NASA/TM-2004-213511

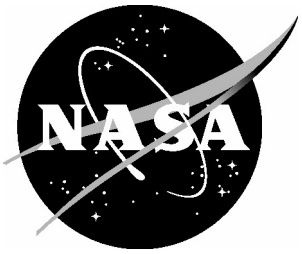

# Optical Diagnostic System for Solar Sails: Phase 1 Final Report

*Richard S. Pappa*
*Langley Research Center, Hampton, Virginia*

*Joseph R. Blandino*
*James Madison University, Harrisonburg, Virginia*

*Douglas W. Caldwell*
*Ecliptic Enterprises Corp., Pasadena, California*

*Joseph A. Carroll*
*Tether Applications, Inc., Chula Vista, California*

*Christopher H. M. Jenkins*
*South Dakota School of Mines and Technology, Rapid City, South Dakota*

*Thomas C. Pollock*
*Texas A&M University, College Station, Texas*

December 2004

The NASA STI Program Office . . . in Profile

Since its founding, NASA has been dedicated to the advancement of aeronautics and space science. The NASA Scientific and Technical Information (STI) Program Office plays a key part in helping NASA maintain this important role.

The NASA STI Program Office is operated by Langley Research Center, the lead center for NASA's scientific and technical information. The NASA STI Program Office provides access to the NASA STI Database, the largest collection of aeronautical and space science STI in the world. The Program Office is also NASA's institutional mechanism for disseminating the results of its research and development activities. These results are published by NASA in the NASA STI Report Series, which includes the following report types:

- TECHNICAL PUBLICATION. Reports of completed research or a major significant phase of research that present the results of NASA programs and include extensive data or theoretical analysis. Includes compilations of significant scientific and technical data and information deemed to be of continuing reference value. NASA counterpart of peer-reviewed formal professional papers, but having less stringent limitations on manuscript length and extent of graphic presentations.

- TECHNICAL MEMORANDUM. Scientific and technical findings that are preliminary or of specialized interest, e.g., quick release reports, working papers, and bibliographies that contain minimal annotation. Does not contain extensive analysis.

- CONTRACTOR REPORT. Scientific and technical findings by NASA-sponsored contractors and grantees.

- CONFERENCE PUBLICATION. Collected papers from scientific and technical conferences, symposia, seminars, or other meetings sponsored or co-sponsored by NASA.

- SPECIAL PUBLICATION. Scientific, technical, or historical information from NASA programs, projects, and missions, often concerned with subjects having substantial public interest.

- TECHNICAL TRANSLATION. English-language translations of foreign scientific and technical material pertinent to NASA's mission.

Specialized services that complement the STI Program Office's diverse offerings include creating custom thesauri, building customized databases, organizing and publishing research results ... even providing videos.

For more information about the NASA STI Program Office, see the following:

- Access the NASA STI Program Home Page at ***http://www.sti.nasa.gov***

- E-mail your question via the Internet to help@sti.nasa.gov

- Fax your question to the NASA STI Help Desk at (301) 621-0134

- Phone the NASA STI Help Desk at (301) 621-0390

- Write to:
  NASA STI Help Desk
  NASA Center for AeroSpace Information
  7121 Standard Drive
  Hanover, MD 21076-1320

NASA/TM-2004-213511

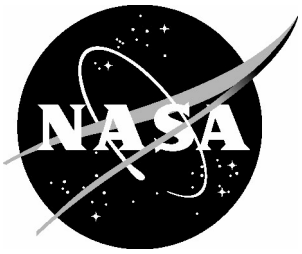

# Optical Diagnostic System for Solar Sails: Phase 1 Final Report

*Richard S. Pappa*
*Langley Research Center, Hampton, Virginia*

*Joseph R. Blandino*
*James Madison University, Harrisonburg, Virginia*

*Douglas W. Caldwell*
*Ecliptic Enterprises Corp., Pasadena, California*

*Joseph A. Carroll*
*Tether Applications, Inc., Chula Vista, California*

*Christopher H. M. Jenkins*
*South Dakota School of Mines and Technology, Rapid City, South Dakota*

*Thomas C. Pollock*
*Texas A&M University, College Station, Texas*

National Aeronautics and
Space Administration

Langley Research Center
Hampton, Virginia 23681-2199

December 2004

Available from:

NASA Center for AeroSpace Information (CASI)
7121 Standard Drive
Hanover, MD 21076-1320
(301) 621-0390

National Technical Information Service (NTIS)
5285 Port Royal Road
Springfield, VA 22161-2171
(703) 605-6000

## *Preface*

NASA's new In-Space Propulsion (ISP) program recently selected teams led by AEC-ABLE Engineering, Inc. and L'Garde, Inc. to develop scale-model solar sail hardware over the next two years, and to demonstrate its functionality on the ground. Both are 4-quadrant, square sail designs with lightweight diagonal booms (<100 g/m) and ultra-thin membranes (<10 g/m$^2$). To support this technology, the authors are engaged in a focused research effort to develop an integrated diagnostics instrumentation package capable of accurate monitoring of solar sail structures such as these during ground and near-term flight experiments. We refer to this activity as the "Optical Diagnostic System (ODS) for Solar Sails" project. Our design is mainly focused on the funded ISP Cycle 1 concepts being developed by AEC-ABLE and L'Garde, but the small size, low mass, low power, and modularity of the ODS design may also make it relevant to a wide range of other solar sails and other gossamer structures.

The approach taken focuses on lightweight optics and photogrammetric techniques to measure solar sail membrane and boom shape and dynamics, thermography to map temperature, and non-optical sensors including MEMS accelerometers and load cells. The diagnostics package must be light: <10 kg initially, evolvable to 2 kg for a 5000 m$^2$ mission sail. It must measure key sail structural characteristics including deployment dynamics, sail support tension, boom and sail deflection, boom and sail natural frequencies, sail temperature, and sail integrity. This report summarizes our work conducted in the initial 6-month Phase 1 period (conceptual design phase), and it complements the final presentation given in Huntsville, AL on January 14, 2004.

## *Acknowledgements*

Many individuals supported the ODS Phase 1 study. We especially acknowledge significant supporting technical contributions from Scott Van Essen at Ecliptic Enterprises, Aaron Gough at South Dakota School of Mines and Technology, and Jon Miles at James Madison University. Additional technical contributors and reviewers include Tom Jones, Chris Sandridge, Eric Walker, Chris Meyer, Al Burner, and Tianshu Liu at NASA Langley; Diane Hurtado, Mike Jacox, and John Junkins at Texas A&M; Mike Fennell at Tether Applications; John Hoppe at Swales Aerospace; and John Rakoczy (our COTR) at NASA Marshall. The Principal

Investigators of the two ISP Cycle 1 sail development teams, Dave Murphy at AEC-ABLE Engineering and Leo Lichodziejewski at L'Garde, consulted with the team on several occasions during the study and provided helpful information related to integration of ODS with their sail systems. Their contributions are gratefully acknowledged. We also thank John Oldson for providing editorial assistance and co-investigator Joe Carroll for making major contributions to the writing of the final report.

## Table of Contents

# Section 1
# What Is to Be Measured and Why

## *1.1 Introduction*

A solar sail diagnostics system has a number of potential uses, including:

1. Determining whether the solar sail is configured and behaving as models predict
2. Answering questions that cannot be confidently answered without a flight test
3. Collecting data that can be used to identify failure mechanisms or other anomalies
4. On later missions, verifying that known problems have actually been solved.

Determining what is necessary and what is sufficient is difficult, given the extremely limited ground and flight test base for solar sails to date, the great difference between solar sails and most traditional (non-gossamer) spacecraft concepts, and the difficulty of providing a proper test environment on the ground (good vacuum, zero gravity or good gravity compensation, etc.). As a result, it is not yet clear exactly what kinds and quantities of data will be most useful, or what a minimum acceptable dataset will be. As discussed below, it is precisely this uncertainty that may be the strongest argument for an Optical Diagnostic System (ODS).

One of the useful things about imaging, and in particular video, is that it is the cheapest and most convenient way to collect huge amounts of data. The richness of the data allows it to be very useful when the system behaves unexpectedly, and it is not clear what is happening. On the other hand, if a solar sail is far from earth, that data needs high compression before downlink to be affordable. Compression is less of an issue for ground-based tests or tests in low earth orbit.

The combination of some form of imaging (even if not highly calibrated) ***plus*** other forms of data (strain gauge, acceleration, attitude, temperature, and maybe even electric fields) may be far more useful than any one form of data by itself. For example, structural vibration frequency may

give the best data on boom stiffness, and waveform analysis may indicate the presence of hysteresis, buckling, or other non-linearities. Such frequency data might be derived from video data or from a Fourier transform of strain gauge or other data. But unless there are other supplementary data, we may not be able to determine why the boom frequency is different from expectations. And if the data seem strange, imagery becomes invaluable, so one can see whether a boom is buckled or incompletely deployed, or whether the membrane has snagged or torn.

Another type of synergism is to use anomalies in data from non-optical sensors like strain gauges to trigger collection of additional higher-rate video imagery, or saving of recent image data that might otherwise be overwritten before download if everything appears normal.

## *1.2 ODS Objectives*

The team has developed the following proposed primary and secondary objectives for ODS, which have been presented in the project reviews during Phase 1:

*Primary:* Gather data in a near-term solar sail flight experiment to validate structural analytical models for confident scaling to larger sizes.

*Secondary:* Observe/measure the unexpected, especially "known plausible" malfunctions

The focus of the ODS project is on development of a integrated diagnostic system suitable for an initial solar sail flight experiment, such as might be sponsored by NASA's New Millennium Program. This diagnostic system may be judged to be unnecessary (or perhaps too massive unless miniaturized) for subsequent solar sail flights if everything behaves as predicted on the initial flight. Or perhaps a subset of the system used for health monitoring rather than validation of structural analytical models would be flown on subsequent development flights or even on early missions. The sailcraft in the initial flight experiment is assumed to be a square solar sail design at least 40 m in size (edge dimension) with four booms deploying from a central

hub that support individual quadrants of highly reflective membrane material. Candidate designs include the two concepts currently under development by AEC-ABLE Engineering Co. and L'Garde, Inc. for NASA's In-Space Propulsion Program.

## *1.3 What the life history of a solar sail suggests about ODS requirements*

In deciding what needs to be measured and why, the team considered what problems might occur during the life history of a solar sail that could be detected by ODS. Our thoughts are summarized below.

### 1.3.1 Materials

The sail membrane and supporting structure must tolerate the sequence of configurations and environments the sail will see. Key environmental issues include energetic UV and ionizing radiation. The responses may vary with rate, temperature, the presence or absence of oxygen or other gases during or after exposure, and with the opacity of the metallization, especially after folding, unfolding, and other handling. Other issues include dryout in vacuum, blocking (sticking of adjacent film layers), extreme temperatures and gradients caused by shadowing or inadvertent focusing of light (especially during deployment), and modification of membrane properties by the surface metallization. Atomic oxygen may not be an issue, because drag would likely cause reentry before a membrane erodes much. As a minimum, ODS images need to be able to indicate the location and geometry of significant tears in the membrane. This may help us distinguish between many of the various failure modes discussed here.

### 1.3.2 Manufacturing

Different sail designs have different requirements on dimensional accuracy of membrane and structure. Critical dimensions may change with temperature, desiccation, and stress history, and they may not change uniformly. Solvent vapors may cause blocking or other problems.

Cleanliness may also have unexpected effects: an early prototype may be dusty enough to prevent blocking or depressurization damage, while a cleaner, flight sail may be vulnerable to one or both problems. It may be important for ODS to be able to see the results of serious manufacturing problems. Anything that imposes uni-axial tension can generate wrinkles. Such wrinkles may be more visible if a sail is in low orbit around earth because the varying position of the lit earth may allow better "wrinkle surveys" than can be done when the only significant light source is direct sunlight.

### 1.3.3 Storage

Storage temperature, duration, pressure cycling, and ambient atmosphere (dryness, solvents, etc.) could be issues. Bimetallic corrosion of the thin membrane coatings before launch could be an issue if both sides are coated with different materials. If a hydrated membrane can act as a polymer electrolyte, it may be necessary to store the sail in very dry air to prevent corrosion. This might best be detected by witness samples stored with the sail and removed before launch, but imagery taken after deployment may also be useful.

### 1.3.4 Launch

During launch, peak depressurization rates inside a fairing are of order 0.05 atm/sec. The sail design must either guarantee adequate venting of any trapped air volumes, or accept random local damage (including membrane bulging or bursting), and possible larger-scale damage due to piston effects of the stowed sail. Perforating the membrane may help if the stowage geometry does not allow too many holes to be sealed by adjacent folds. Imaging the folded sail during launch is infeasible, but we can image the results after deployment, especially with a telephoto inspection camera. Damage seems likely to be limited to exposed folds. The damage location and appearance may help narrow down the range of potential causes.

### 1.3.5 Deployment

Many if not most potential sail failure modes may first become evident during deployment. Booms may buckle; tensile elements may fail, jam, or snag; the membrane may snag or tear;

actuators can jam or otherwise fail; and electronics and/or software can malfunction. Imaging plus opportunistic sensing of other types may be particularly useful at diagnosing deployment-related failures and anomalies. Imaging systems require enough memory, processing power, and downlink bandwidth that also including other sensors (strain, acceleration, temperature, etc.) should not significantly increase system-level requirements.

### 1.3.6 Sail dynamics

Solar sails operate in an environment that provides negligible damping, so the sail design must itself provide adequate structural damping of any possible dynamics that could be induced in the system. Sail developers may need to build and exercise detailed and realistic sail FEA models, with damping parameters realistic for the sail environment, to understand this issue. Only after such models are built and exercised will we know how accurately we need to observe the dynamics in order to characterize damping. Damping by air during ground tests can be fairly high even in a reasonably good vacuum (e.g., 0.1 torr) due to the large surface area and ultra-low mass density of the membranes.

In addition, the perturbing effect of gravity will be unavoidably large in ground tests. Such tests may be far more useful for "stress-testing" our understanding of the sail's dynamics in general, than for directly indicating the likely flight dynamics. The best ground test may involve multiple conditions, none of which simulates flight accurately, but which together exercise what are thought to be the key features of the design, operations, dynamics, and controls.

### 1.3.7 Long-term degradation

Long-term degradation includes the effects of micrometeoroid damage, cumulative radiation on the membrane or electronics, command or control malfunctions, thermal cycling, etc. One issue is whether the sail will retain enough control authority after impact damage, failure of individual control actuators, gross membrane tearing, or other problems. Another is whether the sail can recover from being flipped over onto its back. The sail's effectiveness varies with its reflectivity and area, so any large degradation will be visible, though its cause may not be. Most of the ODS cameras will be monochromatic for highest measurement resolution, but the pan-tilt

inspection head might include one or more color cameras. (See Section 3 for a description of the ODS baseline design concept.) However, the value of color imagery may be limited by degradation of the color filters as they accumulate exposure to bright light. This may require use of special stable filter wheels with a monochromatic imager, rather than the conventional Bayer "mosaic" filter built into most small-format color imaging chips.

A related issue is gradual increases in sunlight intensity during missions that approach the sun. This increases sail temperature and temperature gradients (and hence thermal distortion), and may also affect sail degradation mechanisms.

### 1.3.8 Diagnostics during or after major system failures?

A solar sail may suffer a major structural or control failure. ODS need not remain operational after loss of power or downlink capability, but it may be feasible and worthwhile to retain imaging capability after lesser failures. For example, if a sail flips over, ODS will be on the unlit side (assuming the ODS baseline implementation). If the sail is not totally opaque, useful imaging may be possible until the batteries die. If the sail is opaque, tears and other flaws may be very visible. But such imaging should probably be regarded as an "opportunity" rather than a serious ODS design driver.

### 1.3.9 An early list of "known plausible" failure modes for ODS to handle

The list below was compiled by the ODS team for the kickoff meeting. It has not been reviewed and accepted by either the sail developers or the solar sail program office. We cannot currently guarantee that the baseline ODS design will be able to observe and distinguish between all of these failure modes, but thought it was worth including them for potential use during reviews later in the ODS development process.

Sail booms or ODS camera mast:

- Deployment jamming
- Buckling
- Thermally induced distortion

- Other unexpected bending or twisting
- Lower damping of boom/mast dynamics than expected
- Irregular deployment synchronization (if applicable)

Sail membrane:

- Damage from depressurization at launch (which may have varying effects)
- Damage from sticking or disorderly unfolding that creates stress concentrations
- Tearing due to any cause (grazing micrometeoroid impacts, thermal cycling, etc.)
- Degradation from local heating, UV, radiation, contamination, ODS targets, or …?
- Lower damping of membrane dynamics than expected

Other:

- Getting maximum functionality in unexpected orbits (kick stage malfunction, etc.)
- Failure to separate completely and cleanly (this is apparently quite common)
- Control failures (e.g., controller upset or latch-up curable by cycling power)
- Control actuator malfunction (what sensors should ODS or the sail developer use?)
- Difficulties in recovering from unexpected attitudes (e.g., due to controller upset)

## *1.4 Importance of sail thermal gradients, construction errors, etc.*

The low stresses planned for the sail membranes (<10 psi), in films with a Young's modulus in the 300-900 ksi range, means average membrane strains on the order of 1 to 30 parts per million. Any factors that can cause local length changes at least comparable to this can seriously alter the stress distribution in the membrane. If a small part of a membrane shrinks by more than this compared to the rest of the membrane, it may take all the loads. These concentrated loads may still be low, but they may be large enough to cause tearing, especially if "spiky" transient loads due to flapping, etc., are superimposed on them. Section 6 of the report shows how thermal gradients may cause length changes large enough to be an issue. Also, step-and-repeat membrane assembly techniques may induce cumulative size and shape errors that are hard to control and even harder to quantify. Changes in film tension, temperature, and humidity during assembly may also contribute errors that are only seen after deployment in orbit.

## *1.5 How wrinkles and creases can affect sail dynamic behavior*

Due to their membrane nature, sails have unique features that affect sail behavior. Membranes have two distinct kinds of out-of-plane deformations: wrinkles and creases.

*Wrinkle* – an out-of-plane elastic deformation associated with the no-compression behavior of membranes. (This is the historical use of the term in membrane mechanics.) Wrinkles usually materialize as sinusoid-like waves. They may occur locally or be fully developed over the majority of the membrane surface. See Fig. 1-1.

**Figure 1-1. Membrane wrinkling**

*Crease* – an out-of-plane inelastic deformation associated with "yielding" of the membrane material. (There is some history to this use of the term, particularly in the paper and textile fields.) Creases usually materialize as sharp, cusp-like deformations, similar to balling up a sheet of paper and unfolding.

We have also recently seen a distinctive behavior when allowing small membrane samples with intersecting folds to unfold at very low tension. Complicated "puckers" can form at the intersections of folds. They can "cinch up" during unfolding, even if the initial folds were not creased. It takes modest (but not negligible) tension to remove them, even in 1.4-micron film.

Any parts of the membrane that see no significant tensile loads during or after deployment may retain creases or puckers. They may change local sail dimensions by >>30 ppm. This may actually be quite useful if it provides a self-regulating "slack management" feature to sail regions that might otherwise be slack. But creases and puckers can also potentially concentrate the sun's energy by multiple reflections, possibly enough to cause local membrane overheating and damage, especially in missions close to the sun. The thin metal coatings on the sail membrane may also significantly affect the membrane response to creases and puckers, because the yield strain of the metal is far less than that of the film, and its Young's modulus is far higher.

## *1.6 Measurement Needs and Goals*

There are several important reasons for collecting data on solar sail behavior in space:

- Deployment is so complicated that reliable simulation may be simply infeasible
- Data are needed by theoretical/numerical models, including system-level damping
- Test theoretical/numerical modeling methods, to improve risk reduction analyses
- Characterizing membrane tear propagation in the actual space environment
- Unexpected phenomena are perhaps the most serious challenges to risk reduction

Model validation may be the most critical to solar sailing success. Experimental data must be considered in the context of high-fidelity computational models. The sails are membranes that will wrinkle if they are not kept in tension. Wrinkles and creases reduce the propulsive efficiency of a solar sail, may cause hot spots where membrane overheating can occur, and will likely cause significant departure from what is expected with a biaxially-tensioned membrane. Furthermore, slack directions and areas in the sail represent load-carrying indeterminacy that must be minimized to increase confidence in structural integrity under mission conditions.

There are several solar sail modeling methods that need to be evaluated in deriving ODS measurement requirements. Relevant field variables predicted by these methods include:

- Sail strain
- Lowest several sail natural frequencies and mode shapes
- Static boom shape
- Boom loading
- Lowest several boom natural frequencies and mode shapes
- Static sail shape
- Center of pressure

Other important solar sail measurement tasks include:

- Measure sail support tension
- Measure sail temperature
- Measure boom root loads

- Measure boom tip accelerations
- Observe deployment and report both qualitative and quantitative results
- Observe sails, booms, and other mission-critical components for structural health

We need to estimate the required accuracy of experimental solar sail measurements to avoid either under-designing or over-designing ODS. At a minimum, the experimental data must be at least as accurate as the models to be validated, although several times more accuracy is desirable for higher confidence. But how accurate will the model predictions be? A 7 kPa (1 psi) "skin" or membrane stress in a 21 MPa (300 ksi) elastic modulus sail causes ~3 micro-strain. Values this small are well within the capability of modern finite element (FE) codes. When compared to classical membrane solutions, FE computed frequencies and mode shapes have been shown to compare extremely well. Generally, computational model results will be considered successful if they are within 5% - 10% of experimental "truth."

Center of Pressure (CP) is an important parameter in the design and control of solar sails, as is the Center of Mass (CM). CP is the position through which a force that is statically equivalent to the pressure load acts. The CP-CM offset and its uncertainty are fundamental to solar sail guidance and control [Ref. 1-1]. The CP in some ways is a metric for sail computation not unlike "rms figure error" is for antennas and optics. The CP depends on the global and local shape of the membrane, and hence sail shape is critical for solar sail model validation.

Table 1-1 lists the types of measurements needed for validating structural analytical models and modeling techniques for solar sails.

**Table 1-1. Measurement goals for a 70 m solar sail flight experiment.**

**(Based partly on Ref. 1-2)**

| Parameter | Expected Range | Accuracy Target | Notes |
|---|---|---|---|
| **Deployment Dynamics** | *Qualitative:* Video of entire deploying sail<br>*Quantitative:* Measure trajectories of booms & membranes | *Qualitative*: High-quality video at 10+ frames/sec<br>*Quantitative*: 40mm | This is measured only once, so cameras for this purpose might be located off the sailcraft (e.g., on a carrier platform) or ejected later to reduce sail mass. |
| **Shape** | 0-2 m (est.) out of plane | 20 mm | 20 mm is the mean accuracy for a uniformly distributed grid of targets. |
| **Vibrations** | *Natural Frequencies:* First 5-10 system modes<br>*Damping:* 2% (est.)<br>*Amplitudes:* 1 m (est.) | *Frequencies:* 1%<br>*Damping:* 10%<br>*Amplitude:* 20 mm | Image frame rate at least 2x the highest vibration frequency of interest. |
| **Sail Tension** | 0 to 50 N | 0.1 N | Will investigate in-situ measurement possibilities with L'Garde & ABLE. |
| **Boom Stress** | *Deploy:* 0 - 15 x $10^6$ Pa<br>*Later:* 1 x $10^6$ Pa | *Deploy:* $10^5$ Pa<br>*Later:* $10^4$ Pa | Highest stress levels occur during deployment, but difficult to measure then. Operational stresses much lower and also difficult to measure directly. |
| **Film Stress** | 0 - $10^6$ Pa<br>(Mostly under $10^5$ Pa) | $10^3$ Pa | Very low operational stresses. Can be estimated using measured wrinkle patterns, sail shape, modes, and predictive structural model. |
| **Temperature** | Thermographic map | 10° C | Not listed in the NRA, but important for some missions. |
| **Sail Integrity** | Identified by data trends versus time and/or optical observation | High-resolution imagery, perhaps one quadrant only | If not mass-prohibitive, high-resolution camera will include pan/tilt/zoom capability. |

Also listed in Table 1-1 are estimated ranges of the measurement parameters and an accuracy target for each parameter assuming a sail size of 70 m. Accuracy targets for other sail sizes vary proportionately. This information is based in part on requirements listed for a proposed New Millennium Program ST7 solar sail flight experiment [Ref. 1-2].

Cables that collect loads from the sail membrane quadrants and carry them to the booms complicate the structural configuration of the sail. The cables and membranes carry tensile

loads, while the booms carry compressive loads and some bending. Boom loads are likely to be small (perhaps only a few Newtons), and the resulting deflections should be small, if the structure has enough damping. Sail loads are also likely to be small, but deflections may be considerably larger than those of the booms due to the relative differences in stiffness. The wide range of stiffness, coupled with potentially large sail displacements and nonlinear material behavior, makes it challenging to predict sail response. The dynamic response of membranes, due to their no-compression/wrinkling character, is extremely challenging to accurately predict. This implies that, even under the best situations, any sail diagnostics measurement package must be designed to work with considerable uncertainty with respect to structural model predictions.

## *1.7 Optical diagnostics*

Photogrammetry is the science of measuring the location and size of three-dimensional (3D) objects with photographs [Ref. 1-3]. The image analysis procedures are related to those used in surveying. When dealing with time sequences of images, this technology is often called "videogrammetry" (or "videometrics") instead of "photogrammetry," although either term is acceptable [Ref. 1-4]. Modern close-range photogrammetry uses digital imaging sensors (either CCD or CMOS) and computer data analysis. It can measure hundreds or thousands of object points simultaneously. Measured sets of object points, also known as "point clouds," can characterize static shape. Sequences of images can characterize structural dynamic properties (i.e., vibration) as well.

Digital photogrammetry records the object from at least two camera positions and calculates 3D coordinates of discrete points on the object's surface by triangulation of light rays. These discrete points can be natural surface features, but when high accuracies are required, natural features can be inadequate. Solid-colored circular targets are usually installed on the object when highest measurement accuracies are required.

Rigorous statistical analysis is used in the numerical processing so a covariance matrix and other statistics indicating accuracy, precision, and reliability accompany the 3D coordinates. Such statistics are especially necessary when spatial deformation is indicated by the difference

between sets of coordinates obtained at different times. This enables decisions to be made at specific levels of confidence about what shape and position changes occurred in the object. The photogrammetric technique is extremely flexible, able to acquire measurements simultaneously over the surfaces of large objects. It has been proven by successful application to monitoring spatial deformation of a wide range of structures, including various gossamer research structures [Ref. 1-5].

The measurement accuracy achieved with photogrammetry depends on several inter-dependent factors including:

- Size and geometry of the test structure
- Number of cameras and their image resolution
- Camera synchronization (for dynamics measurements)
- Locations and pointing directions of cameras
- Illumination conditions
- Clarity and contrast of surface features (targets)
- Camera and lens characteristics
- Image compression procedures
- Camera stability
- Calibration and data analysis procedures

As will be shown in Section 3, we studied a variety of camera geometries during Phase 1. Those with the widest range of camera viewing directions (e.g., from the center and each corner of the sail) had the highest photogrammetric measurement precision. But they also had the highest expected integration cost, so the ODS baseline concept was restricted to cameras mounted only on a central camera mast. The baseline concept assumes that the camera mast is mounted on the sun side of the sail and views a grid of sunlit photogrammetry targets. An alternative implementation that is still being studied is mounting the camera mast on the back side of the sail instead (or in addition to a front-side mast) and using translucent photogrammetry targets that are visible from the back. In this report, we will assume the mast is on the front side.

## *1.8 Thermal imaging*

Thermal gradients on the sail can cause relative size changes that are large compared to the average tensile strain of a few parts per million. This has led to an interest in thermal mapping of the sail as part of the ODS concept.

However, there is an important integration problem: the ODS cameras need to be mounted on the sunlit side of the sail (in the baseline concept), while thermal imagers should give much better data if they image the back of the sail, which has ~10X higher thermal emittance than the front. This implies using a separate back-side mast and imager installation. This will raise development and integration costs. In Phase 2 we will examine how accurately we can measure membrane thermal emissions using compact low-power passively cooled thermal imagers, for both sun-side and anti-sun-side imager locations.

A comparably critical issue that will be examined in Phase 2 is whether we may be able to ascribe any measured thermal imaging differences unambiguously to one or more of the following potential causes:

- illumination differences (direct or reflected)
- local solar absorptance differences, due to degradation or contamination
- local longwave emittance differences, or
- different reflected longwave radiation, if the sail is in low orbit around earth.

## *1.9 Non-imaging diagnostics*

The mass, power, signal conditioning, memory, and downlink bandwidth needed for imaging swamps that of most other sensors, so it may be feasible to add various other sensors to ODS without significantly driving the ODS design. Such sensors can be particularly valuable if they can enable on-board (autonomous) selection of subsets of the image data as being of more than average interest (e.g., just before and after a sensed acceleration or strain transient). The main criteria are complementarity, synergism with the imaging data, and fairly easy integration.

## *1.10 Recommendations*

Most of the recommendations relating to "what and why" are actually addressed in later sections of the report that focus in more detail on individual aspects of the ODS design. But two recommendations seem worth making here:

### 1.10.1 Developmental testing of ODS

ODS should use a wide variety of tests during development. Often the best tests are early and very informal ones. Sometimes poorly conceived early tests are the ***most*** instructive, if they occur early enough in development. Developmental imaging of prototype sails is also a key opportunity to assess what diagnostics may be useful in flight: what is unexpectedly useful or useless on the ground may also be so in flight. But one has to think through the implications of relevant differences in dynamics, environment, lighting, etc., between development and flight.

Perhaps even more important than testing ODS on prototype sails is testing single imagers with representative photogrammetry targets on small membrane samples that can be folded and then unfolded and hung at low tension. This gives the most representative membrane creases, wrinkles, and "optical noise." One can also provide far better lighting and black baffling for such tests than is feasible for tests on larger prototypes. Such tests should help quantify glare and glint problems (see Section 4.1). This in turn will help optimize many aspects of the ODS design, including number of cameras and pixels, lens and lens shade design, and overall layout.

### 1.10.2 ODS architecture trades

We really don't know yet how much data we can afford to collect, how easy it will be to do real-time compression and/or analysis on that data to minimize on-board storage and/or downlink needs, or how much ODS data an actual flight experiment will be able to send to earth, either in real time or after storage in some on-board archival memory. This should be addressed as flight experiment concepts become more specific. It appears worthwhile to keep more than one data handling architecture option open until more is known about the consequences, likely developmental problems, and possible flight opportunities.

## *1.11 References*


1-1. Wie, B., "Dynamic Modeling and Attitude Control of Solar Sail Spacecraft," Final Report, JPL Contract No. 1228156, January 2002.

1-2. Price, H., "Solar Sail Technology NMP ST7 Opportunity," Website: http://nmp.jpl.nasa.gov/st7/ST7_TA_Solar_Sail.pdf, May 2001, p. 13.

1-3. Atkinson, K. B. (editor), Close Range Photogrammetry and Machine Vision, Whittles Publishing Company, 2001.

1-4. El-Hakim, S. F. (editor), *Videometrics and Optical Methods for 3D Shape Measurement*, SPIE Proceedings No. 4309, January 2001.

1-5. Pappa R. S. et al., "Photogrammetry Methodology Development for Gossamer Spacecraft Structures," *Sound and Vibration*, Vol. 36, No. 8, August 2002, pp. 12-21.

# Section 2
# ODS Requirements Derived to Date

## *2.1 Status*

The requirements in this section were presented by the ODS team to the project office at the Phase 1 final review on January 14, 2004, but they have not yet been officially endorsed. They are subject to change in Phase 2.

## *2.2 Keywords and Notation*

The following keywords and notations have special significance herein.

**[ ]** The use of square brackets for requirements shall indicate values which are approximate or negotiable.

**Shall**. A keyword indicating a mandatory requirement that must be implemented.

**Should.** A keyword indicating flexibility of choice with a preferred alternative that shall be considered.

**May**. A keyword indicating a flexibility of choice with no implied preference. It can be interpreted as permission. Such statements are generally included for clarification; silence on a subject is equivalent to "may".

**Will**. A keyword expressing a commitment by some party to provide something.

All sentences containing the keywords "shall" or "should" shall be interpreted by designers and implementers as instructions; they should be expected to be contractually or formally binding. Any sentence not containing one of these keywords may be interpreted as informational.

The following definitions are not used in this document, but will be used in later versions of the requirements:

**Inspection (I)** is the verification of compliance by the examination of documentation (the results of prior lower level verifications, drawings, vendor specifications, software version descriptions documents, etc.) or by direct examination of an attribute (dimensions, weight, physical characteristics, computer program code, etc.)

**Analysis (A)** is the verification by evaluation of data by generally accepted analytical techniques to determine that the item will meet specified requirements. Analytical techniques may include systems engineering analysis, statics, analog modeling, similarity, and computer simulation.

**Test (T)** is an empirical verification of operation of all or part of the subsystem under controlled conditions to determine that quantitative design or performance requirements have been met. It includes the collection and subsequent examination of quantitative data. Tests may rely on the use of instrumentation and special test equipment to measure the parameter(s) that characterize the requirement.

**Demonstration (D)** is an empirical verification of operation of all or part of the subsystem under controller conditions to determine that qualitative design or performance requires have been met. Demonstration relies on observation/recording of functional operation not requiring the use of elaborate instrumentation, special test equipment, or quantitative evaluation of data.

Sail size is defined as the outer edge dimension of a square sail.

*Note: This sail size definition may need clarification for specific sail designs. For example, since the sail's outer edges are usually curved, we may want to use sqrt(area), or quadrant hypotenuse, or tip-to-tip distance of adjacent booms. This will be examined further in Phase 2.*

## *2.3 Definition of Requirement Levels*

1. **Level 1** requirements are between Customer and PI. They may be qualitative, "big picture," or goals and thus require qualitative flowdown to clarify them. In the tables on following pages, all level 1 requirements are shown in bold on a gray background.

2. **Level 2** requirements are between primary project system elements. For this project, the system elements at this level are: ODS, Sail (the actual propulsive structure), Sailcraft, Modelers, Testers

3. **Level 3** requirements are between subsystem elements of a system. ODS is the only system that is decomposed at Level 3. The full complement of subsystems is TBD but includes: Cameras, Avionics, Photogrammetry Technique (maybe?), etc.

The requirement level is indicated in the following tables by the number of fields in its ID.

## *2.4 Functional Requirements (Level 1 reqts are bold on gray)*

| ID | Title | Requirement | *Rationale* |
|---|---|---|---|
| **1** | **Sail Shape** | **ODS shall provide spatial measurements at sufficiently high frequency to determine sail shape, natural frequency, damping and modes and mode shapes** | **This is quantitative.** |
| 1.1 | Sail Out-of-Plane | ODS shall measure out of plane sail displacements to an RMS precision of [0.025% of sail size (5 mm for 20 m sail)]. | |
| 1.2 | Sail Motion | ODS shall measure out of plane displacements up to a frequency of [2] Hz. | Derived from models of first 10 mode frequencies. |
| 1.3 | Sail Modes | ODS shall provide measurements that support determination of the first [10] vibrational modes | |
| 1.4 | Sail Sampling Interval | ODS shall use a spatial sampling interval of [4 % of sail size] or better (less). | |
| 1.5 | Boom Measurement | ODS shall measure straightness and twist of the sail booms at [not less than 5] locations along their length to an RMS precision of [TBD]. | |
| 1.6 | Boom Motion | ODS shall measure lateral displacements of the sail booms up to a frequency of [2] Hz. | |
| 1.7 | Measurement Method | ODS shall utilize photogrammetry as a primary sensing method. | This supports ability to find “deflated” shape. |
| 1.8 | Measurement Timing | ODS shall have the capability to take a set of measurements of the entire sail system within [0.02s] (Simultaneously with respect to 2 Hz time scales). | |
| **2** | **Sail Stress** | **ODS shall provide adequate data to infer the stress state of the sail system** | |
| 2.1 | | ODS shall accommodate load and strain sensors. | |
| **3** | **Deployment Monitoring** | **ODS shall observe and record sail system deployment, qualitatively monitoring sail system health and integrity** | |
| 3.1 | | ODS shall have the capability to image the entire sail system continuously. | |
| **4** | **Post-Deploy Health Monitoring** | **ODS shall have the ability to qualitatively monitor sail system health and integrity after deployment** | **Needs definition of what health and integrity are.** |
| 4.1 | | ODS shall have an inspection capability that can resolve features of [0.1% of sail size]. | |
| 4.2 | | ODS shall have the ability to globally monitor sail health. | |

## *2.5 Implementation Requirements (Level 1reqts are bold on gray)*

| ID | Title | Requirement | *Rationale* |
|---|---|---|---|
| **5** | **Mass** | **ODS shall weigh less than 10 kg, when used for 20 m sail vehicles. The ODS design should be evolvable to 2 kg on a 5000 $m^2$ sail or otherwise provide options for attaining this mass target.** | |
| **6** | **Power and Data** | **ODS shall operate within a power budget of 25 W. ODS shall require a daily data budget of <1 Gbyte/day.** | |
| **7** | **Flightworthi-ness** | **ODS shall use technology and architecture that are evolvable to a space flight system.** | |
| 7.1 | Mission Assurance | ODS architecture and electronics shall be designed with consideration for acceptability according to a typical mission assurance plan. | |
| 7.1.1 | Radiation Environment | ODS shall be designed for a radiation environment consistent with high LEO (~1000 km). | |
| 7.1.2 | Design Life | ODS shall withstand its design environment for a minimum of [6 months] with a goal of [2 years]. | |
| 7.1.3 | Redundancy | The ODS design shall provide for functional and/or block redundancy as appropriate to match ODS reliability with host reliability requirements. | |

## *2.6 Programmatic Requirements (Level 1 reqts are bold on gray)*

| ID | Title | Requirement | *Rationale* |
|---|---|---|---|
| **8** | **Validation** | **ODS shall be validated by comparison with more accurate instruments such as those already commonly used at LaRC** | |
| **9** | **EM Demonstration** | **ODS EM shall be demonstrated (fully integrated, with form, fit and function) during deployment of a 20 m sail.** | |
| **10** | **PB Operation** | **A prototype ODS shall be operational at Plum Brook for the 20-meter tests.** | |
| 10.0.1 | Form, Fit & Function | Plum Brook ODS shall have functionality of a spaceflight ODS, and as much of the fit and function of a flight ODS as practical. | |
| 10.0.2 | GSE | All GSE required for ODS operation at Plum Brook shall be provided by the GSE team. | |
| **11** | **No PB Interference** | **ODS shall not impose new requirements on Cycle 1 10- or 20-meter sail systems.** | |
| 11.1 | Interference | ODS shall not interfere with Cycle 1 testing at Plum Brook. | |
| 11.2 | Interface | ODS shall not mechanically interface with the Cycle 1 testing hardware. | |
| 11.3 | No Targets Needed | ODS shall have some functionality without targets. | L'Garde sail will not have targets in 10m & 20m sails. |
| 11.4 | Environment | ODS shall operate in same environment as Cycle 1 Hardware at Plum Brook: down to [0.1] Torr, in the range [-10 to +50 °C]. ODS may provide heaters to mitigate low temperature but should account for such heaters in its power budget. | |

## *2.7 Requirement for failure tolerance: sensor strings only, or full system?*

The project office has requested that ODS have an additional Level 1 requirement to be one-failure tolerant. There are 2 major reasons for this. The first is the roadmap to a space flight system. A space flight system will have to be one-failure tolerant. The second reason is for in-vacuum testing of ODS on large prototype solar sails: it is not acceptable to break vacuum, repair ODS, and re-pump the chamber to repair ODS failures.

The Level 1 requirement may be worded something like this, "ODS shall provide the requisite data for validation of structural models while being tolerant to one failure per string."

Fault tolerance is easy to do on many aspects of the design, especially if it just requires redundant sensors and signal conditioning circuits. But it is not easy to do everything that way, such as with data compression, flight computers, and other avionics. We need to clarify whether ODS needs fault tolerance just at the single-sensor-string level, or higher up. For example, all sensors at a single boom tip will share common power and datalines to the hub, or common autonomous power and wireless links to the hub. Does each such boom-tip assembly require redundancy?

Additional sensors are particularly useful if they provide some additional value, but then losing them degrades the system. So paradoxically, adding a single sensor that provides more insight into system dynamics may degrade the system redundancy, compared to using a suite of 4 sensors, any 3 of which can provide the “required” data.

It appears best to answer this question on a case-by-case basis. For example, an extra MEMS type accelerometer and signal conditioning requires minimal extra mass, power, and data rates, and some geometries may allow complete solutions using “any 3 of 4.” But in the case of cameras, the mass, power, cabling, and data rate implications are non-trivial, and redundancy requires complete image area overlap. So redundant accelerometers may make more sense than redundant cameras. Or we might arrange for the pan-tilt inspection head (Section 3 discusses the baseline ODS design concept) to include a camera that can substitute for any single failed fixed camera. Or other camera views of most of a quadrant may allow “good enough” analysis most of the time. So another question is whether and how much degradation is allowed after a single sensor failure, for each type of sensor.

The additional more serious question is what requirements for redundancy ODS should have inboard of the sensors, where redundancy can lead to far higher complexity and introduction of obscure failure modes. Here again, case-by-case study and decisions may be critical. A consistent requirement of fault tolerance may have far more serious implications than requiring tolerance of most but not all component failures.

# Section 3
# ODS Baseline Design Concept

## *3.1 Geometries considered for sail photogrammetry*

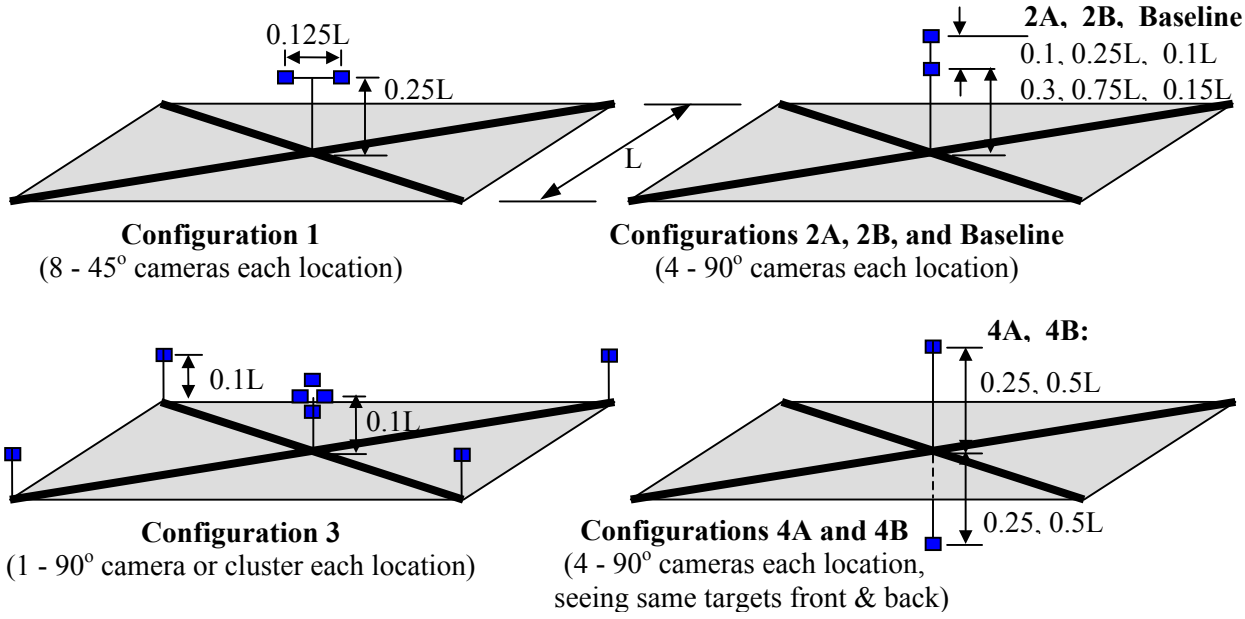


**Figure 3-1. Four configurations and variations considered, including final baseline design**

### 3.1.1 Strengths and weaknesses of each configuration

Photogrammetry infers 3D object positions from 2D imagery using multiple viewpoints for depth perception. The short baselines in Configurations #1 and #2 reduce depth perception. The main difference between these configurations is that #1 has the poorest depth perception near the left and right edges while #2 has poorest depth perception near the center. By contrast, #3 has good 3D precision everywhere because each quadrant is viewed from all 3 of its corners. It is also the most robust, especially if each boom-tip camera views the whole sail. A failed camera reduces precision but several complementary views are retained of each location on the sail. But #3 is also the hardest to integrate, with 5 camera masts and considerable high-bandwidth cabling. Configuration #4 is similar to #2, but has a much larger baseline. But it also requires some form of target (TBD) that is visible from both the front and the back of the sail.

### 3.1.2 Configuration downselect issues and process

At the kickoff meeting, the ODS team recommended configuration #3 as the baseline. But the integration complexity (5 camera masts and long cables), plus concerns about putting additional mass at the tips of the booms, led to immediate rejection of this design.

Configuration #4 led to 3 concerns about the aft boom. One was that any aft mass would tend to destabilize the sail, if it could move the overall vehicle CM aft of the sail plane. Another concern was an integration issue: it requires a way to mount camera masts on both the front and the aft side of the sail or its payload. This might conflict with payload design or interfaces to the booster. A third concern was constraints on sail membrane design imposed by the need for target visibility from both the front and the back side. Ensuring back side target visibility may require locally masking the sail during aluminization, or removing the metal later, or punching holes in the sail and patching them with translucent targets, or other similarly invasive approaches.

The above problems led us to focus on configurations #1 and #2. But front-mounted booms also have problems. One is that if their product of length and mass moves the vehicle CM too far forward, the sail can become excessively stable. Then the sail requires much more control authority to tilt to large angles to the sun, as is needed for high tangential thrust. For modest ODS masses, this should not be a problem, and may actually provide a benefit to the payload: the CM offset may allow the main sail payload to mount slightly aft of the sail plane to provide the desired near-neutral stability, rather than having to be packaged partly in front and partly aft of the center of the sail structure to ensure a suitable CM location.

In considering configurations #1 and #2, yet another boom concern surfaced. The L'Garde design minimizes sail weight by discarding a support package after deployment, and it does this by releasing it in front of the sail, after which the sunlit sail accelerates aft, away from the support package. Hence we seem to require a tilted and/or offset camera mast on the L'Garde sail. Configuration #1 might raise more concerns about support package re-contact after release. This plus a later differentiation of functions for the two camera locations led us to concentrate on configuration #2: a single central front-side camera mast, with sail-view cameras at two heights.

The ODS baseline design concept assumes that the front-side camera mast deploys and latches in place once, and then cannot change its length afterwards. Therefore, triangulation to determine sail shape requires two camera stations along the mast. This assumption was made because the team is not aware of any candidate inflatable mast technologies designed for in-space retraction. In any event, adding retracting motors or other devices to allow the camera mast to change length in space is expected to require a significant mass and cost penalty. But this possibility needs to be examined further. Perhaps a new mast technology will make it feasible to vary camera mast length. If that can be accomplished, the ODS team will reconsider using only a single platform of cameras, and doing photogrammetric triangulation by varying the camera mast length. Of course, this assumes the sail shape does not vary during the time required to acquire the two image sets.

## *3.2 Evolution of the baseline camera configuration*

As noted in Section 3.1.1, the easy-to-integrate configuration #2 has poorer viewing geometry and hence depth perception than #3 or #4. But viewing geometry is not the only factor that affects photogrammetric precision: camera quality also is critical. One can compensate for smaller baselines by using higher-resolution imagers. The selection of a small-baseline configuration led us to focus on raising image quality to compensate. Some early concepts considered VGA-type imagers with 640 x 480 pixels; by the end of the study, our main focus was on SXGA imagers, with 1280 x 1024 pixels. Another change was even more important: using more cameras, each with a narrower view. This is discussed in more detail in Sections 4 and 5 of the report, but the 5 main arguments for using many cameras can be summarized here:

1. Using more cameras with narrower views reduces overall lens mass ***and*** improves resolution;
2. Having separate views of "near" and "far" regions allows more precision from fewer pixels;
3. Using more views limits the effects of sail glare to smaller fractions of the total sail area.
4. Using 4 cameras in a cluster to replace a single camera with a fisheye lens is more reliable if it is properly designed (only one-fourth of image area is lost by a camera failure).

5. Fisheye lenses have much more barrel distortion (correctable, but better to avoid altogether) than normal camera lenses.

But greatly increasing the number of cameras has diminishing returns. Most of the benefits really seem to come from having ~4 views per quadrant (the baseline concept uses 1 near-field view plus 3 narrower views of different "far" parts of the quadrant). Splitting the coverage this way also allows much of the quadrant to still remain visible even if strong reflected glare wipes out one or two camera views.

The other major change in the design concept was to specialize the functions of the two viewing locations. The lower platform is the primary cluster, with 4 cameras for each quadrant. The upper platform is mainly an inspection platform, with 3 cameras bore-sighted together on a pan-tilt head. Our initial concept for the inspection camera used a zoom lens, but we think the platform will be lighter, cheaper, more robust, and photogrammetrically more stable if we use multiple fixed-focal-length lenses bore-sighted together, with different fields of view. The wider views provide context for the narrower views. The widest-view camera may cover a full quadrant or more, while the next narrower view might be slightly narrower than the "far" view cameras on the lower platform, and can be used with them for good depth perception of ~10% of the sail area at a time. The narrowest-view camera allows high-resolution imagery of seams, tears, boom details, and other regions of interest anywhere on the sail.

### 3.2.1 Key consequences of this design evolution

One consequence of the specialization of the two viewing platforms is that we have very good full-time observing of the whole sail (other than small regions lost to glare), but full multi-view 3D photogrammetric solutions for only ~10% of the sail area at a time. This would seem to be a considerable loss, but there is another key factor here: the sail components have a variety of constraints on their size and shape. If the booms are not buckled, they are of known length, and the only uncertainty then is the extent of bending and/or twisting. We measure that with an additional set of 4 narrow-view cameras, one near the base of each boom, aimed radially outward along the boom. They view targets and natural features along the length of the boom. This

geometry provides the highest photogrammetric sensitivity for measuring boom bending and twist, which both occur parallel to the imager plane.

Similarly, the distance between targets on the sail is set during assembly, and will only change by significant amounts if the sail sticks together, tears, or becomes very slack. All these phenomena should be observable. Hence we do not need full 3D solutions all the time over the whole sail: just good imagery, plus an ability to infer the 3D shape from the images and known constraints, plus a way to test our inferences locally by using the inspection cameras plus the main array for full 3D photogrammetry. Deriving the process of estimating 3D sail shape (and sail dynamics) from image data from lower-platform cameras only plus known constraints will be a key effort for the ODS team starting in Phase 2 of the project.

Increasing the number of cameras and the number of pixels per camera greatly increases the amount of raw data to be handled. As discussed later in Section 8.1, we found that we could get good images and centroid estimates even with high compression (~24:1). This means that despite a large increase in raw data per image set, we have less data to download than the initially planned raw data volume. Selective download can reduce this further.

We have baselined all monochrome ("black and white") cameras, except possibly for one camera on the pan-tilt platform. It may make sense for the narrowest-view camera to be either a color or multi-spectral camera, if it is determined that color features might provide indication of contamination, degradation, or other phenomena that would not be visible in monochrome views.

## *3.3 The final baseline ODS design*

Our original configuration (proposed, but then rejected, at the kickoff meeting) had both cameras and other sensors at each corner of the sail. The corner-mounted cameras have gone away, but other distributed sensors have remained. The final baseline ODS configuration shown

in Fig. 3-2 shows those sensors, the boom-view cameras, the main observing camera cluster, and the inspection pan-tilt head.

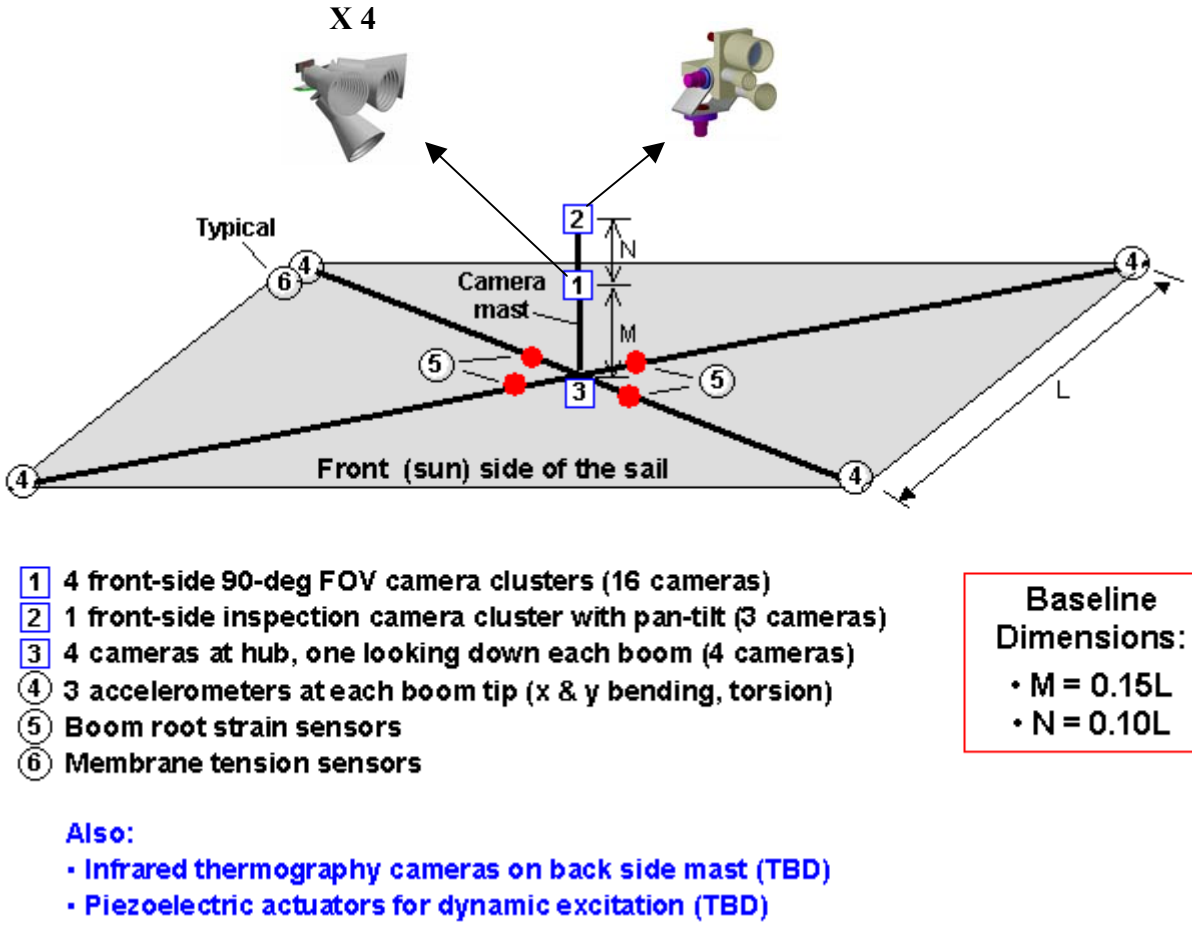


**Figure 3-2. Baseline ODS design**

## *3.4 Other solar sail optical diagnostic concepts considered*

### 3.4.1 Imaging from dedicated inspectors: free-flying, tethered, or "virtually tethered"

Early in the project we considered dedicated inspectors, either free-flying or tethered. One problem with a free-flying inspector is keeping up with the sail during the mission because of the continuous light-induced sail acceleration. The inspector delta-V should not be a problem for brief periods only, especially during deployment (when sail acceleration is less). We considered

using L'Garde's support package as a host platform, but it stays attached until deployment is complete, so the most useful images would be missed.

An interest in keeping the inspector nearby for later viewing opportunities led to questions about tethering the inspector. The problem here is that sail acceleration is low enough that it will be hard to ensure tether deployment and also prevent rebound. The added component mass, complexity, and risks of a tethered inspector, which needs active attitude control, reliable damping of tethered oscillations, and its own power supply, seemed to greatly exceed those of the short central camera mast needed for configuration #2. Delivering power through the tether may make it stiff enough to be more like a poorly designed mast than a tether. Hence we focused on cameras mounted on a relatively rigid mast.

We also considered one other concept: a "virtual tether." If a solar sail is in a twilight sun-synchronous LEO orbit, it can counteract drag by canting to the sun and wobbling as it goes around its orbit, to keep the leading edge somewhat sunward. The sail is also displaced away from the normal orbit plane (by ~400m for a 20 g/m$^2$ test sailcraft) by solar pressure. It can actively maneuver to stay roughly that distance from a free-falling inspector. That "inspector" could even be an existing imaging spacecraft in a suitable orbit, whose mission is non-critical enough that risks from a test of this nature would be acceptable. Pursuing this was beyond the scope of the ODS study, but may merit study if early flight tests in twilight orbits are considered.

### 3.4.2 Imaging from the ground or other spacecraft?

There is an interesting question of what one can learn by imaging a 40m solar sail from the ground. The best imaging would be either from nearly any equipment at a really good site, or from tracking telescopes with adaptive optics. AMOS (the Air Force Maui Optical Site) has both a good site and good optics. There is an annual AMOS users conference in the September timeframe. A web link to the conference is: http://www.maui.afmc.af.mil/conferences.html

Since what we are observing is bright, we can use short exposure times and modest apertures. This allows an imager to "freeze" turbulence. This gives distortion rather than smearing. Multiple images taken at high data rates may allow deconvolution of the turbulence.

It may also be possible to get imaging by orbiting assets on a non-interference basis. But reflecting huge amounts of light toward them might cause problems with their sensors.

It is possible that the solar sail membranes will be quite wrinkled even a considerable time after deployment. High-speed images from a row of imagers on the ground (every few miles, for 50 miles or so) might be quite useful in determining the "light map" even if the imagers can't resolve any details of the sail.

### 3.4.3 Imaging of other solar sail tests

The Znamya-2 solar sail deployment test occurred in 1993. A 20-meter thin film structure was deployed from the Progress M-15 spacecraft using centrifugal force. Deployment was done after Progress left Mir, but while it was still nearby. Cosmonauts on Mir imaged the experiment using available equipment. Figure 3-3 shows two web images of the Znamya in space.

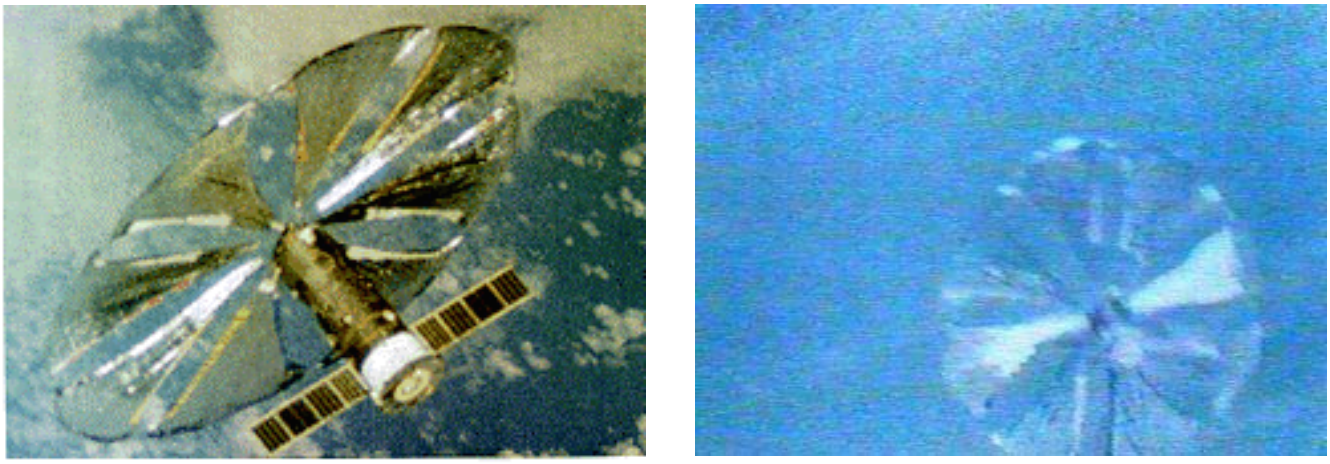

**Figure 3-3. Images of 20-meter Znamya-2 sail after deployment, taken from Mir**

The Planetary Society's Cosmos 1 solar sail flight experiment will have a small optical diagnostics system. The planned camera views are shown in Fig. 3-4.

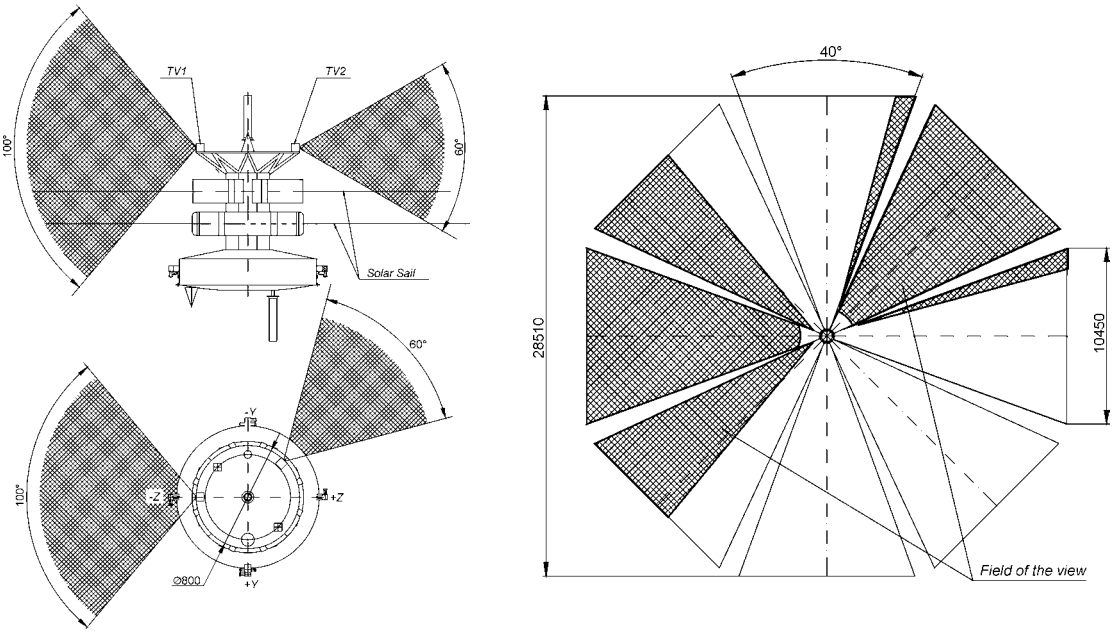


**Figure 3-4. Planned camera views in Planetary Society's Cosmos 1 solar sail flight test**

## *3.5 Some open issues on ODS design*

### 3.5.1 Integrating sun and/or star-tracking cameras into ODS?

If there is a need to determine the sail thrust vector very accurately based on sail orientation data, we may need a sun and/or star camera co-mounted with the main ODS camera cluster. We cannot determine the orientation of the sail in inertial space without knowing the ODS cluster's inertial orientation. Mounting star trackers elsewhere limits ODS inertial accuracy to the accuracy of our estimate of bending between the cluster and the star tracker. The main drawback for this star tracker location is that a much better lens shade is needed: both the sun and the sail limit the star views. A final decision need not be made now, because we can use additional imagers of the same kind we plan to use, but with more suitable lenses, lens shades, and software.

### 3.5.2 Should the distributed non-optical sensors be a part of ODS?

The ODS team may possibly have a better grasp of what sensors are most useful to complement the imaging than the solar sail developers currently do. In addition, we may use anomalies detected by those sensors to trigger retention of imaging data that will otherwise be overwritten, and we may make more use of that data in combination with the imaging data (for model verification) than the sail developers do. So we have a vested interest in the nature and quality of that data. Furthermore, there is one ODS team and there are currently two sail contractors, so having the ODS team take responsibility for this is perhaps a more efficient use of limited funding.

But when it comes time to actually integrate a suite of sensors into a single flight sail design, it is more appropriate to have the ODS team play an advisory role, and give the sail contractor full responsibility to procure, integrate, and test distributed non-optical sensors and their signal conditioning, power supply, and data links. Integration seems likely to be both the costliest and the riskiest part of this effort, so it may be reasonable for the sail developer to take the lead. Both sail designs may have some other electronics and wiring out to the ends of the booms, so this effort would not be entirely unrelated to their current tasks. A final decision is not needed now, but it may be worth consideration as part of the overall program planning for solar sails.

# Section 4
# Lighting and Target Design

## *4.1 Lighting: Effects of lighting and glint on camera design & performance*

A significant issue for ODS design is reflected glare and glint from the sail. In most cases, at least one imager will view an intense specular reflection of the sun. Over much of the rest of the sail, wrinkles and creases can cause local specular reflections to the imagers. The width of each glinting feature as seen by an imager will often be <<1 pixel, so the brightness recorded by the imager will be far less than that of the light source. But full glare from the sun can be ~60,000X brighter than a target, while the diffuse reflection from a non-glinting sail is only ~2% as bright as a target. So even "micro-glint" can impede image analysis, either by generating false targets or by throwing off centroid position estimates of actual targets.

ODS bears some similarity to at least three other types of fairly common optical tasks: conventional photogrammetry, startracking, and finding an adversary approaching from the direction of the sun. But the overall task is quite different from any one of those three tasks.

The rest of this section discusses the problems resulting from the extremely wide range of potential "optical noise" or "stray light," in order of decreasing light intensity, as follows:

- Potential permanent sensor damage from focused sunlight
- Partial or total loss of useful imaging when glare is too strong
- Difficulty finding & centroiding targets and other features where glint is highly variable
- Difficulty in evaluating long-term changes in diffuse reflectivity if glint is significant

And there is also one positive aspect of glint: glint variations may have diagnostic utility.

Figure 4-1 illustrates the basis of the glare problem. Clearly, when a highly reflective solar sail flies at an angle to the sun's rays, the ODS cameras on a sun-side mast will see bright specular reflections from somewhere on the side of the sail that is closer to the sun. At greater inclination angles, the bright spot migrates outboard but still occurs somewhere on the sail except at the steepest inclination angles. Less-intense light scattering towards the cameras also occurs from elsewhere on the sail, even when the sail is perpendicular to the incoming light. Of course, normal billowing (and local scalloping in the L'Garde sail design) of the membranes will affect this simplified behavior, causing the effects to shift spatially, but they will still occur.

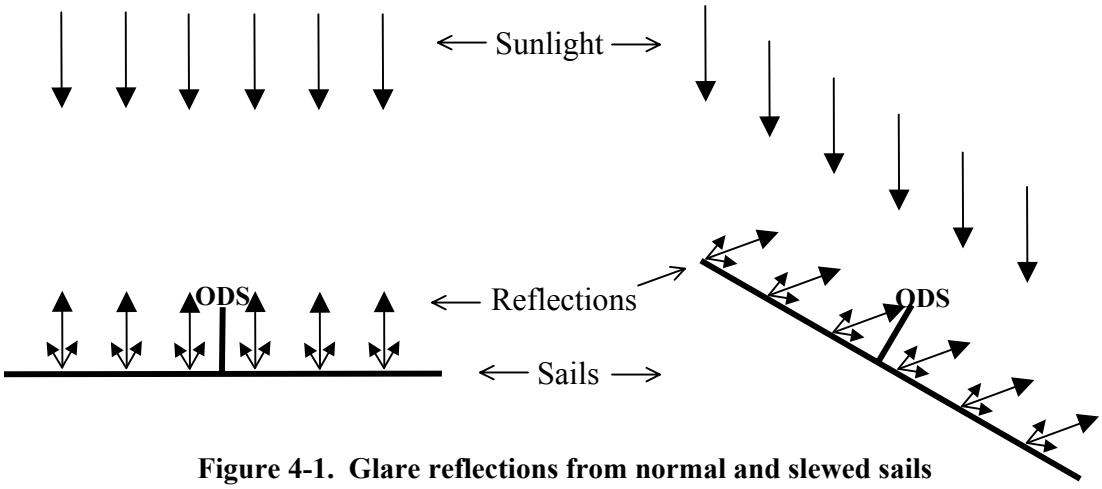


**Figure 4-1. Glare reflections from normal and slewed sails**

4.1.1 Damage from focused sunlight

The brightness of the specular reflection of the sun will be ~85% that of full sunlight, due to the imperfect specular reflectivity of the membrane. However, the sail will generally have some local curvature. If the membrane is concave in the region of the specular reflection, the "sunspot" focused onto the imager may be larger and may involve several times more energy than in a direct image of the sun through the same imager lens. The realistic worst-case ratio is not known, but is likely to be "at least several."

One imager supplier (FillFactory) says that their STAR250 and STAR1000 imagers will not be damaged by focused sunlight except by direct overheating sufficient to cause local chip damage. Rough calculations suggest that this should not be a problem unless the local sail

curvature provides high concentration. If this is a concern, we can use smaller lens apertures. But beyond f/4 to f/5.6, lens resolution may be degraded too much.

Another option is an infrared (IR) cutoff filter. This eliminates half the energy, but less than half the signal. It also improves resolution, for several reasons. One is that IR photons have the longest wavelengths and hence are hardest to focus to a small spot. Perhaps more importantly, an IR cutoff filter will also eliminate most "wandering photoelectrons." Most IR photons are absorbed deeper in the chip and can travel further before being captured by a pixel photodiode on the surface. Eliminating the IR-generated "wandering photoelectrons" can improve image resolution. It may also allow more of the overall desired level of smearing to be provided by the optics. This allows use of smaller and simpler lenses. A narrower-cut filter (perhaps green only) can improve the ratio of signal to heat input even more. It will also simplify lens color correction, further easing the requirements on the optics. Easing the requirements on the optics may in turn allow smaller lens shades to be used, reducing the size and mass of each ODS camera cluster.

### 4.1.2 Glare-induced degradation of image quality

When reflected sunlight falls on an imager, or even just on its lens, the images will have artifacts at various locations from multiple specular reflections off lens surfaces. There will also be a diffuse sheen from light that bounces off imperfectly black matte surfaces onto the image. Using 4 imagers per quadrant, each with its own lens and lens shade, will generally limit the resulting image degradation to only 1-3 images of 16 total. Fewer images will be affected on average if image coverage overlaps less. This conflicts with a preferred 10-20% image overlap for photogrammetry, and will require trades later as a part of detailed ODS design.

The high glare brightness vs. target and sail brightness make stray light suppression critical. Good lens shades will be essential. Also, narrow-pass filters (e.g. green only) allow anti-reflection lens coatings to perform better. Robert Breault (see www.breault.com) has described a basic strategy for stray light suppression in an elegant 4-step sequence:

1. List all surfaces that if lit can scatter light onto the detector.

2. List all surfaces that can be directly illuminated by undesired sources.
3. Eliminate any surfaces that are on both lists: that is the key issue.
4. After that is done, minimize the amount of light that can get between those lists.

Breault also says that looking for a "better black" is literally the last thing you should do in stray light control. A very poor black might be ~3% reflective, and a very good black ~0.6%. That means that having 3 bounces off bad coatings is better than 2 bounces off very good coatings. And very good coatings can introduce other problems. For example, Martin Black (now Equinox Interscience's Deep Space Black) is a very porous black anodize. The porosity helps provide multiple bounces locally, but it also attracts and snags dust and other contaminants. And it is not compatible with knife edges--because forming it rounds any edges and then forms a very open foam around those edges. So maybe a knife-edge design that is less black but smooth enough to keep clean will end up being better by the time it is launched and deployed. For more detail on stray light control and black surfaces, see Refs. 4-1 to 4-3.

In low earth orbit, reflections of clouds off a sail can cause problems, because they will often be roughly as bright as sunlit matte white targets. The earth view factor can exceed 30%, and much of that may be covered with clouds, so sail tests in low earth orbit may result in target-recognition problems more of the time than do solar sail missions beyond low orbit.

### 4.1.3 Glint issues with sails at low tension

"Glint" is here used to refer to specular reflection from creases, wrinkles or other regions smaller than a pixel in at least one direction. This can result in pixel brightnesses anywhere in the ~3:000:000:1 brightness range between the full intensity of a specular reflection and the ~2% diffuse reflectance of the sail. Glint should not be a serious problem if the film is under enough biaxial tension to remove stowage creases and avoid the wrinkles which occur with uniaxial tension. In "suitably tensioned" sails, seam and edge imperfections may be the major source of glint, and targets might be kept far enough away from such features to prevent problems.

But if the sail membrane tension remains low during and after deployment, creases from stowage may never fully straighten out. This may cause glint to be both high and variable across

the sail. It seems unlikely that ultra-thin membranes will form creases only at the intended folds when large quadrants are folded. Pleats will also form in random locations, especially when the folded sail is folded again at right angles to the initial folds. If some of these pleats pass close to targets, they may result in residual creases and glint that induce target centroiding errors.

In addition, simple tests on samples of aluminized 1.4 micron Mylar® film showed that unfolding it at very low biaxial tension created complicated puckers in small regions. Membrane tensions well above 1 psi seem necessary to remove the puckers. For films like aluminized Mylar® or CP1 (with specific gravities near 1.4), a tension of 1 psi occurs 0.5 m or 20" above the bottom of a hanging sample of film. Hence one cannot test samples much larger than this without applying tensions far higher than 1 psi. If the film is supported in "trampoline" mode, gravity self-loads scale with the radius of curvature. They are ~1 psi in each direction per meter of local radius of surface curvature. Hence on earth, only small film samples can be handled at low enough tensions to be representative of flight conditions.

Earth-based tests of far larger membranes necessarily apply far higher membrane tensions than the ~1 psi biaxial tension planned in orbit. Even static "trampoline" support of large membranes will apply far higher loads than expected in orbit. For example, if a quadrant 10 meters across the diagonal is supported at the corners under low enough tension to sag ~0.5 m in the middle, then the radius of curvature in the middle is ~30 m. The weight of the film will impose a tension of ~30 psi in each direction. One could provide operational tensions on this scale in flight sails, but that would increase the required boom strength and stiffness. And such tensions would assist tear propagation in the membrane. This would require the sail membranes to include some form of rip-stop network to prevent propagation of tears.

### 4.1.4 Effects of glint on optimum level of image defocus

The optimum level of image smearing for best centroiding is a function of the pixel-to-pixel noise level in the image. If noise is low, then the best centroiding should use significant, multi-pixel defocus (smearing). But if pixel-to-pixel noise level is high, as it may be, then centroiding errors will be lower if centroid calculations use fewer pixels (with shorter "moment arms"). The optimum amount of smearing may be much less than normally used in either photogrammetry or

startracking. This in turn has a bearing on lens design and filter selection. As noted earlier, an IR cutoff or narrow-band visible filter can reduce the number of wandering photoelectrons and the difficulty of providing a given image resolution. On the other hand, most suitable imager chips have significant variations in light sensitivity across each pixel. This results in centroiding artifacts if smearing is too low. With new small-format sensors having pixel pitches in the 3-8 micron range, and medium-speed lenses (~f/4-5.6), it may be harder to limit the smearing to the level desired over the whole image than to ensure that there is enough smearing.

## *4.2 Lighting trades for Plum Brook or other large-scale ODS tests*

During Phase 1 we investigated the implications of lighting at the 30m Plum Brook vacuum chamber, where it was originally intended to test ODS on 20m prototype solar sails in 2005. Recently, we have learned that this ODS testing at Plum Brook **has been cancelled**. However, most of the results are relevant to other large-scale ODS/sail tests that may be done elsewhere. The issues and potential costs are significant if we want to obtain not just useful data on sail dynamics, but also realistic images. The main topics are brightness, flash vs continuous illumination, the spectrum, number, size, and positioning of the lights, and the value of black backdrops under and around the sail.

### 4.2.1 Brightness

We don't need and can't afford one-sun brightness (~100,000 lux), but we want "adequate" lighting for ~5 Hz frame rate images. Assume the exposure time for each image is the full 0.2 second. In orbit, we can use ~f/4 lenses and still have millisecond duration exposures. (Lenses much slower than f/4 would probably have worse resolution due to diffraction.) At Plum Brook, using faster lenses (f/1.4 to f/2) and 0.2-second exposures allows much dimmer lights. We also have the constraint that the lighting must be adequate for ground diagnostics using normal video cameras.

We don't need to fill the “pixel light buckets" but if we don't fill them some reasonable fraction of the way full, then shot noise starts to limit centroiding accuracy. With a PB-0300

CMOS sensor, 0.2-second exposure, and f/1.4 lenses, 100 lux lighting should fill the pixel buckets for normally lit bright white diffuse surfaces. On the other hand, "glare" surfaces can be far brighter than white. We would not be able to distinguish white targets from glare and glint if white surfaces filled the buckets. It might make sense for bright white to fill the buckets <1/2 full, so we can more easily distinguish glare from white targets. Then we might be able to get by with 50 lux lighting, or slower lenses than f/1.4.

### 4.2.2 Continuous vs flash illumination

Flash illumination looks considerably more cumbersome and expensive to realize, especially with multiple light sources (which we plan to have to see the effects of various lighting angles). The main value of flash is for synchronized exposure of all pixels on all imagers, despite the rolling focal plane shutters that are on most of them. This should not be an issue, because we think we can tolerate the small top-to-bottom delays (which can be a modest fraction of the exposure time). In addition, we can synchronize different imagers by periodically turning the light on and off. Flash lighting would also constrain the ground diagnostic imaging, which probably wants to be straight video. Both in orbit and on the ground, we can centroid based on single images. Then we can use this small dataset to compute a "simultaneous centroid" for each target, by adjusting the positions some small fraction of the time between exposures A and B, based on the row centroid (and hence exposure time offset) of each target.

### 4.2.3 Number of light source positions

It seems very expensive to try to collimate light before it hits a 20 m sail in large-scale ground tests. If we use a centered light source, the only part of the sail that will look like it would with the sail normal to the sun is the center. Outboard parts of the sail will look as they would look if tilted somewhat away from the sun, because of divergence of the light from the central source. We need to be able to switch to at least one off-axis light source, high up on the sidewall of the chamber. This would let us see what things look like on a sail quadrant that tips toward the sun. We may also want to put 2 lights against the wall halfway between two booms, perhaps 5 and 10m above the sail. Parts of the closest quadrant would then look as they would look at larger tilt angles to the sun. Such lighting would be strongly variable between the near side and

the far side. The near side would probably be of more interest since it would have more glare problems, which we need to evaluate to decide how much lens shading is needed. An alternative is a single movable light source, but position reproducibility might be a problem.

#### 4.2.4 Light spectrum

We can use full-spectrum lighting of some type, or low-pressure sodium. Low-pressure sodium would eliminate chromatic smearing (this would be useful given the larger-aperture lenses we may need at Plum Brook). On the other hand, it seems poor in many other respects, including any color ground diagnostic imagers and any test documentation pictures we might want. So we will tentatively assume some form of full-spectrum lighting (incandescent, metal halide, or other).

#### 4.2.5 Size and kind of each light source

The sun subtends 1/107 radian at 1 AU. If the light is ~25m away, a sun-like source would be 23 cm in diameter. We do not think we need anything that small, but on the other hand, we think we do not want anything far larger than that if we can avoid it. Much larger sources would decrease the brightness of glint, and hence perhaps mislead us about how much we should be concerned about glare from wrinkles and creases. But if there are any electronics cables and/or support lines suspended over the sail, we would like the light source illuminating each spot on the sail to be much larger in diameter than the cable width, so these cables don't cast noticeable shadows. This is less of an issue if glint-related testing is done separately, on small samples.

This suggests that we may want one very bright and moderately compact light, rather than an array of 8-foot fluorescent tubes. And we want to focus as much of its output onto the square sail as possible, and as uniformly as possible. We would also like to absorb everything else before it reaches the sail and has a chance to scatter into the camera. One option that might work is a light source for a projector of some type: both the lamp and its cold mirror and condensers.

Another option is a single metal halide lamp with appropriate optics. Metal halide lamps have a good color balance, which may be useful for the diagnostic videos and documentation

photos. There are commercially available 1000W lamps that start out with 110,000 lumens. If we can deliver half of that to a 20x20m square sail area, the resulting light level is ~140 lux. Any other form of wide-spectrum lighting may generate far more waste heat for the same amount of light provided. For example, we would need about 5kW of incandescent lighting to equal 1kW of metal halide. The actual light source for metal halide is very small, so we could reflect and focus it efficiently (as we could with incandescent lighting) to cover the sail. But we don't know all the details, nor the complications that will come from putting such lamps in cooled pressurized boxes in vacuum. But for tests not done in vacuum, metal halide lamps may be very workable due to their high intensity, compact size, good color balance, and modest heat rejection requirements for any given light output.

Note that during setup, having multiple bright lights at different locations will be useful because the deep shadows from one source could be problematic. We might also put up the black backdrops fairly late in the installation process (after readying them early).

### 4.2.6 Black backdrops

There is one other important lighting-related item. We need black backdrops to obtain representative images: at least black polyethylene film, with a reflectance of ~3%, but preferably flocked black fabric, with ~0.6% reflectance. We want it on the chamber sidewalls, from the floor to at least ~15m up. It will make a large difference in the utility and representativeness of our images. It should also make any photos for distribution both more realistic and more dramatic. Black backdrops do reduce the lighting level by absorbing scattered light. But we need to minimize scattered light.

We also need the floor under the sail to be black. One reason is that it will get most of the light early in deployment, during boom deployment and the first part of sail deployment. Scatter off it will make the images of the boom less representative. The other thing is that a very black backdrop in the images (at least under the booms) will make images of the open-construction ABLE boom and L'Garde truss structure more representative. The boom itself is nearly black (graphite composite, except for any targets and non-black fittings). So to see what the boom would look like, given nearby glare from the sail, we need a background significantly blacker

than the graphite-fiber composite boom elements. Hence we may need strips of flocked black fabric at least under the booms, and black polyethylene film (or conductive-loaded black polyimide) elsewhere.

#### 4.2.7 Conclusions

Tentative recommendations for illumination at Plum Brook are as follows:

| | |
|---|---|
| Steady vs flash | Steady |
| Brightness: | >100 lux normal lighting on sail? |
| Spectrum | full color (metal halide?) |
| Light positions | center plus edge (as high as possible), plus 1-2 partway up wall |
| Light size | 20-30 cm apparent source? |
| Black backdrops | Yes, on sidewalls & floor; black poly ok; flocked fabric better. |

## *4.3 Targets and Targetless Concepts and Issues*

Original ODS ground rules required that we be able to do some optical diagnostics without dedicated targets, and that we recommend target concepts to improve on this. The key issue affecting the visibility of targets in images is the uncertain "optical noise" of glare and glint from the sail, discussed in Section 4.1.

#### 4.3.1 Targetless imaging

There are at least 3 "inherent optical targets" in the current sail designs:

1. The edges of the membrane
2. The boom structure
3. Construction seams

Unfortunately, these features are all linear rather than point targets. As a result, there is a reduced dimensionality to any shape solutions derived from them, except where visible structural

details (as there are in both the ABLE and L'Garde booms) indicate specific points along the line feature. Imperfections in the seams generate glinty scatter, but the glinting locations change with the lighting angle. Therefore it may not be feasible to use seam imagery for 2D location data.

There are at least 3 other forms of useful data in images of the sail itself. One is that any serious boom or membrane failures should be visible. Tears in the membrane that allow a view of the gap should be visible, because the sail's diffuse reflectivity (1-2%) is far brighter than the space background. Any large boom or membrane deviations from expected shape will generally involve buckling or other visible features. If such features are visible, the primary role of ODS will be helping us understand them and their cause; photogrammetric accuracy will be of secondary importance. If such features are not present, then we can reasonably assume the booms and sail are intact. We can use that assumption to constrain interpretations of all other visible features. In particular, we can infer that deviations from the expected target positions on intact tensioned sail quadrants viewed at an angle are due mostly to out-of-plane displacement. Once we estimate those displacements we can estimate their necessary in-plane effects (due to cosine effects) and iteratively refine the overall estimate of both in-plane and out-of-plane deformations of the sail.

A second form of useful data is that the sail's diffuse reflectivity may significantly deviate from Lambertian with near-normal illumination and near-grazing views. This needs testing with samples of representatively handled sail membrane. If this is the case, then we may be able to infer something about the radial component of membrane slope from brightness variations over the sail. But such variations can also be due to glint. Hence we may need to limit use of this technique to areas with low glint. (Glint can be estimated both from significant excess background brightness and also from spiky variations in brightness as the local slope changes.)

A third form of useful data is glint statistics themselves: higher glint at larger viewing angles suggests increased creasing and wrinkling. Wrinkling indicates current uniaxial tension, while creases can provide indications of both current tension and peak tension since deployment.

### 4.3.2 Target shape

For intentionally added targets, we can consider circles and ellipses, other solid-colored shapes, and more complicated "coded" targets. Coded targets allow automated unique identification of each target by software. But coded targets have to be quite large to cover enough pixels to allow identification. This may not be critical because we may be able to automate target identification from the overall pattern of targets, at least for fully deployed un-torn sails, especially if targets are laid out in a simple pattern. Automated identification may be hard during deployment or if a serious anomaly occurs, but such cases can be dealt with manually (at some cost and delay). Square targets or other shapes with sharp corners may impose local stress concentrations on the sail membrane, so circles or ellipses are preferable. Automated target recognition may be easier with circles than with ellipses, but the highly oblique view of distant targets requires properly oriented high-aspect-ratio elliptical targets to generate a circular image. And even then target images will be elliptical whenever the membrane deviates from the expected shape, or if the production technique does not easily lend itself to appropriately orienting each elliptical target. A more valuable clue for both recognizing and uniquely identifying individual targets may be the overall pattern they make.

One further target shape issue is whether the target should have uniform brightness or a Gaussian brightness distribution (or at least a feathered edge). Hard-edged targets that modify the membrane properties in any way are more likely to cause local glint at the edge if there is any buildup of slack there. (This was the case in the spray painted targets provided at the Phase 1 final review.) Glint at the edge of the target can cause an error in centroiding estimates. On the other hand, it may be easier to obtain a single uniform level of target brightness than to smoothly vary it as desired. We can probably deal with either hard- or soft-edged targets, but we should characterize their mechanical and optical properties before making a final decision.

### 4.3.3 Target brightness

White targets may be ~50X brighter than the diffuse background brightness of the sail membrane, but only ~1/60,000 as bright as a full specular reflection of sunlight off the sail. And there will nearly always be such an area on the sail. Around that region, there will be a region

with a wide range of average brightnesses due to glint covering some fraction of a pixel. The brightness of those pixels can be anywhere between ~60,000X and 2% of the target brightness.

One can make targets "brighter than white" over a certain range of lighting and viewing directions by blazing them somewhat like a diffraction grating, but it may be hard to do that over the full range of lighting and viewing angles that are required while also keeping the brightness uniform (to minimize centroiding errors) and predictable (to ease distinguishing targets from glint). Other options are colored or fluorescent targets. But one cannot make the target bright enough in any wavelength region to outshine high glint or direct glare, and such targets are likely to run warmer than the rest of the sail. Overall, it seems both easier and more useful to try for uniform and stable matte white targets. SRS Technologies has demonstrated the capability to apply ultra-lightweight diffuse white targets to their CP1 membrane film during manufacture, and simple experiments during Phase 1 showed that ~2 micron thick spray painted targets can be applied to aluminized Mylar®.

Matte white targets will be far brighter than the sail membrane over most of its area, and much dimmer over a very small area. In a halo around the glare spot (which is generally closer to the center of the sail than to the edge), one might even distinguish a target from a comparably bright region of sail by its brightness uniformity (if nearby glare doesn't overwhelm the image).


**Figure 4-2. Sample 1.25" dia. target disks**

**Figure 4-3. Target on sail**

Figures 4-2 and 4-3 show prototype targets before and after installation on a preliminary CP1 sail. This particular membrane has been folded and relocated several times, which caused the dense permanent creasing visible in Fig. 4-3. Note that the sail glint in the photograph ranges from being significantly dimmer to being much brighter than the target itself. The target in Fig. 4-3 appears grayer than it actually is (it is, in fact, bright white) because the autoexposure electronics in the camera have incorrectly assumed an average gray scale for the picture of 18%.

### 4.3.4 Target size

Photogrammetric target centroiding accuracy is best if the target is at least several pixels high and wide (5-10 pixels is typically optimal) and is surrounded by a several pixel wide, uniformly bright annulus that is either much brighter or much darker than the target. We cannot ensure this with a solar sail. In the near field, the target can be several pixels across, but glare and glint may often be highly variable around the target. In the far field, the oblique view may greatly reduce glint and glint variability. We may be able to have targets several pixels wide, but ~5:1 foreshortening from the view angle may make it hard to justify targets >>1 pixel high. The billow will improve the view of far-corner targets, but any flapping could make them periodically considerably less visible.

But we may not need the farthest targets to subtend several pixels in height. Even the image of an ideal point target will usually spread over several pixels due to pixellation, lens limitations, and wandering photoelectrons. (In fact, limited smearing can aid centroiding.) The real far-field question is how many pixels high the target image must be to generate enough photoelectrons for the software to find the target and compute its centroid accurately enough. Even small sunlit targets should provide plenty of photons; the real issue is the background optical noise from sail glint.

There is a clear tradeoff between required target size and overall pixel count. If we use four times as many pixels to image a region of sail, then each target will cover as many pixels even if it has only half the linear dimensions and one-fourth the area. And the centroiding errors in pixels can be comparable, so having more pixels and smaller targets will reduce RMS centroiding errors by roughly half. Hence the final selection of target size and overall pixel

count (number per imager times number of imagers) should be made as a combined trade study to provide some desired accuracy at minimum total cost (i.e., marginal target cost vs marginal imaging system cost). One option is to use several different target sizes, with larger ones used either for the outboard strips or at least for the targets in the far corners of each quadrant.

One other size factor is that if the target brightness cannot be kept uniform, then smaller targets may reduce errors since brightness variations can themselves induce centroiding errors. But if these errors can be characterized in advance, they can be accounted for. And they should be fairly fixed, so errors will have more effect on estimates of sail static shape than on sail dynamics.

#### 4.3.5 Target spacing and pattern

It may be worth varying the target spacing in some distinctive way that allows unique target identification from target spacing. But this makes intuitive shape estimation more difficult because the image "looks" noisier. Several intermediate options may be worth considering. One is uniform spacing plus an extra target at a different location on each row for an independent check on target identification. Another option is uniform spacing in one direction and non-uniform spacing in the other. It may be easier to fabricate and fold the targets and to visually interpret the image if the targets run down the middle of each strip (i.e., uniform spacing normal to the outer edge of the sail quadrant), but with non-uniform spacing along the strip length.

Another option is simply a uniform grid (which is easier to apply and to visually interpret) with a smart enough routine to identify the overall pattern, or to recognize that it cannot do so confidently. Or one could lay down a nominally regular pattern but make more effort to measure the actual target positions than to place them precisely. (This can be done with a high-end photogrammetry system.) This may introduce a pattern of random errors large enough to aid target verification, while not large enough to be visually misleading.

### 4.3.6 Number of targets

The more targets there are, the more modes of vibration we will be able to discriminate (if their vibration amplitude is large enough to be sensed). But one might also, by modeling and analysis, select a suite of target positions that allow robust separation of many modes using both spatial and temporal variations, without using large numbers of targets. This may be compatible with a philosophy of variable along-strip spacing and uniform cross-strip spacing. Also, the edges of each quadrant can serve as additional target features, though of reduced dimensionality. Because of this reduced dimensionality, we still need to have point-like (or possibly crossing-line) targets near the edge. But we can use the observed position of the edges of the quadrant to constrain the overall solution.

The number of targets may be driven mostly by a compromise between poor diagnostics with too few targets, and excessive hand labor and/or risk of damage during sail fabrication if there are too many targets. By comparison, it seems less likely that any analysis will be able to conclude that the first N modes ***must*** be discriminated but that all higher modes can be ignored.

Another factor that affects both the pattern and the overall number of targets is that the targets probably need to be away from the folds in the sail, and preferably far away from them. This may help keep targets from affecting the unfolding (if they affect film stiffness at all), as well as reducing local "glint gradients" around the targets that could bias centroid estimation

### 4.3.7 Optical targets for booms

The 4 boom-view cameras should see a boom-and-target view like that shown in Fig. 4-4, looking out through an ABLE boom. A similar pattern of boom elements and targets should be feasible on the L'Garde booms if the cameras look through the "V" truss structure (the spreader system) on the sunlit side of the booms. The targets can be either sunlit if they are tilted for a good combination of lighting and visibility, or they can be retroreflective if the boom-

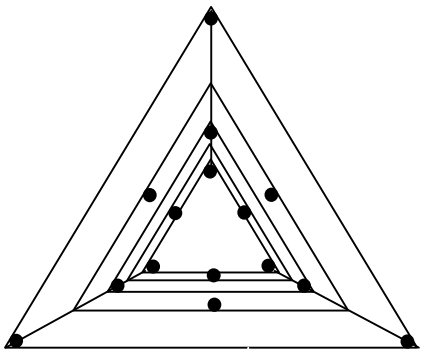

**Figure 4-4. ABLE boom & targets**

view cameras have LEDs or other light sources adjacent to their lenses.

## *4.4 Recommendations*

### 4.4.1 Implications of glare and glint on design, and the need for membrane optical tests

When we choose an imaging chip for use in flight, one key factor is how sensitive to damage it is from focused sunlight, and whether it requires some sort of mechanical shutter and controls to keep it from seeing the sun. Adding shutters may drive ODS mass and risk of component failure, so such an option should not be considered lightly. Glare and glint also drive lens shade, lens, and camera housing design, and need early and adequate attention. They are also critical to target detection and centroiding. Section 11 discusses this topic in more detail and recommends near-term tests on suitably handled and lit membranes. These tests are best done on small folded and unfolded samples hanging under low tension. The tests can be done independently of the larger-scale ODS/sail tests and much earlier than those tests.

### 4.4.2 Target design recommendations

For both the AEC-ABLE and L'Garde sails, matte-white round or elliptical targets appear best. It is not yet clear how large they must be to ensure visibility and accurate centroiding. This should become clearer if the Phase 2 effort includes tests of sail glare and glint statistics as recommended in Section 4.4.1.

For the ABLE/SRS sail, in which the targets may be applied in a roll-to-roll process, it might be best to apply targets down the middle of each strip, or on every $N^{th}$ strip. It may be costly to customize target elongation and orientation from target to target, or spacing from strip to strip, but it may be feasible to use several different target sizes and/or degrees of elliptical elongation for different subsets of the strips. In the case of the L'Garde sail, where the targets may be spray painted on during assembly of each quadrant, local variations in the target size, shape, orientation, and spacing may be more feasible simply by changing the spray paint mask.

Finally, it is not yet clear how many targets are needed, but 100-150 per quadrant currently appears to be acceptable to both the sail developers and to the ODS team. We also need to ensure that the positioning of targets allows the overlap regions between adjacent camera views to have enough common targets for good photogrammetric registration of the adjacent images.

## *4.5 References*


4-1. Stray Radiation V, 18-20 August 1986, San Diego, CA; Robert P. Breault, chair/editor; SPIE Vol. 675. Breault's recommended stray light analysis procedure is on page 11. Also see SPIE volumes 511, 967, 1331, 1753, and 2260, all on the same subject, all with Breault as editor.

4-2. Equinox Interscience's Deep Sky Black coatings, at: www.eisci.com/deepsky.html

4-3. Optical Characterization of Black Appliques, K.A. Snail et al, Proc. SPIE, Vol. 2864, pp 465-474. The article is available online at: www.esli.com/downloads/SPIEArticle.pdf

# Section 5
# Camera Configuration and Design

A wide variety of issues contributed to our design decisions and/or recommendations on camera configuration and design. This chapter discusses these design issues and describes our recommended baseline camera configuration.

## *5.1 Factors that limit target centroiding accuracy*

### 5.1.1 Summary

One of the main design drivers for ODS is good accuracy in estimating the position in images of photogrammetry targets and other features of interest. Another important factor is good angular and brightness resolution of visual details so we can better see the condition of the sail. Good visual resolution conflicts somewhat with best centroid estimation because optimum centroiding can involve intentional smearing of point features over several pixels (but this can also be done on the ground with software). The low angular resolution and poor grayscale in the images of Znamya shown in Section 3.4.3 should reinforce the value of sharp images. The lists below indicate key design factors for the images and imagers.

Image characteristics

- Size, brightness, and brightness uniformity of targets or other features being imaged
- Optical noise from the sail within a few pixels of the feature being analyzed
- Bright glare from other regions that can reach that part of the imaging by scattering

Imager characteristics

- Pixel field of view (pixel pitch/lens focal length)
- Lens point spread function
- Imager point spread function and sensitivity map across each pixel

- Any system electrical noise that degrades the stability of the camera grayscale

### 5.1.2 Determination of pixel centroiding errors on an early-model CMOS imager

We had a concern about centroiding errors that might come from using active pixel CMOS imagers, which are known to have large local variations of light sensitivity across each pixel. This led us to do a simple test. Rather than precisely moving the camera or a point light-source from one image to another, we used a single image of a black/white edge running across the image at a slight angle. The camera was a Photobit PB-0300 8-bit VGA imaging chip (640x480). Its photodiodes cover only 20% of each pixel's area, but the peak quantum efficiency is ~25%. This means that other parts of the pixel contribute some photoelectrons. The lens was an f/1.3, 8.5mm lens, stopped down to ~f/4 after focusing. (The lens did not have marked f/stops.)

Post-processing started by taking the difference between vertically adjacent pixels. We selected a reference row by finding the highest positive difference between adjacent rows in each column, and offsetting that by 1 if the value in RefRow+1 was higher than that in RefRow-1. Then an edge centroid was computed using only 4 pixels: RefRow-2, RefRow-1, RefRow, and RefRow+1, by calculating the center of gravity of differenced pixel values in those 4 rows. This gave a list of 640 centroids, one per column in the image.

The next step was to find a smoothed local average centered on each column but not including it. This average used 10 columns on either side, with triangular weights. The difference between the smoothed local average and individual column values was only 0.08 pixel RMS.

In a real ODS image, one would compute vertical centroids of each target using perhaps 3-5 adjacent columns of pixels (depending on the width of the target). This should reduce the error by of order Sqrt(NCols). Including both row and column errors should increase the total centroid error by ~41%. Overall, ODS may do better or worse than this, depending on the actual imaging chip used, the lens quality and amount of defocus, the algorithm, etc. The point of this test was to see whether the intra-pixel sensitivity variations of active pixel CMOS imagers might severely

limit centroiding accuracy. It appears this will not be a problem, even with an extremely simple centroiding algorithm and an imaging chip that may be more susceptible to centroiding errors than many newer chips are.

## *5.2 Why we may need ~20 cameras, and what views they should have*

### 5.2.1 Do we really need 4 cameras per quadrant?

The baseline ODS design concept used a cluster of 4 stationary miniature cameras as shown in Fig. 5-1 to image each sail quadrant from the lower camera platform. Four medium-view-angle cameras need not weigh more than 1 wider-view camera with comparable angular resolution, because a single camera will require a much larger imager, lens, and lens shade. And a single camera will not be able to provide comparable glare rejection, and it may not be able to equal the lens performance of a cluster of smaller cameras. This section discusses these issues in more detail.

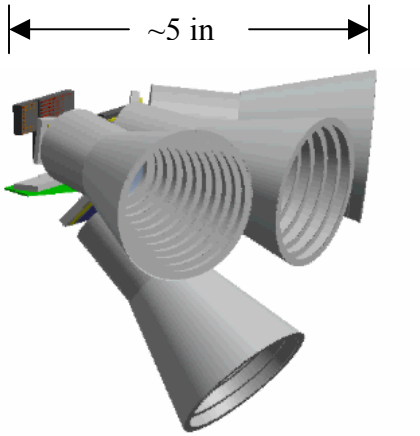


**Figure 5-1. Cluster Concept**

First, using many cameras allows us to have many lenses and lens shades. Then strong glare in one image need not blind the image of a whole quadrant, but just a fraction of the quadrant. Strong glare will generally occur in at least one quadrant, so going from 1 to 4 cameras per quadrant may reduce the typical “lost coverage” from ~25% to ~6% of the sail area. That also suggests that we may want to limit the overlap of adjacent images. Overlap means wider coverage, and hence wider "acceptance angles" for lens shades, and hence susceptibility to glare over a wider angle. On the other hand, modest overlap will allow viewing of more of a sail region whose main imager is blinded by glare, so this argument should not be overused.

Another argument for using several cameras per quadrant is that it lets us get by with fewer pixels overall, by using different lens focal lengths to compensate for different distances and view angle cosine effects. If we had only 1 wide or super-wide angle view per quadrant, most of the pixels would cover the nearfield, and we would need far more than 16 x 1.3MPixels (our current plan) for the same RMS error in estimated target positions. Centering the imager off the lens axis could also reduce variability of scale factor, but it requires far higher correction of off-axis lens errors. This would require much larger and heavier lenses and lens shades, and would not address the glare problem.

The arguments for multiple narrow-view cameras can also be used for a larger number of views than 4 per quadrant. But many of the benefits of many views come just from separating the views into near and far regions. Locating ODS on a central boom of modest height means that the near region covers most of the subtended solid angle of the sail, but only a small part of the total sail area. Glare will typically be far worse in some part of the near region than further away. This leads to the question of how many "far" views should be used per quadrant. The view of the far regions of a quadrant is a long, narrow, panoramic view, with a height of ~15-30$^{o}$ but a width of 90$^{o}$ (plus overlap). Most small-format imaging chips have 1:1, 4:5, or 3:4 aspect ratios, so we need at least 2 imagers to cover 90$^{o}$ of width while not wasting most of the image height, and 3 or 4 imagers to keep the average positional errors estimated from the far images comparable to those in near images. The final decision may hinge on the details of what views we should use, how many pixels we need overall, and on whether clusters of 4 rather than 5 cameras may simplify the structure of supporting electronics.

### 5.2.2 Degree of desired image overlap

The precision obtained from photogrammetry is due to the combination of rich image data and sophisticated processing. This can determine not just best-fit positions of different targets, but often also their relative locations, and sometimes even the lens distortions of the imagers used. Doing this requires viewing many of the same features from multiple angles. One of the desired photogrammetric processing procedures (known as relative orientation) requires at least 6, and preferably more, non-collinear targets to appear in adjacent images. Having triangular

overlap areas is best. Hence there may be reason for at least 10-20% overlap of adjacent images, and one tiling geometry may be better than another. The overall image tiling geometry sets the overlap geometry, but the amount of overlap can be adjusted as desired by varying the lens focal length and coverage for some or all of the views.

At the other extreme, a large overlap in ODS camera views will make glare a problem in more images. The best solution may be to provide enough overlap of adjacent images to allow good relative image registration, while trusting pre-flight data on lens distortion characteristics and the relative camera positions (but not orientations) of different imagers in a cluster or in the overall lower-platform ODS assembly of 16 cameras.

We want good geometric stability between imagers, and between each lens and its imaging chip. If handling, launch, and thermal cycling don't cause the imaging chip and lens elements to move (which we can check from common targets), then we can do long-term filtering of relative pointing estimates from targets in two adjacent views. If we want 1/10 pixel accuracy, and we have 5.2 micron pixels, we need to limit cumulative relative lens and imaging chip motion to <0.5 micron after ODS gets to orbit. Problems might occur for several reasons, including: ratcheting of clamped joints or failure of adhesive bonds after thermal cycling, potting compound dry out, or relaxation of a bulge in the imaging chip if air leaks out from the air gap in the sealed imaging chip package.

### 5.2.3 Camera view strategy: quadrant-centered, or boom-centered?

We have baselined a “quadrant-centered” cluster of 4 cameras per quadrant. But a boom-centered approach may also merit study. It aligns the diagonal of each wide-angle view with a boom, and covers the inner ~half of its length. For a given wide angle view angle, having the diagonals aligned with the booms covers the booms and sail further into deployment using only those 4 cameras than do geometries that don't align the far corners with the booms. This reduces the number of images needing to be captured and stored, or allows higher image capture data rates.

A boom-centered approach also better fits the "peaky" azimuthal distance variations to the far edge of the sail: it is >40% further away at the corners than in the middle of a quadrant. So ODS might use 15 mm lenses to view the corners, and a pair of 11 mm lenses to handle each far view region between corners. This gives higher magnification at the corner, whose targets are both further away and viewed more obliquely. This seems more efficient than using one wider-angle view centered on the quadrant, and two longer lenses, going from there out to the corner of each quadrant. If later analyses suggest that higher accuracy is desired in mid-quadrant, we may want to stay with a quadrant-centered cluster, but if equal accuracy is desired over the entire sail, or if higher accuracy is desired near the corners, boom-centered clusters may make more sense. This issue will be examined more in Phase 2.

## *5.3 Camera lenses*

ODS requirements on lens design are not extreme if we use 4 or more cameras for each quadrant and do not require imaging of the sail using low levels of artificial light during eclipse. We have plenty of photons and slow dynamics, so medium-speed lenses (~f/4-5.6) may be adequate. Significantly slower lenses could provide enough photons, but the small-pixel imagers that enable a small ODS require medium-speed lenses for good resolution. The size of a lens shade for a given effectiveness may scale with the diameter of the front lens element, if it is easier to reduce external than internal scattering. Hence it may make sense to use a lens with a fairly small front element and larger elements closer to the imager.

We can tolerate significant image geometric distortion (which is typically barrel distortion) as long as it remains stable through launch vibrations and camera thermal cycling. We may possibly be able to correct for distortion and even camera thermal expansion well enough by predictive analysis, while using actual pre-flight imaging tests to calibrate each camera for focal length, lens/imager misalignment, point spread function, and relative position. If so, then we can use common-target image data in space just to generate accurate camera aim estimates.

### 5.3.1 Commercial, modified commercial, or custom lenses?

Many compact medium-speed lenses have been developed for non-zoom megapixel electronic cameras with various imager formats. Some of these lenses appear quite suitable optically for ODS. But the ODS environment also poses non-optical demands on the lens. It is not yet clear whether we should use stock lenses without modification. For example, many lenses use one or more very thin elements. We need to ensure that the lens barrel is vented well enough that the fairly quick depressurization during launch does not impose excessive loads. Also, many optical glasses discolor when exposed to proton radiation at the intensities found in the van Allen belts, solar wind, or solar flares. This affects the front element most, which in turn shields the other lens elements to some extent. Ceria-doped glasses are tolerant of radiation, so it may make sense to either make the front element out of a ceria-doped glass or add a flat ceria-doped filter in front of the lens. Extensive ultraviolet (UV) exposure may also darken cements used to form cemented doublets. Here again, a ceria-doped element or filter may be useful, because ceria-doped glasses also absorb UV. In addition, some lenses apparently use compliant spacers that are compressed externally during final lens testing to "tune" the lens. If such spacers or other materials outgas onto lens surfaces, optical clarity can be significantly reduced. Finally, we must ensure that our lenses have acceptable focus shift and other changes with temperature, and stable properties after many thermal cycles, especially if one or more early solar sail tests occur in non-twilight earth orbits.

For initial ground tests, it appears feasible to use stock lenses developed for CMOS imagers, as long as they can tolerate a fairly slow depressurization. For flight, more development will be required, but the required development effort is very familiar to team member Tom Pollock and the optics group he works with at Texas A&M. Some companies have indicated a willingness to adapt stock lenses (such as adding a color filter or ceria-doped front element) for a reasonable lot charge. This may conceivably allow use of "modified stock lenses" for flight.

### 5.3.2 Flatness of field requirements

For the image to come to a focus in a plane, the lens must meet the Petzval condition:

$$n_1 f_1 + n_2 f_2 = 0$$

This can be achieved with a combination of positive and negative lenses. For multiple elements, it is more accurate to use the reciprocals. Then displacement of an image point at height $y_i$ from the paraxial image plane is (as shown on the web site www.wolfram.com):

$$\Delta x = \frac{y_1^2}{2} \sum_{j=1}^{m} \frac{1}{n_j f_j},$$

where the sum is over layers with indices of refraction $n_j$ and focal lengths $f_j$.

Flat field correction is important to ODS because it affects the uniformity of defocus across the image. We can tolerate modest variations in smearing over the image, but we do not want large variations. The minimum lens solution might be an achromatic lens to reduce spectral smearing, plus a negative element (perhaps adjacent to or even bonded to the front of the imager package) for improved focal-plane flattening. Larger numbers of elements can better null out coma and other errors over a wider field, and need not greatly increase lens mass or cost, especially if we can use or adapt a stock lens design. We could end up using a lens similar to that shown below:

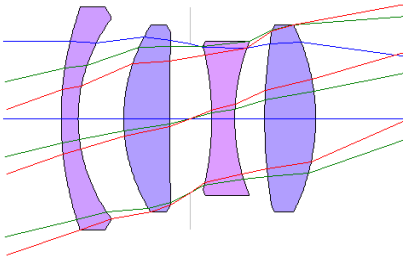

**Figure 5-2. 4 Element Lens and Ray Tracing**

### 5.3.3 Narrow-band filtering for improved resolution?

Since we have lots of photons in space, we can ease the lens requirements by filtering out everything except a modest spectral band, perhaps near 550 or 600 nm. This should ease chromatic and flat-field correction, and can eliminate most wandering photoelectrons (see below). Wavelengths near 550-600 nm are short enough to allow fairly good image resolution, but long enough for a strong signal (many photons and near-peak quantum efficiency). Long

wavelengths also have a lower rate of change of chromatic correction with wavelength than shorter wavelengths do.

### 5.3.4 Strawman lens specifications

- Stock C/CS-mount lenses will be specified if at all feasible.
- All lenses will have fixed aperture and fixed focal length.
- Telephoto on pan/tilt stage may require a focus motor; all other lenses are fixed focus.
- All structural components will be metal.
- Lubricants, if any, will be removed.
- All refractive elements will be glass.
- Front element or filter may be ceria-doped, if ODS environment requires it.
- Image plane may be tilted to achieve best focus at extreme edges of the sail.
- Cemented doublet elements are acceptable if optical epoxy resin is used in assembly.
- Spacing between elements at the element edge will be >=0.5mm (unless cemented).
- Primary optical criterion is the Modulation Transfer Function, MTF; secondary criterion is spot size.

## *5.4 Imaging chip options*

### 5.4.1 CCD vs CMOS imaging chips

There are two basic families of solid-state imagers to consider: CCDs and CMOS. Charge Coupled Devices (CCDs) are used in high-end imagers. They can have remarkably high quantum efficiency and remarkably low noise, but they degrade significantly when exposed to ionizing radiation. (In fact, they are often said to be the most "radiation soft" chips known.) An expected improvement in radiation hardness for space-capable imagers was the main reason for work on Complementary Metal-Oxide-Silicon (CMOS) imagers at JPL. This led to the formation of the Photobit company, which later became Micron Imaging. The commercial growth of CMOS imagers has been driven more by the higher degree of integration and lower mass-

production costs offered by CMOS chips, but the main feature of interest to us may be improved radiation hardness.

But CMOS imagers do have annoying idiosyncrasies. They have variable sensitivity across each pixel due to the row and column conductors and multiple active electrical elements in each pixel. But the tests described above in Section 5.1.2 with an early Photobit imager suggest that this variation need not seriously limit centroiding accuracy if we use a suitable amount of defocus (>1 pixel worth). CMOS imagers also have a higher noise floor than CCDs. That should not be an issue with ODS because we have so many photons that the major noise contribution for well-lit targets and other features will probably be shot noise, which is proportional to the square root of the number of photoelectrons in a pixel well. This is set by physics and can only be varied by using deeper wells. This requires larger pixels and hence larger imagers. CMOS also has a "wandering photoelectron" problem. Photoelectrons generated deep in the chip can wander 1-2 pixels away from where they are generated before they are captured by a photodiode. Longer wavelengths tend to be absorbed deeper in the chip, so this problem occurs mostly with photoelectrons generated by infrared photons.

CMOS imagers may have moderately worse resolution, photometry, and centroiding than CCDs. But frame-transfer CCDs have similar photometry problems unless they have good microlenses, and microlenses can degrade centroiding. A shortwave pass filter can minimize wandering photoelectrons, and they may not degrade centroiding as much as they degrade visual resolution. CCDs may have a moderate resolution advantage for equal pixel view angle, but CMOS imagers with moderately more pixels can counter it. This will result in a larger raw image size, but once it is compressed to the same usable resolution there may not be much difference. And if onboard target centroiding is done (TBD), the centroid downlink data volume should depend only on usable resolution, and not pixel count.

These cameras will probably run warm, especially in cases where reflected glare doubles the sunlight incident on the camera cluster. This will increase dark current. This tends to be more of an issue with CMOS than with CCDs. But our exposure times can be short, even with fairly slow lenses, so we may not have a problem here. And when there is "enough" light (i.e., when

pixel exposure exceeds Sqr(RMSDarkNoiseInPhotoelectrons), then dark noise is less of an issue than shot noise, which depends only on Sqrt(PhotoelectronsPerPixel).

As CMOS imaging capabilities have improved, so have CCD chips: new chips take far less power, and offer pixels as small as 2 microns. They may be competitive for ODS if the radiation environment is modest. If the main focus of a flight experiment is deployment plus maneuvering in low earth orbit, CCDs may be fine. But if ODS must work well on missions lasting years without carrying heavy shielding to protect each of the ~24 imaging chips, CMOS is preferable.

### 5.4.2 Should we use frame-transfer or "rolling focal plane" imaging chips?

Both CCD and CMOS imagers are available in two types. One has a storage capacitor adjacent to each pixel, and a means of transferring charge between the pixel and the storage capacitor. This "frame transfer" topology allows simultaneous start and end of the exposure of all pixels on the imager. But it results in reduced quantum efficiency, larger chip area, and poorer centroid estimation. Only a small fraction of the available CCD and CMOS imagers operate this way, so it also greatly reduces the selection of potential imagers.

The other option involves different readout strategies for CCD and CMOS. In CCDs, the whole image slowly ratchets down, and at each step, the columns in a bottom read-out row are rapidly ratcheted into a readout cell. If the imager cannot be shuttered during readout, the smearing can be estimated and subtracted from the image. In CMOS imagers, the "charge buckets" stay in position, but one row at a time is read out. Hence reset of each row should occur a fixed time before readout, and hence also row-by-row. This results in a "rolling focal plane" exposure, with a typical ~30 millisecond time offset between the top and bottom of each frame.

Other things being close to equal, it appears preferable to use a frame-transfer imager. But the sail dynamics are slow enough that a ~30 millisecond variation in exposure time may not matter much in most cases, and other factors may be dominant. For example, the most suitable Micron frame-transfer chip has 12 micron pixels, while a comparable Micron rolling-focal-plane chip has 5.2 micron pixels. This makes a large difference in camera size (housing, lens, and lens-

shade), which becomes more important if ODS has ~24 cameras. In cases such as transients at the beginning and end of deployment, continuous imaging might allow reasonable interpolation to create synthetic "fixed time" images. Or computer simulation models can generate "synthetic focal plane views" that have a similar top-to-bottom variation in time.

### 5.4.3 Should we use color or monochrome imagers?

Many compact CCD and CMOS imaging chips are available in both monochrome and color versions. They are electrically identical and differ only in that the color version has a mosaic filter deposited on the image area. The usual mosaic is a Bayer pattern: a checkerboard that is half green-sensitive pixels, with the other half split between red and blue. Green is favored since human visual acuity is usually better with green than with red or blue.

Monochrome imagers seem preferable for most ODS cameras. One reason is that color imagers with mosaic filters result in poorer centroiding. Also, the mosaic filter materials may outgas, fade, or otherwise degrade in the persistent sunlight, even with good UV filtering. And we do not expect to see much in the way of color features in the sail anyway. Using monochrome imagers also allows narrow-band filtering for improved optical performance, as suggested in Section 5.3.3. Filtering with color imagers would simply make them low-performance monochrome imagers. However, it may make sense to use a color imager for one of the inspection cameras. This can use either a conventional mosaic filter or perhaps a multispectral filter wheel, which may be both more stable and more useful (but larger, more expensive, and less reliable).

### 5.4.4 Some candidate SXGA CMOS imaging chips

| Imager | Pixel pitch in microns |
|---|---|
| Micron MT9M001 | 5.2 |
| Omnivision OV9121 | 5.2 |
| National Semi LM9638 | 6.0 |
| Fill Factory IBIS5-1300 | 6.7 |

Micron MT9M413 12.0

5.4.5 Why should ODS use ~20 megapixels to cover the sail?

The more pixels we use, the smaller the targets can be and still be found against background noise, and the better the centroiding will be. In particular, wherever noise is bad enough to compete with target brightness (and that will certainly occur in the region around the specular reflection point on the sail), the noise will be highly variable, and the target will not be. So if the minimum dimension of the target is several pixels in that region, then we can find the target because its pixels are the right brightness, not just "bright." That suggests we want targets well over 1 pixel high close to the central boom, where glare and glint are likely to be most serious. That is easy to get, even with wider-angle lenses for the near field than for the far field. It also suggests that we may want to limit defocus or smearing to the minimum that gives acceptable centroiding, rather than the larger amounts that may give optimum centroiding.

5.4.6 Should the main photogrammetric cluster also include star tracking cameras?

The cameras in the main ODS cluster can have fairly stable relative geometry since they can mount near each other, and might even use a common housing. There may also be a reason to add one or more star trackers of comparable accuracy to that cluster. Then we can relate the observed sail dynamics to inertial space and not just to the cantilevered camera cluster itself. What we need is one or more of the same kind of imaging chip, but with faster lenses, much better lens shades, and suitable software. The best look angle will involve a trade between direct glare from the sun, and reflected glare, glint, and sheen from the sail membrane.

A more "natural" location for star trackers is on the anti-sun side of the sail, perhaps integrated into the main sail payload. This eases sunshield requirements, but it may complicate interpretation of ODS data if we cannot accurately relate ODS images to inertial space. Similarly, accurate steering of the sail may require relating a best-fit sail plane to inertial space. That can be done more accurately if the star tracker is closely coupled to the photogrammetric cluster viewing the sail. Another alternative is to add targets to the camera mast so we can

directly measure its distortion (static and dynamic) using the wide-angle views in the main camera cluster.

## *5.5 Boom-view camera issues*

Besides the main photogrammetric cluster with its ~16 cameras, the ODS baseline concept includes 4 cameras nearly in the sail plane, one looking outward along each of the diagonal booms. They can use the same imaging chips, but with longer-focus, narrower-view lenses (~$10^{o}$). This allows them to see boom bending and twisting very well, as should be easy to imagine if one considers the boom view sketched earlier in Fig. 4-4. But accurately estimating boom-camera look angles relative to each other and to the main camera cluster may be difficult. These cameras don't have overlapping views (by intent), and it is not clear whether their look angles relative to each other can be kept stable in both sail designs.

If the 4 boom-base cameras do not connect to each other structurally, but only to the boom base, their relative orientations may be perturbed by primary structure flexure. The question is whether we have any way to estimate the relative look angles of those 4 cameras with respect to each other and the main ODS cluster many meters away. We can measure flexing along the length of each diagonal boom very well, but our errors in estimation of the boom dynamics relative to each other may be >10X worse, both in steady-state error and also in dynamics, unless we can accurately relate the boom-view camera look angles to each other.

A related issue is that the longest camera baselines we have are between the boom views and the two other camera clusters (main and inspection). This can only provide 3D photogrammetric strength in views of a boom and adjacent sail features if we can relate the look angles of the cameras at each end of a baseline to each other. This might be done either by redundancy in the image data or by other data or constraints on mutual look angles or dynamics. The upper clusters can easily see the boom-view cameras, but we cannot easily add an upward-looking camera to a boom-view cluster because that camera would have to look nearly into the sun. So we may lose

our two longest baselines unless we have other means of establishing the relative look angles of both cameras compared to the baseline between them.

As noted in Section 5.4.6, we can put targets on the camera mast. If we put them at the base and halfway up to the main cluster, the 4 wide-angle cameras on the main cluster can view the targets. That should help us accurately measure most of the mast dynamics and any cluster tipping. But resolution of boom twist will be weak, and boom-view tipping cannot be viewed but must be inferred based on dynamic or other constraints.

Team member Tom Pollock has studied the dynamics of floppy 4-armed crosses. Three common modes are "Swastika" (rotation of the center in one direction, and the tips in another), a "scissors" mode, and one where 3 arms go in one direction and the 4th goes in the opposite direction with 3X larger amplitude. Adding our camera mast may give very interesting and poorly damped dynamics. If the dynamics may impede interpretation of our data, then we may need to measure them, to relate our long-baseline look angles to each other accurately.

## *5.6 Inspection cameras and pan/tilt head*

We started off assuming the inspection camera would have a zoom lens, and realized that we might get better imaging, lower mass and cost, better reliability, and much better inspection-camera aiming data if we bore-sighted wide- and narrow-view cameras together on a pan/tilt head. Bore-sighting several small cameras also allows us to use one color imager on the pan/tilt head. (It seems prudent to include at least one multi-spectral imager out of ~24 cameras). Costs will probably be lowest if we use the same imager and support electronics that we use for the quadrant-view clusters and boom-view cameras, but with different lenses. The other imagers are all organized in clusters of 4 with shared support electronics, so the inspection platform can fairly painlessly use 4 imagers (with perhaps one of them being a star tracker if there is no better use for it).

One camera can have a quite narrow view (a few degrees). It may be able to see sail details smaller than the diameter of its own lens aperture. To see such small details over a range of distances, adjustable focus is needed, and hence a focus motor and control logic. Focus control need not be perfect. After some initial adjustments under ground control, it may be enough to adjust focus in an open-loop manner as a function of the commanded tilt angle (which approximately controls the distance to the sail region viewed).

The thermal imager discussed in Section 6 will have a narrow enough view that it will also need to mount on a pan/tilt head to see the whole sail. Thermal imaging signal/noise ratio is far worse on the front than on the back, but may be "good enough." Mounting the thermal imager on the inspection pan/tilt head would simplify integration, and the wider-angle optical views can provide precise aiming data for the thermal imager for cases when that may not be reliably inferred from the content of the thermal image. (This may not be a problem if the optical targets are also brighter than the rest of the sail at long wavelengths.) Hence it is possible that the pan/tilt inspection platform will include a thermal imager if our work during Phase 2 shows that we can get good enough imaging from the front side of the sail to be diagnostically useful.

Figure 5-3 shows a candidate layout for the inspection platform, with multiple bore-sighted imagers mounted offset enough to look straight down without their view being obstructed by the camera mast they sit on. Figure 5-4 shows a design for a biaxial drive (that can be modified for ODS purposes) for a pan-tilt head from the company that built the robotic arms for the two Mars Exploration Rovers.

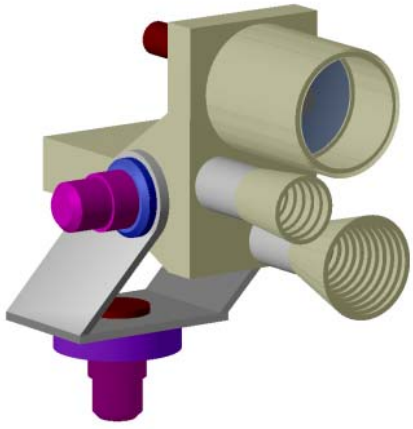

**Figure 5-3. Inspection Platform Concept**

**Figure 5-4. Alliance Spacesystems Inc. Biaxial Drive**

## *5.7 What parameters drive system mass*

We have baselined ~24 cameras for ODS, which is a far larger number than we originally expected. Obviously a significant part of the overall system mass will scale with the number of cameras. Other things being equal, a 24-camera ODS will be heavier than a 12-camera ODS. But other things are not equal: using larger numbers of cameras may allow reductions in individual camera, lens, and lens shade mass enough to pay for much or all of the mass of a larger number of cameras. One early ODS camera design was <20 grams/camera for a VGA design. The lens, housing, lens shade, and imager plus support circuitry on a small circuit board each weighed ~5 grams. The actual design may weigh moderately more, especially if each camera has large amounts of flash memory to store raw data, but even here the camera mass may be <40 grams/camera. So even with 24 cameras and local image storage for each, the total camera mass may be less than half the allowable total ODS mass of 2 kg.

The rest of this section discusses some of the issues considered in selecting the types of cameras, which led to the expected mass being small enough that we can afford up to 24.

If one compares two cameras with the same number of pixels, field of view, and sunshade performance, and one has twice the pixel pitch of the other, then the camera housing, lens, and sunshade dimensions will also differ by a factor of 2. The smaller camera should be lighter by a factor of 4, if "minimum gauge" or radiation shielding are dominant, by a factor of 8 if they are not. So if other things are roughly equal, smaller is much better.

Now consider a different case, where larger pixels have the same pixel noise and quantum efficiency. The lens needs 2X the focal length, but only needs the same photon throughput, so it can use the same aperture diameter and hence 2X the lens f/number. The lens and lens shade should be the same size, but the lens might be slightly simpler and lighter. Diffraction-limited angular resolution should be the same (2X the f/number, 2X the pixel size). It is just the imager and housing (including lens barrel) that should be heavier, by a factor of 4 to 8. It seems likely that the real world may lie between these cases, so "much but not all" of the camera mass may

scale at a rate between the 2nd and 3rd power of the pixel pitch. Lenses may have a resolution that falls short of diffraction-limited by a factor of 2 or more, but if the performance shortfall does not itself change drastically with lens size, then the overall sensitivity of camera mass to pixel pitch should not change much.

Other factors that affect system mass include the number of cameras, the required thermal stability of the housing (aluminum vs invar), any imaging chip radiation shielding that may be needed, sunshade design and size, processing electronics including compression and memory, cabling, and structure to support the main camera clusters stably with respect to each other. If we use aluminum lens barrels and camera housings, the image size on the focal plane (in pixels) will increase with temperature because aluminum expands more than silicon does. The lens elements also respond to temperature, both with size changes and also with refractive index changes. (Thermal expansion of glass "should" decrease its refractive index, but polarization changes with temperature, and this can swamp density change effects.) With medium-speed lenses, focus shifts and distortion changes should be less of an issue than scale-factor changes due to the lens moving away from the imager proportionately more than the silicon imaging chip expands. Scale factor changes can be estimated and compensated for if we measure housing temperature and keep thermal gradients small enough to minimize any need for higher-order corrections.

## *5.8 Recommendations*

Our tentative recommendations on the optical imagers are as follows:

| | |
|---|---|
| Configuration | 6 clusters of 4 cameras (pan/tilt, booms, 4 quadrants) w/shared electronics |
| Imager type | CMOS?, monochrome, no microlenses, 10-bit data, row-by-row exposure |
| Imager format | ~1280x1024 pixel array, small pixels (~5u?), glass-sealed ceramic pack |
| Lenses | Modified stock, f/4-5.6, fixed focal length and focus (except inspection) |
| Filters | Ceria-doped; IR cutoff or narrow-pass visible (near 550 or 600nm?) |
| Lens shades | Fairly large, to reject strong glare from close to region being imaged |

| | |
|---|---|
| Housings | Aluminum alloy, black coating on inside and white on outside |
| Fields of view | TBD (some overlap, but perhaps less than usual in photogrammetry) |

## *5.9 References*


Micron Technology, Inc, CMOS image sensor page: http://www.micron.com/products/imaging/

Omnivision Products; 9000 series camera chip:
http://www.micron.com/products/imaging/products/MT9M001.html

Fill Factory, Ibis5-1300 and STAR (rad-hard) CMOS sensor pages:
http://www.fillfactory.com/htm/products/htm/ibis5/ibis5.htm
http://www.fillfactory.com/htm/products/htm/star.htm

National Semiconductor LM9638 product folder: http://www.national.com/pf/LM/LM9638.html

Janesick, J.R. *Scientific Charge-Coupled Devices*. SPIE Press, 906 p,. 2001

Universe Kogaku America page on lenses for CCDs: http://www.ukaoptics.com/ccd.html

# Section 6
# Thermography

## *6.1 Motivation for investigating thermography for solar sails*

Monitoring sail temperature during flight demonstrations can be important. Sail temperature is driven by front-side absorptance and rear-side emittance, and temperature changes indicate changes in one or both parameters. In addition, knowledge of the temperature field and associated thermal strain distribution is necessary to predict sail loads and dynamics. Average membrane tensions of 1-10 psi are planned, so mechanical strains will be only a few parts per million. Small temperature gradients across the surface could result in thermal strains exceeding mechanical strains. We are just beginning to study the effect of this on sail static shape and loads, and possible effects on sail dynamics. It might even affect sail control loop stability.

Team member Joe Blandino et al. demonstrated the effect of temperature variations on a spot-heated membrane [Ref. 6-1]. The center was heated 55˚C warmer than the rest of the membrane. (Conduction in the plane of thin membranes is minimal.) The heated region expanded and became visibly slack.

## *6.2 Thermal modeling of solar sails*

To better understand the temperature distribution that the sail may experience in space, a thermal model was developed. The sail was modeled using square elements. Figure 6-1 shows the radiation from the sun and interactions with space on one element. Radiation exchange between elements is neglected since the view factors are extremely small. In the front, the mean sail shape is concave but the self-view factor is modest, and the front-side emittance is very low due to the aluminum coating. On the back side, emittance is high, but billowing makes the sail quadrants convex, so only wrinkles and other small-scale features will allow the high-emittance back surface to "see itself" at all. And the view factor of such views will be small. One can

make an intuitive estimate of the importance of such views by imagining the best-fitting sphere to a locally concave region. The self-view-factor is roughly equal to the fraction of the full sphere's area that the local "dimple" covers. That will generally be only a few percent, except very close to a sharp crease that has not been straightened out. Conduction through the membrane is assumed perfect, and conduction in the plane of the membrane (mostly in the aluminum coating) is neglected because local radiative equilibrium dominates in-plane conduction over distances larger than a few millimeters. Average front and back side emittance values are assumed (i.e., the spectral nature of these values is neglected).

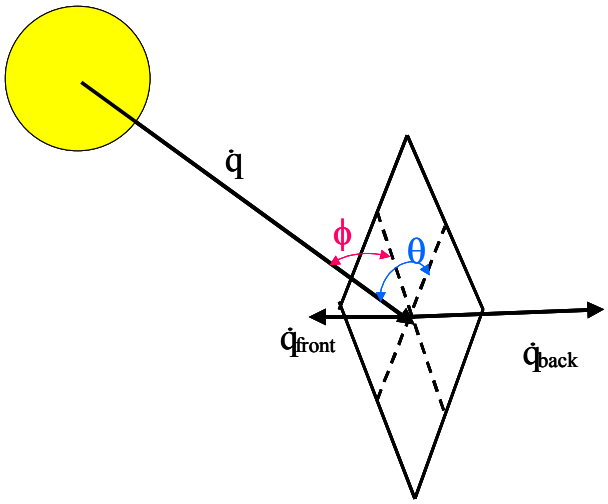


**Figure 6-1. Radiation interactions for a sail element**

An expression for the temperature at any point on the sail surface is obtained by performing an energy balance on the sail. The expression for temperature is

$$T_s = \sqrt[4]{\frac{\alpha_f \dot{q} \cos\phi \cos\theta}{\sigma\left(\varepsilon_f + \varepsilon_b\right)} + T_\infty^4} \tag{1}$$

where $T_\infty$ is the background temperature, $\alpha_f$ is the front side absorptance, $\varepsilon$ is the emittance (front and back), $\sigma$ is the Stefan-Boltzmann constant, and $\dot{q}$ is the normal solar flux. This is essentially the expression given by Salama et al. [Ref. 6-2]. The two angles are projections of the angle of incidence on planes normal to the sail and to each other. The solar intensity on the surface varies with overall sail orientation with respect to the sun, but it also varies with the billowed shape of

the sail. To approximate the billowed shape of the sail, photogrammetry was used to measure the gravity sag of one quadrant of a 2-m sail model. The general shape is shown in Fig. 6-2. The gravity sag is greater than the billow due to light pressure in space, but the data in Fig. 6-2 can be scaled in the *x*, *y* and *z* dimensions. Thus it can be used for any sail size and billow depth.

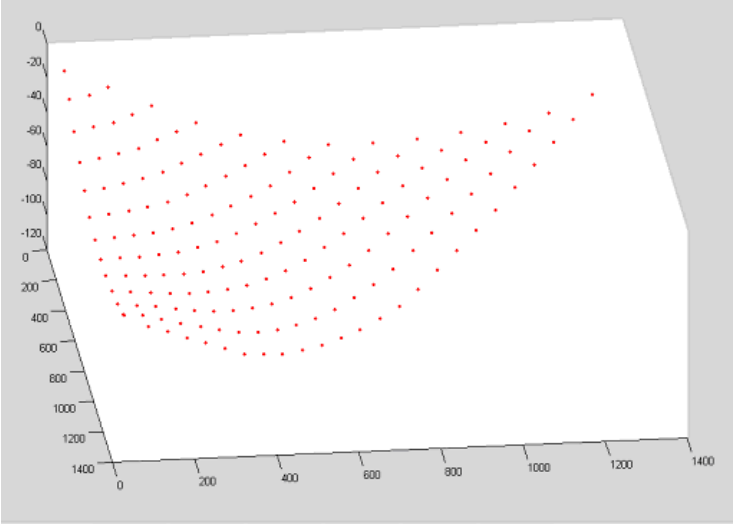


**Figure 6-2. General sag shape used to estimate solar sail light pressure billow. Dimensions in mm.**

We considered a 40 m square sail 1 A.U. from the sun. We estimated the temperature distribution for sail angles of 0˚, 22.5˚, and 45˚ away from normal to the sun, and billow depths of 0, 0.2 and 1 m. We assumed a Kapton® sail, aluminized on the front only, with $\alpha_f$ *=0.09,* $\varepsilon_f$=0.04, and $\varepsilon_b$=0.50. Table 6-1 presents the average sail temperature and temperature range, $\Delta T$, for the 3 sail angles and billow depths.

**Table 6-1. Sail temperatures for various sun angles and billow depths at 1 AU from sun**

| Billow Depth | Sun-sail angle = 0˚ | | Sun-sail angle = 22.5˚ | | Sun-sail angle = 45˚ | |
|---|---|---|---|---|---|---|
| 0.0 m | –21.9˚C | 0.0˚C | –26.6˚C | 0.0˚C | –42.7˚C | 0.0˚C |
| 0.2 m | –21.9˚C | 0.2˚C | –26.8˚C | 0.5˚C | –43.3˚C | 1.0˚C |
| 1.0 m | –21.9˚C | 0.3˚C | –27.9˚C | 2.3˚C | –45.7˚C | 5.2˚C |
| | $T_{avg}$ | $\Delta T$ | $T_{avg}$ | $\Delta T$ | $T_{avg}$ | $\Delta T$ |

The temperature differences are modest, but they can result in dimension changes that exceed the mean strains caused by sail tension. Table 6-2 shows the coefficient of thermal expansion for 3 sail materials and the resulting thermal strain due to temperature differences.

**Table 6-2. Sail thermal strain for three candidate materials**

| Material | Coef. of Thermal Exp. | ΔT | $\varepsilon_{Thermal}$ |
|---|---|---|---|
| **Kapton®** | $2.0\times10^{-5}/^{\circ}C$ | 0.2 ˚C | 4.0 με |
| | | 0.5 ˚C | 10.0 με |
| | | 1.5 ˚C | 30.0 με |
| **CP1 colorless polyimide** | $3.7\times10^{-5}/^{\circ}C$ | 0.2 ˚C | 7.4 με |
| | | 0.5 ˚C | 18.5 με |
| | | 1.5 ˚C | 55.5 με |
| **Mylar®** | $1.7\times10^{-5}/^{\circ}C$ | 0.2 ˚C | 3.4 με |
| | | 0.5 ˚C | 8.5 με |
| | | 1.5 ˚C | 25.5 με |

To compare the mechanical and thermal strains, Table 6-3 lists the 3 candidate materials and strains caused by a 68,940 Pa (10 psi) mechanical load, the upper limit of what has recently been discussed for solar sail membrane tensions. For Mylar® and Kapton®, thermal expansion exceeds the mechanical strain if the temperature difference exceeds ~1.2°C. For CP1, thermal expansion exceeds the mechanical strain even for temperature ranges under 0.5°C. If the sail membrane sees average tensile loads smaller than 68,940 Pa, which is likely, then the temperature gradients required for thermal effects to greatly redistribute loads will be proportionately smaller.

**Table 6-3. Membrane mechanical strains for three materials under 68,940 Pa (10 psi) tension**

| Material | Tensile Modulus | $\varepsilon_{mechanical}$ |
|---|---|---|
| Kapton® | $2.96 \times 10^9$ Pa | 23.2 με |
| CP1 | $4.20 \times 10^9$ Pa | 16.4 με |
| Mylar® | $3.79 \times 10^9$ Pa | 18.2 με |

Measurement of the sail membrane temperature hence seems quite valuable for understanding structural behavior in space. Temperature gradients across the sail surface can

develop due to variations in metallic coatings, sail orientation to the sun, and the billowed shape of the sail. The cases presented illustrate that only small temperature gradients, perhaps well under $1^{o}$C, are necessary for the thermal strain to become larger than the mechanical strain. Because the thermal strains will be significant, their effect on sail dynamics must be considered. This will be studied more in Phase 2.

## 6.3 *Optical properties of solar sails*

The approach described above assumes uniform solar absorptance and thermal emittance values over a typical membrane. Exercising the model shows that small perturbations in optical property values can generate significant changes in the temperatures and temperature differences predicted, and hence in thermal distortion and the resulting mechanical load distribution. Thus it is important to characterize and consider in a thermal model the wavelength dependent or spectral emittance and absorptance.

A sample of Kapton® polyimide film (Product 100HN) was acquired from Dunmore Corporation and later tested at Surface Optics Corporation (SOC) for spectral reflectance and transmittance. Dunmore first tested the film for quality conformance. Its properties were: film thickness: 0.001 inches; aluminum adhesion test results: 0.0%; emittance: 0.02; surface resistivity: 0.72 ohms/sq. SOC used the following test matrix to characterize the spectral reflectance of the samples: test coated and un-coated sides in similar fashion; acquire Hemispherical Directional Reflectance (HDR) (total reflectance), Diffuse Directional Reflectance (DDR), and Specular Directional Reflectance (SDR), where SDR ($\lambda$) = HDR ($\lambda$) – DDR ($\lambda$). The tests included the 2 to 25 micron wavelength region, which covers a small part of the energy in the solar spectrum, and most of the long-wave emittance spectrum. The tests were run at 20 °C (room temperature), 60 °C, 100 °C, and 140 °C; with incident angles of 20°, 50°, and 70°; with average, perpendicular, and parallel polarization. The tests focused on temperatures warmer than shown in Table 6-1 because polyimide sails (of Kapton® or CP1, for example) seem most attractive in missions that go significantly closer to the sun than 1 AU. A brief synopsis of the results is provided below.

The spectral reflectance of the coated side of the membrane is relatively constant with both wavelength and polarization. It varies modestly with angle of incidence and temperature. Nearly all the reflected energy is specular, and the diffuse portion increases inversely with angle of incidence. An average value of reflectance, ρ, weighted with respect to temperature and angle of incidence offers a reasonable basis for thermal calculation. A representative depiction of spectral reflectance for coated Kapton® 100HN is provided in Fig. 6-3.

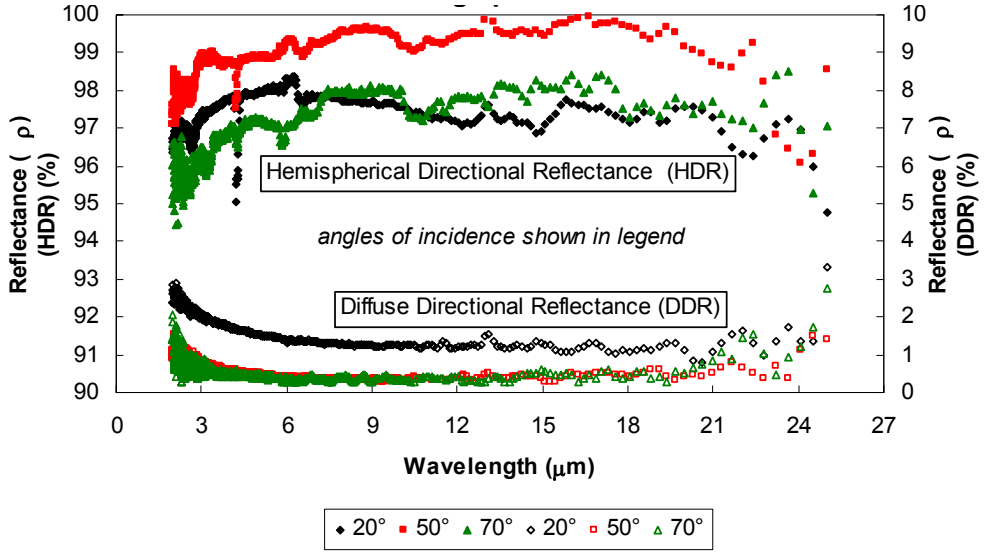


**Figure 6-3. Spectral reflectance for coated Kapton® 100HN at 61.7 °C for average polarization**

The spectral reflectance of the uncoated side of the membrane is highly variable with wavelength but mostly unaffected by polarization. Reflectance varies significantly with angle of incidence and insignificantly with temperature. The portions of reflected energy that are specular and diffuse vary significantly with wavelength and angle of incidence. An average value of reflectance, ρ, does not offer a reasonable basis for thermal calculation, so spectral analysis is needed. Representative spectral reflectance for coated Kapton® 100HN is shown in Fig. 6-4.

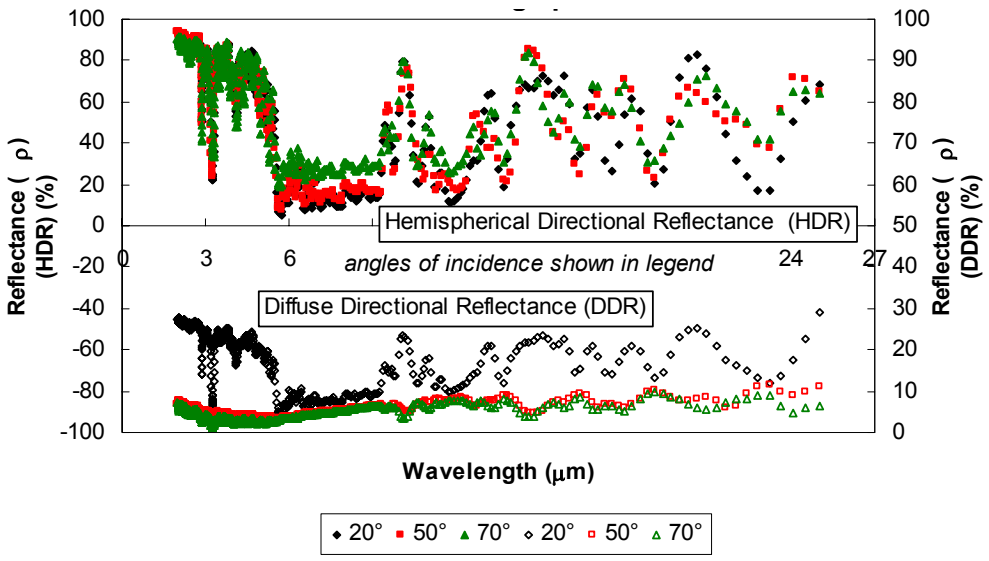


**Figure 6-4. Spectral reflectance of uncoated Kapton® 100HN at 103.2 °C for average polarization**

Spectral transmittance (see Fig. 6-5) should be evaluated and considered in any thermal analysis. A preliminary analysis suggests that 1-mil Kapton® transmittance can be an important factor in the infrared. A heating element placed behind a membrane sample may transmit energy through the membrane comparable to that emitted by the membrane. Transmission of direct sunlight may be less of an issue except directly looking at the sun, since very little of the sun's radiation is in the long-wave thermal region used by the Indigo thermal imager.

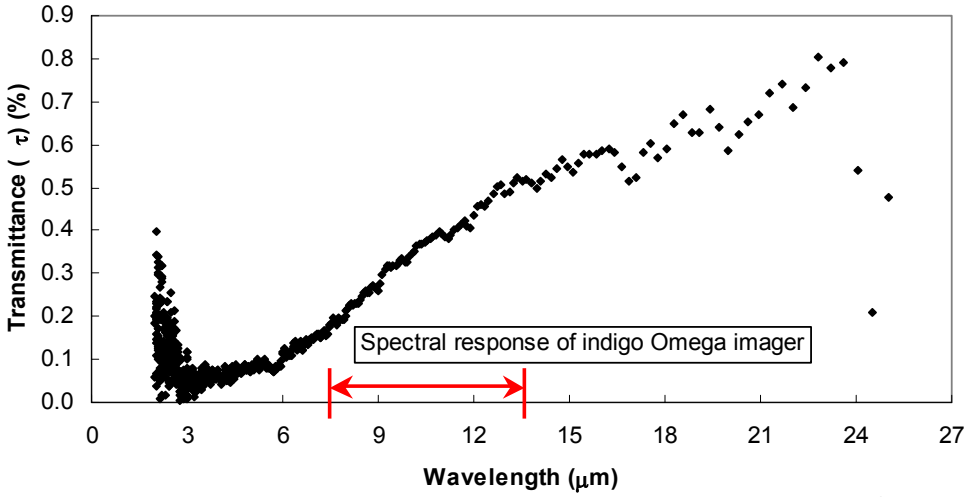


**Figure 6-5. Hemispherical directional transmittance, one-side-coated Kapton® 100HN, normal**

## *6.4 COTS thermography equipment and testing*

We tested the indigo Omega (long-wave) miniature microbolometer-based imager [Ref. 6-3] to determine the feasibility of that approach for thermography. This new imager is very small, low mass (<120 grams), and has excellent image quality. It uses an uncooled 160×120 array of microbolometers based on vanadium oxide. It is sensitive to the 7.5-13.5 micron wavelength range. It acquires images at 30 Hz and features a noise equivalent temperature difference (Netd) of less than 85 mK. Its temperature detection range is –40 to 55 °C (extended).

We collected infrared image data from a 0.5m x 0.5m, 1-mil aluminized (on one side) Kapton® sample. We collected images using both an Omega and also 2 other high-quality thermal imagers that we had available: an Agema Thermovision 870 (mid-wave) infrared scanning system and a CMC Electronics Cincinnati TVS-8500 (mid-wave) infrared imaging system. These two systems are laboratory-grade instruments and the TVS-8500 represents the state of the art in Stirling-cooled, mid-wave focal plane array technology. The Thermovision system is old technology but robust and flexible in its operation. They both use shorter-wavelength ranges than the Omega.

We placed the three imagers behind a shield to minimize stray ambient reflections from the surroundings. We then placed the Omega and Agema side by side at the centerline of the membrane, positioned the CMC unit near the top of the membrane, and then heated the membrane with a circular resistive element centered behind the membrane. The images collected with the Omega and Agema units are shown in Figs. 6-6 and 6-7, first with no power applied and then with power applied at three different levels.

Specular reflections are apparent in all the images, but are more easily distinguished in the monochrome images produced by the indigo Omega system. At low power setting the warmed round region begins to be seen in the center of the membrane, and in the images for medium and high power setting (Fig. 6-7), the effects of natural convection become apparent.

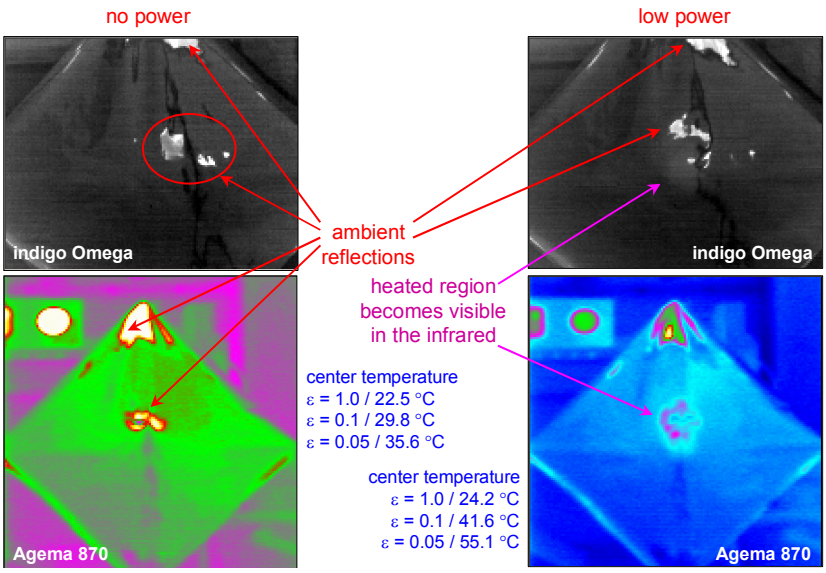


**Figure 6-6. Infrared images of 0.5-m, 1-mil aluminized Kapton® sample, at ambient temperature (left) and with low heater power at center (right)**

The Agema system calculates target temperature based upon a proprietary algorithm that considers three inputs from the user: $T_{ambient}$ (temperature of the surrounding atmosphere), $T_{reflected}$ (a nominal average blackbody temperature of the objects surrounding the target), and ε (an estimated average target emittance). The temperature data listed in Figs. 6-6 and 6-7 show the sensitivity of a "true" temperature calculation to the average emittance assumed for the calculation.

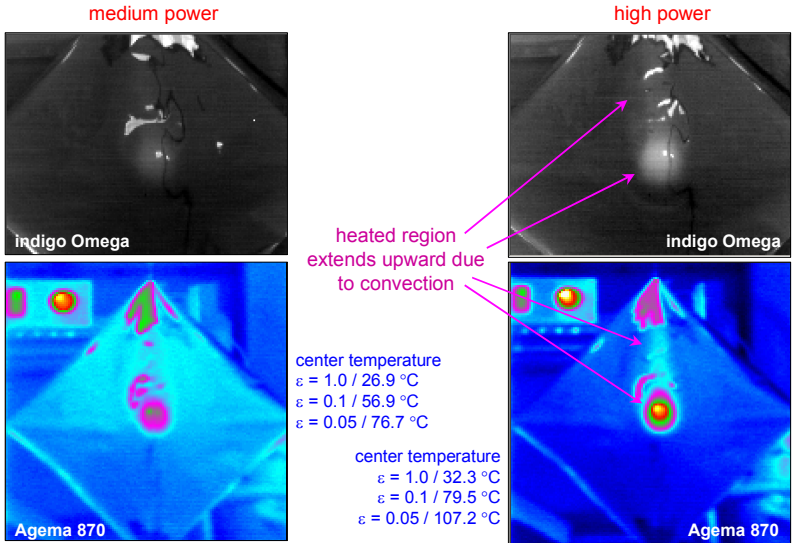


**Figure 6-7. Infrared images of 0.5-m (on side), 1-mil aluminized Kapton® sample, with medium heater power at center (left) and high heater power at center (right)**

## *6.5 Trades between back side and front side thermography*

The main advantage of back side thermography is a far larger signal and somewhat lower noise, and hence a far better signal-to-noise ratio. The low front side membrane emittance reduces thermal radiation from the sail and efficiently reflects "noise" radiation from other objects. Particularly with sails in low earth orbit, the emitted signal may be swamped by a reflected longwave earth signal, which varies with cloud cover and height and is hence not easy to estimate and compensate for. On the back, the emittance is much higher, and reflected "noise" is weaker. But front-side thermography from the inspection platform should greatly ease integration, by eliminating any need for an aft mast and another pan-tilt head. The signal would be small, but it could be useful, especially if the front side longwave emittance can change due to sputtering, oxidation, contamination, etc. In Phase 2, we will explore more what might be learned from front-side thermography.

## *6.6 Significance of optical property knowledge and nonuniformity*

According to equation (1) in Section 6.2, if the sunlight and effective longwave radiant ambient temperature are constant, the membrane temperature should scale with $(\alpha_f /(\varepsilon_f+\varepsilon_b))^{0.25}$. Hence changes in front-side solar absorptance or front or rear longwave emittance will affect the temperature. Since sail absorptance is low (~0.09), even modest changes due to contamination or other factors may make a significant difference in temperature and hence thermal distortion. Changes in emittance could also have an effect. But here things are more complicated. For example, if most of the thermal emittance is on the back, an increase in back emittance will drop the temperature but have little effect on the overall radiation emitted from the back: that will scale with $\alpha_f\varepsilon_b /(\varepsilon_f+\varepsilon_b)$, or (since $\varepsilon_f<<\varepsilon_b$) with $\sim\alpha_f$. Hence back side thermography may see front side absorptance changes much better than it sees back side emittance changes. Front side thermography should be sensitive to both absorptance changes and emittance changes, especially those on the front: the emitted energy scales with $\alpha_f\varepsilon_f /(\varepsilon_f+\varepsilon_b)$. So paradoxically, front-side thermography, despite its weaker signal and stronger noise, may detect more membrane property

changes—but only if the signal-to-noise is "high enough." (But it may not tell us what parameter changed.) All of these issues need further investigation.

## *6.7 Recommendations*

The good sensitivity and low mass, power, and cost of thermal imagers like the new indigo Omega described in Section 6.4 may make such imagers an attractive part of ODS. The ODS baseline design currently assumes the thermal imager will be located on the back side of the sail because it faces deep space. But putting the imager on the inspection pan-tilt head on the front side of the sail may significantly ease ODS integration costs and constraints, and hence makes it easier to justify doing it. Doing thermography from the front results in much weaker signals and stronger noise, but the results may be sensitive to changes in more of the sail's optical properties. For now, we will continue to assume that an additional support mast and pan-tilt unit is needed for a back side installation of the thermal imager until the suitability of moving it to the front can be unambiguously determined.

Many questions still need to be answered, including:

1. Can compact, low-power imagers like the indigo Omega be qualified for use in space?
2. Can front side thermography with microbolometer-based instruments like the Omega provide useful images of the sail?
3. What can such images tell us about sail properties, degradation, or other phenomena?

## *6.8 References*


6-1. Blandino, J. R. et al., "The Effect of Asymmetric Mechanical and Thermal Loading on Membrane Wrinkling," *AIAA Structures, Structural Dynamics, and Materials Conference*, AIAA paper 2002-1371, April 2002.

6-2. Salama, M., McInnes, C., and Mulligan, P., "Gossamer Sailcraft Technology," Chapter 19 in Jenkins, C. H. (editor), *Gossamer Spacecraft: Membrane/Inflatable Structure Technology for Space Applications*, AIAA Progress in Astronautics and Aeronautics Series, vol. 191, 2001.

6-3. Webpage on Indigo Systems Omega thermal imager: www.indigosystems.com/product/omega.html.

# Section 7
# Distributed Non-Imaging Sensors

As noted in Section 3, we originally planned to have cameras not just in the center but also at each corner of the sail. This required distributed wiring that would also be able to handle various other distributed sensors, so such sensors were included in the study. To reduce expected ODS cost and mass, the solar sail program decided to limit the cameras to a central boom at the hub of the sail, which is located on the front side in the our baseline concept but potentially can be used on the back instead. Nevertheless, there remains a potential requirement (specifics are still TBD) for distributed sensors, and this is still within the scope of the ODS team's work. This section of the report lists the options and issues we see for the various distributed non-imaging sensors and their support hardware. This distributed subsystem must fit within the overall mass, power, cost, and "easy to integrate" constraints of the overall ODS.

## *7.1 Distributed sensor options and recommendations*

The main focus in this area was sensors that complement the imaging sensors or provide data that could aid decisions about what imaging data to collect, retain, and/or download. Some of the categories below were included based on only a cursory assessment and need a more careful evaluation. The only categories discussed in detail are items 1-5 below.

### 7.1.1 Measurements considered

1. 3-axis acceleration at each boom tip (to measure boom bending and torsion)
2. Component temperatures (as convenient)
3. Strain at root of each boom (near hub), and perhaps along one or more booms
4. Membrane tension (at one or more support points of each quadrant.)
5. Laser-based systems (e.g., the LDRI)
6. Charging of local exposed non-grounded surfaces (to determine importance of grounding)
7. Diagnostic feedback from sail control actuators (motor currents, position, temperature, etc.)
8. Housekeeping data from distributed sensor support electronics (temperature, voltages, etc.)

### 7.1.2 Accelerometers

We considered conventional high-end accelerometers (Q-flex, etc.), lower-mass piezo-electric sensors, and some fairly new MEMS devices from Analog Devices and Silicon Designs. The option that now looks most attractive is the Silicon Designs SD1221 seismic-grade MEMS accelerometer chip. It has a ±2 g full-scale range, 2000 g shock tolerance, an internal temperature sensor, and RMS noise of ~2E-6 g/Sqrt(Hz). Figure 7-1 shows the SD1221. It weighs only 0.62 grams, is <1 cm square, and requires ~10mA at 5V. Signal output is a differential analog pair, with voltages each ranging from 0.5 to 4.5V. Taking full advantage of its accuracy and low noise requires a closely coupled analog-to-digital converter.

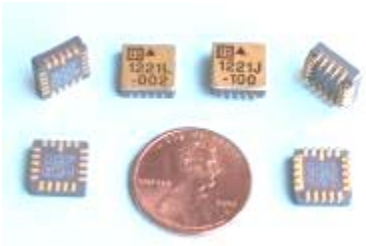


**Figure 7-1. SD1221 accelerometers**

### 7.1.3 Temperature sensors

We considered the temperature sensor options listed below:

1. DS1820 family (digital output; –55C to +125C; "party line" can handle many sensors)
2. AD590 (current proportional to absolute temperature)
3. Thermistors (good over moderate temperature range)
4. Thermocouples, for wide temperature range (use any of the above as a reference temp)
5. Optical fiber temperature sensors (require a large central electronics element)

The Dallas/Maxim DS1820 family is an unusual digital-output sensor with "party line" wiring. It can only provide outputs in the -55C to +125C range but can survive a wider range. The "party line" wiring may simplify integration because 3 wires (and in some cases 2) are enough to provide power, commands, and data return from dozens of sensors. It is attractive in cases where many temperature sensors are needed and wiring must be minimized. It is available in various packages from TO-92 down to a 0.7x1.4x2mm chip-scale package. The DS1820 is one family of sensors and communication chips that use the Dallas "1-wire" protocol. That protocol may be a useful option for getting distributed sensor data to the central ODS package.

The AD590 has a nominal output current of 1uA/K over a 4-30V supply range. The current output reduces noise problems in most installations. Thermistors are generally used on devices exposed to only a modest temperature range because of their exponential variation of resistance with temperature. Thermocouples have a wide temperature range capability but also a low signal, so they are prone to noise problems unless wiring is short and/or well shielded. Optical fiber sensors are the lightest sensors, but their signal conditioning is (currently) the heaviest and most expensive.

### 7.1.4 Strain gauges and load cells

We considered the strain gauges and load cells listed below. The support electronics for optical fiber sensors are fairly substantial and may not be easy to miniaturize. And optical fibers respond to both stress and temperature, and hence would probably need thermal compensation. Furthermore, distributed (averaging) strain sensing does not uniquely indicate boom shape changes. But this technology is rapidly improving it so needs to be watched. Signal transmission distances of more than 100 meters are possible over fiber and the sensor weight is negligible. Currently, options 1 and 2 appear to have much lower risk.

1. Foil type uniaxial or rosette strain gages for boom root (from Measurements Group)
2. Sub-miniature load cell (Entran ELFM for ground tests; similar to flight hardware)
3. Optical fiber strain gages (single point)
4. Optical fibers for distributed strain sensing for boom shape determination.

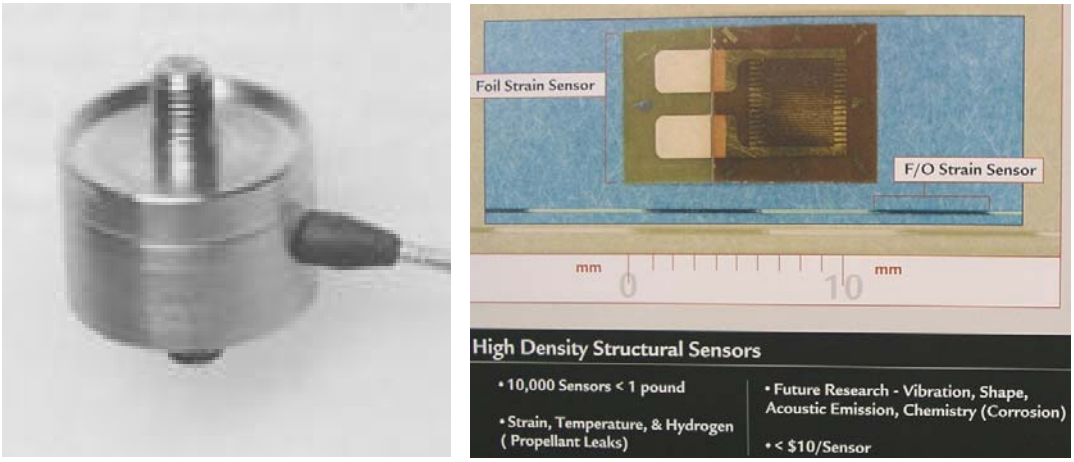


**Figure 7-2. Precision Measurements miniature load cell and some strain sensor options**

### 7.1.5 Laser Dynamic Range Imager

The Laser Dynamic Range Imager (LDRI) was developed by Sandia National Labs and NASA JSC and was used on Space Shuttle mission STS-97 in Dec. 2000. It is an interesting sensor for possible use for in-space shape/dynamics measurement of solar sails. It is an active, scannerless range imager that provides range information at each pixel of a video image. The illumination source is a diffused infrared laser beam. Although capable of measuring the shape of large diffuse objects at video rates, the low diffusivity of aluminized membranes makes it extremely difficult to receive adequate signal return for a full-field solar sail measurement. However, it could measure a field of attached diffuse targets. Technical contacts are Bob Nellums at Sandia, and George James and George Studor at JSC.

## *7.2 Sensor support electronics, power, and data transmission*

In a large-scale gossamer structure, shielded analog wiring of any length will drive system noise, mass, and installation cost. The larger the structure, the more critical it is to digitize data locally, either at the sensor itself or in a nearby support module. Data transmission issues drive the support electronics design because wireless options require the support electronics package to provide its own power. Based on this understanding, we discuss data link options and issues first.

### 7.2.1 Wired vs wireless links: power and data options and issues

We considered the options listed below for connecting distributed sensor support electronic modules to the central ODS package located at the hub of the solar sail:

1. Concepts using wire for power and communications (RS422, RS485, LVDS, 1-wire)
2. Harms-Goubou (RF mostly trapped around a single conductor)
3. Short-range RF techniques (wireless modems, Bluetooth, etc.)
4. Short-range optical techniques (IrDA or laser in free space, fiber, or L'Garde boom)

Concepts using wires allow the ODS host platform to provide power to the remote electronics modules. But the larger the structure, the more the wiring weighs and costs to install. The "1-wire" approach uses a shared power/signal line plus a second wire as a ground. It may be the lightest and easiest to integrate, but it limits power and data rates. A 2-pair option may be significantly more capable: a power/ground pair, plus a differential signal pair.

Let us assume a 4-wire cable: either power + ground + signal pair, or a redundant "1-wire protocol" pair. We can use a design similar to the ProSEDS wire, namely 7 strands of 28AWG aluminum magnet wire twisted around an 8x400 Kevlar® core braid for strength. The twist is tight enough for the wires to clamp the core firmly and also to accommodate tensile load cycling without yielding the wire. Here we might twist 4 polyimide-insulated 30AWG wires around a 3x400 Kevlar® core. This design weighs 0.75 grams/meter, and the resistance of each conductor is 0.6 ohm/meter. The wire-twisting operation is compatible with occasional swapping of one pair to reduce cross coupling between the pairs. On a 70m sail, we would need ~200m of cabling. The mass is ~150 grams, <8% of the allowable ODS mass. If the cabling also delivers power and commands to boom-tip vane actuators, 150 grams may be very acceptable. A power-loop resistance of ~60 ohms may be acceptable if ultracaps in the module provide load leveling.

Wireless options require the remote support electronic packages to include solar cells. The low power needed places a premium on design simplicity, such as fixed body-mounted solar cells. High-end triple-junction solar cells reduce the required cell size and hence the module area that must face the sun. If it is desired to collect data during eclipse (including eclipse of the small solar array by other sail features, or shading caused by boom rotation during deployment), then the module also needs batteries, or at least ultracaps, plus suitable charge-control circuitry.

An additional issue with all 3 wireless data link options is possible obstruction of the signal path by sail features, either during deployment, normal operation, or anomalies. The best solution may conceivably vary with the sail design. For example, the inflated L'Garde booms may be able to act as RF waveguides, allowing use of Bluetooth or other protocols well beyond their normal range. If the inner surfaces are shiny enough, the booms might even act as optical

guides. (The L'Garde boom can bend enough for the ends to not have direct visual contact, so the inside surface treatment and its effect on RF and optical transmission may be critical.)

Our current baseline is wired connections. But we don't yet know whether the actual wiring can be anywhere near as light as the ProSEDS-derived concept suggested above (~0.75 grams/meter), or will be enough heavier that wireless concepts (and the resulting complexity of autonomous power supply, etc.) merit further study. If the wiring is exposed, it may need to be either shielded or redundant, either of which may significantly increase wiring mass.

### 7.2.2 Other design issues

Once the decision for wired vs wireless concepts is confirmed, the full sensor support electronics module can be designed. Functionally, this system is like an attached picosat. It needs power conditioning, sensors, signal conditioning, an FPGA or computer, and command, control, and communications. But rather than thinking of this in terms of satellite design approaches and costs, a more instructive perspective may lie in the work that DARPA and other organizations are doing on distributed sensor and communication networks.

A recent NIAC study of an ambitious global-monitoring concept (see Manobianco reference in Section 7.3) summarizes recent work on "Smart Dust" concepts and approaches (sensors and complete systems in the milligram class), and includes a 5-page bibliography reviewing work in this area. The Smart Dust work is far too developmental for ODS, but it is an indication of the direction in which distributed sensing systems are headed, and it seems very relevant to future gossamer spacecraft concepts. The discussions of issues like A/D conversion and local wireless data links at minimum power are clearly relevant to our needs.

Besides power and communications issues, other issues to be considered with the distributed sensor support modules include the following:

- Electronics radiation tolerance: latchup, functional interrupt, upset, and total dose
- Amount of local/distributed memory (esp. if data is desired before com-link is functional)
- Local vs central computational capability (FGPA vs 8-bit vs 16-bit vs 32 bit CPU)

- Amount of development required (commercial package vs custom-built)
- Degree of sophistication of software if it uses a CPU

### 7.2.3 Compatibility and synergism with sailcraft and other spacecraft needs

It is worth putting some care into the distributed-sensing aspect of ODS system design because it may be useful over a range of applications. For example, it may make sense for the L'Garde design to use a wireless link to command control surface actuation at the ends of their booms. It is also relevant to health monitoring and control of other gossamer structures. It is even relevant to large non-gossamer structures such as the International Space Station (ISS), where the complexity of the integration process may justify a wide range of autonomous distributed systems. For example, the floating-potential probe package developed by NASA Glenn and installed on ISS several years ago provided its own power and had a wireless link to ISS to reduce integration issues.

More immediately, we need to ensure that our thoughts and recommendations on sensors and support electronic concepts are at least compatible with, and preferably strongly synergistic with, any needs the sailcraft developers have for distributed power, control, and monitoring on their sail. Because of the issues of compatibility and potential synergism, and the fact that integration costs may dominate at least for wired options, we need to work closely with the sail developers during the next study phases to ensure that our work is relevant.

## *7.3 References*

John Manobianco, Global Environmental MEMS Sensors (GEMS): A Revolutionary Observing System for the 21st Century. NIAC Phase I Final Report on USRA Grant Number 07600-093, December 2002. Includes 5 page bibliography, much of it covering recent work on "Smart Dust" and related concepts.

Silicon Designs accelerometer page: http://www.silicondesigns.com/SelectChart.html

Analog Devices AD 590 product page (also, many other useful product lines) http://www.analog.com/Analog_Root/productPage/productHome/0,2121,AD590,00.html

"BASIC STAMP" microcontroller page, at Parallax Designs:

http://www.parallax.com/html_pages/products/basicstamps/basic_stamps_oem.asp

Mission Research Corporation, Santa Barbara: Advanced Instrument Controller
http://www.mrcsb.com (Note: Now part of ATK—AIC ref. not found)

Spectrolab (Boeing) solar cells: http://www.spectrolab.com/prd/space/cell-main.asp

Entran load cells: http://www.entran.com/ltoc.htm

Vishay Measurements Group: http://www.vishay.com/company/brands/measurements-group/

Maxim (Dallas Semiconductor) Single Wire Digital Output Temperature Sensor page:
http://www.maxim-ic.com/products/sensors/1_wire.cfm

# Section 8
# Avionics System Issues and Design

## *8.1 Evolution of thinking on data volume, compression, and operating mode*

Our thinking in this area evolved considerably over the course of the Phase 1 study. The centroid testing described in Section 8.1.2 was a significant factor. We describe the evolution chronologically because it highlights the alternatives we considered and what led us to our baseline concept.

### 8.1.1 Early perspectives

We initially thought that image compression hardware would be so bulky and slow that it would make more sense to do compression as a post-processing operation on stored raw data rather than in real time or on stored data in each camera head. This led us to consider storing raw data. This in turn led us to consider using two different forms of compression: JPEG2000 or something else that provides visually useful information (especially low-rate images downloaded near real time), and another that does accurate target centroiding directly from the raw data to provide even lower bandwidth data that is very accurate. This reduces the bandwidth required for both visual and centroid downloads while retaining the raw data in case selective downloads are desired later.

This approach allowed the system to be decomposed into 4 pieces with fairly simple and well-defined interfaces: cameras to capture images, memory to store the raw image data, an image compression algorithm to operate on stored image data, and a separate centroiding algorithm. The simple interfaces and low throughput requirements (other than storing the raw image data) might simplify development. Note that with this philosophy, any questions raised by ground analysis of either the centroid or visual data might be answered by requesting download of the relevant raw data still in archival memory, or less-compressed forms of that data.

### 8.1.2 Centroiding tests on compressed images

We knew compressing images could reduce target centroiding accuracy, but we did not know by how much. We addressed this uncertainty by centroiding some high-quality target/sail images before and after compression. This allows us to quantify centroid shifts as a function of the compression algorithm and compression ratio. LaRC provided sample images to Ecliptic. Ecliptic used both JPEG and JPEG2000 methods to compress the images to various extents, and then LaRC used centroiding algorithms on both the raw and compressed images. We did not include MPEG compression because it relies on high similarity between consecutive frames, and we want to interleave images from many cameras on one compression device. MPEG may merit consideration if we want higher data rates and if hardware compact enough to use at each camera becomes available, or if we want to do compression on stored data.

The results for 8 targets are shown on the next page (X and Y centroid shifts in pixels) for several different compression ratios using both JPEG and JPEG2000. Overall, the errors associated with compression seem quite modest. The wavelet-based JPEG2000 method provided similar results (both visual and centroiding) typically at ~3X higher compression ratios than with the older JPEG algorithm, which uses discrete cosine transforms (DCT). But as might be expected, the newer JPEG2000 algorithm is computationally more intensive.

### 8.1.3 Baselining of real-time compression

These promising centroiding results suggested that we could compute centroids accurately enough from compressed image data that we might not ever need to download raw image data. This led us to consider again whether we could compress the image data in real time because then we could significantly reduce the amount of on-board memory required to store images until download. The onboard storage requirement was mainly driven by the deployment phase, which requires longer sustained imaging than is required later. Based on additional analyses, Ecliptic indicated that real-time compression by a single compressor should be feasible at the desired imaging rates, within the current specified ODS power and mass budget. The architecture compresses images from different cameras in sequence. That requires a buffer memory for each camera as shown later in Figure 8-4 (as part of the “camera electronics” module).

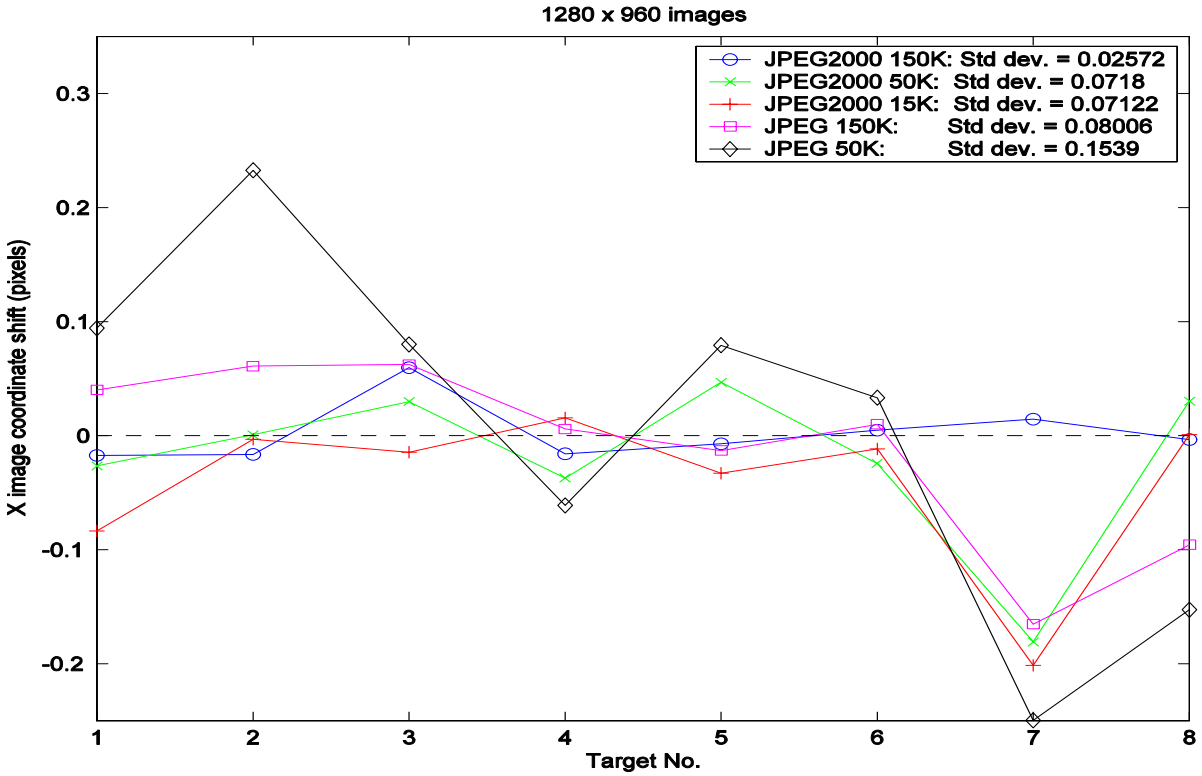


Figure 8-1. Compression Test: X Image Coordinate Shifts

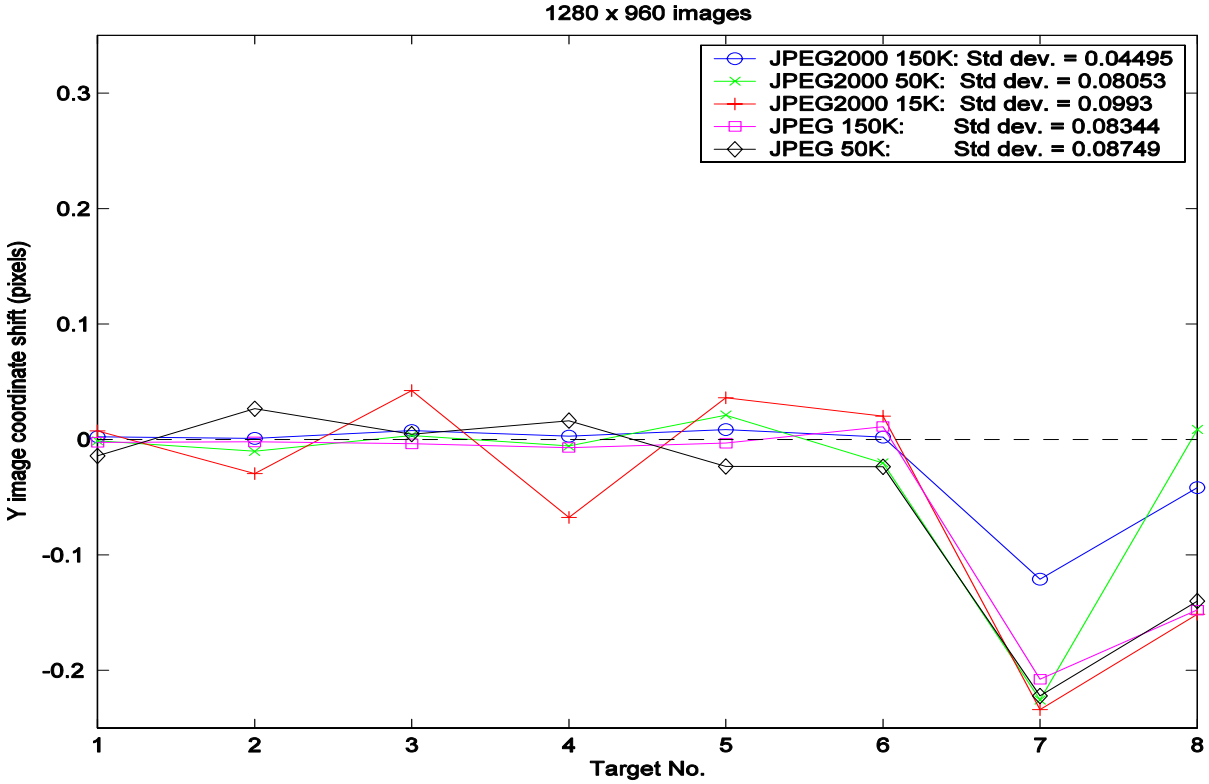


Figure 8-2. Compression Tests: Y Image Coordinate Shifts

### 8.1.4 Centroiding as an auxiliary form of image compression

In parallel with the above study of real-time compression, we also looked at real-time centroiding. The main value may be download of more useful data in real time. The effective compression ratio of centroid data may be of order ~2000:1. This compression ratio assumes that a set of twenty 10-bit SXGA images includes ~1600 usable bright spots (including multiply imaged targets and "false targets"), and that each bright-spot centroid requires ~80 bits to characterize its position, brightness, size, shape, and other features.

Centroiding should take far less computational power than JPEG2000. Preliminary analyses suggest that scanning the images to find bright spots may take more time than computing centroid position. One way around this is to use low-level logic to "snoop" on the two high-order bits of the image data during readout from the imager. Non-zero high-order bits can trigger capture of timer values. These timer values indicate the column and row of candidate bright spots. After the full image is downloaded and available for random-access readout, an algorithm can check each bright spot detected and decide whether to process it. It can use criteria such as nearby glare, contrast with surrounding pixels, brightness, size, shape, uniformity of target brightness, and other indicators that should preferentially select real targets over glint or glare.

This procedure is not incompatible with also doing conventional image compression using JPEG2000, MPEG, or other algorithms. It is an additional option that provides extremely compressed but directly useful data with a minimum of special hardware and computer power.

### 8.1.5 Estimated data budget (capture, compression, and download)

One can limit the amount of data to download by limiting how much is collected, or compressing it real time, or later, or by being selective about what to download or how far to send it. Limiting collection (i.e., reducing image resolution or image rate) is simplest but gives the least useful data. It is not yet entirely clear whether compressing it in real time will be more or less demanding (in power, mass, and developmental cost) than storing it and compressing it more slowly later. Other options include downloading only a subset of the captured images (e.g.,

every Nth image, plus those acquired during any interesting events such as accelerometer spikes). Then we would analyze those images and other data to decide what else to download. We might even overwrite some imagery before it is downloaded if deployment proceeds normally. Also, if the first mission occurs in LEO, or at least starts there, it may be feasible to collect and download large amounts of data without requiring high compression. It seems worth examining these options in more detail later as their implications and the likely mission details become clearer.

Table 8-1 shows a preliminary data budget. It assumes only 8-bit data for each pixel, and it assumes higher-rate imagery at the start and end of deployment than during the hour in between, with a peak of 80 frames/second to be compressed. Dynamic tests and triggered-event needs do not exceed those of deployment. The budget shows the contributions of the different types of activities and the importance of compression and centroiding in reducing download needs.

**Table 8-1. Estimated ODS Imaging Data Volume Requirements**

| Parameter | Units | Sail Deployment Activities | | | Dynamical Surveys | | Triggered Events | |
|---|---|---|---|---|---|---|---|---|
| Mission Phase | | Release | Deploy | Lock | Imagery | Centroids | Imagery | Centroids |
| Duration | s | **60** | **3600** | **60** | **300** | **300** | **120** | **120** |
| | | | | | | | | |
| Image Format, X | | 1280 | | | | | | |
| Image Format, Y | | 1024 | | | | | | |
| Pixels | Mpx | 1.31 | | | | | | |
| Pixel Depth | bits | 8 | | | | | | |
| Image Size | Mb | 10.49 | | | | | | |
| | | | | | | | | |
| Frame Rate | fps | 4 | 0.5 | 4 | 4 | 4 | 4 | 4 |
| Active Cameras | | 8 | 20 | 20 | 20 | 20 | 20 | 20 |
| **Raw Pixel Rate** | **Mpx/s** | **42** | **13** | **105** | **105** | **105** | **105** | **105** |
| **Raw Data Rate** | **Mb/s** | **336** | **105** | **839** | **839** | **839** | **839** | **839** |
| Raw Data Volume | MB | 2517 | 47186 | 6291 | 31457 | 31457 | 12583 | 12583 |
| | | | | | | | | |
| Compression Ratio | :1 | 25 | 80 | 25 | 80 | 2000 | 80 | 2000 |
| **Compressed Data Volume** | **MB** | **101** | **590** | **252** | **393** | **16** | **157** | **6** |
| Compressed Data Rate | MB/s | 1.7 | 0.2 | 4.2 | 1.3 | 0.1 | 1.3 | 0.1 |
| Total Deployment Data Volume | | ----- | **942** | ----- | | | | |
| | | | | | | | | |
| Downlink Data Rate | kbps | | 100 | | 100 | 100 | 100 | 100 |
| Downlink Efficiency | | | 90% | | 90% | 90% | 90% | 90% |
| Downlink Duration | hr | | 23 | | 10 | 0.4 | 4 | 0.2 |

## *8.2 Maturation of real-time JPEG2000 compression scheme*

The major issue here is whether flight-worthy JPEG2000 compression hardware and software will allow a sustained throughput of ~80 SXGA images/second (1280x1024 pixels each) with acceptable system mass, power, and cost. Better hardware is becoming available over time. The real questions are what throughput we will actually need, and whether suitable flight-worthy hardware will be available when the design must be frozen.

Our recommendation is to pursue development as funds become available, while periodically reviewing what image capture rates are really needed. If the desired imaging rates increase beyond what JPEG2000 compressors can handle, or if we run into other difficulties, MPEG options and/or a backup architecture described below may be worth attention.

### 8.2.1 A developmental backup to real-time compression: storing raw data in flash memory

It appears feasible to download raw image data into high-capacity, serial-access NAND flash memory chips. We need 10 memory chips per imager. Sequenced latching of pixel data allows 4 pixels of 10-bit image data to be buffered into 5 flash chips with a 48Mpixel/sec readout rate and 12MHz flash chip data rate. To capture even a single image, 2 banks of 5 chips are needed. One bank stores several lines of image data into a page buffer while the other goes off-line and programs the page into non-volatile memory. Those 10 memory chips can do sustained image capture at any desired rate up to the maximum for the imager (on the order of 30Hz). The highest-capacity chips now available are 1Gx8 Samsung chips. Ten such chips can store 6553 raw SXGA images. This allows 1 Hz imaging for over an hour, plus bursts up to 30Hz for much shorter periods that may be of particular dynamic interest such as the very beginning and end of deployment. Added images can be captured once earlier images have been post-processed or discarded. A single microcontroller might control 4 or more cameras, including image capture, real-time centroiding, and low-throughput software-based JPEG2000 compression.

The most risky aspect of this concept may be the high consumer demand and resulting delivery backlog for serial NAND flash chips due to their popularity in electronic cameras and other products. Cost, mass, power, and radiation tolerance should be less serious issues.

## 8.3 *Baseline avionics architecture*

Figure 8-3 shows the baseline ODS configuration. A central command and data handling (C&DH) computer provides overall instrument control and the single point interface with the host spacecraft. The 23 focal planes of the baseline configuration are divided into three groups by function and location. These are the boom view cameras (4 focal planes), the sail view assemblies (16 focal planes), and the inspection (pan/tilt) assembly (3 focal planes).

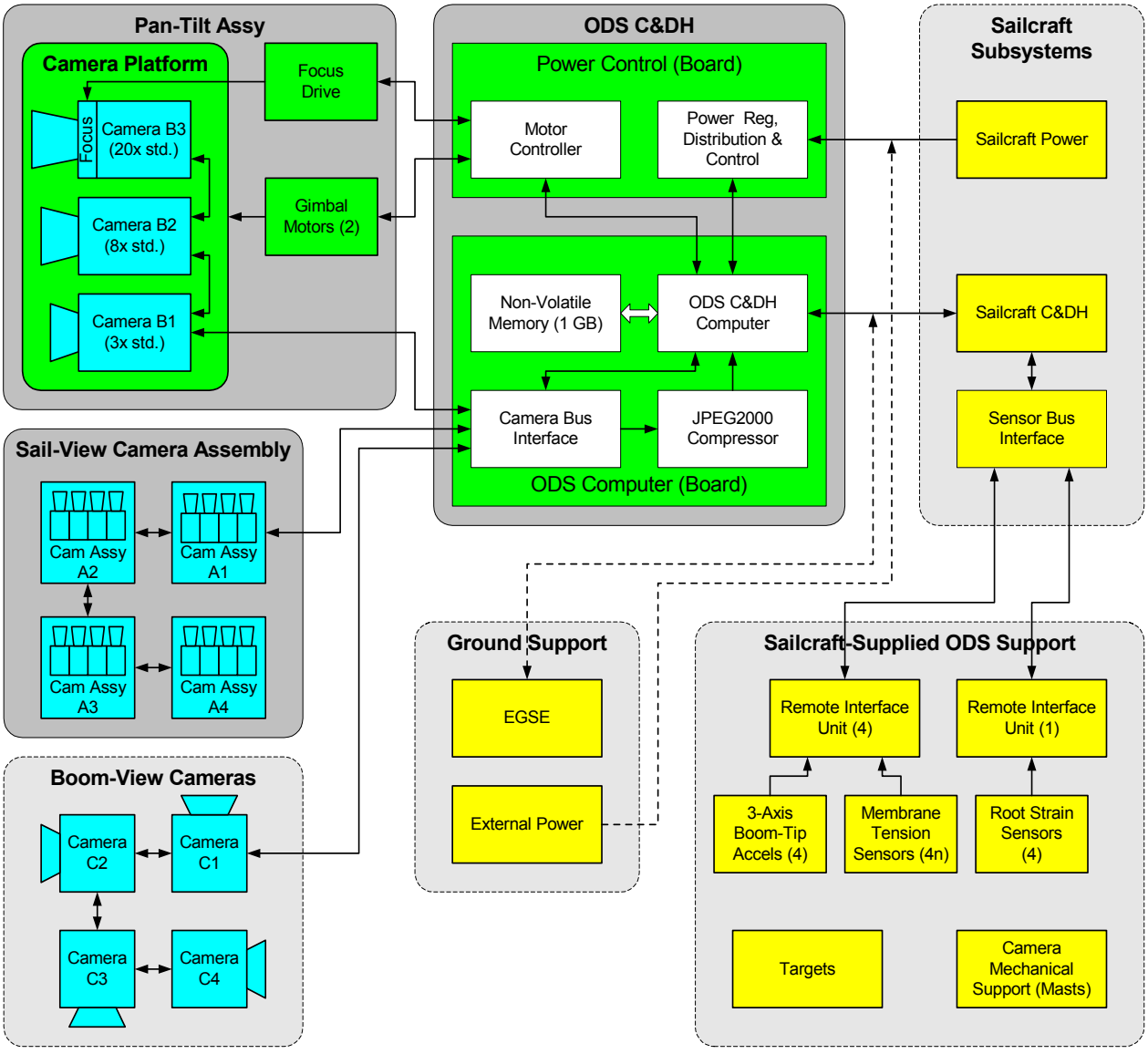


**Figure 8-3. Avionics System Block Diagram**

Imager control electronics will be distributed to each camera head, with a FPGA handling low level controls such as detector control, auto-exposure, and windowing (see Fig. 8-4), as well as buffer management, real-time centroiding, and communication with the C&DH system. Although each sail view assembly contains 4 Focal Plane Arrays, it is logically one camera and has one set of control logic (see Fig. 8-4). The other two camera groups (boom view and inspection assembly) use similar logic in different configurations. Each camera assembly communicates with the CPU over a bi-directional, synchronous serial LVDS link. Within each imager group, the individual imagers are daisy chained together. This shares bandwidth but reduces cabling requirements.

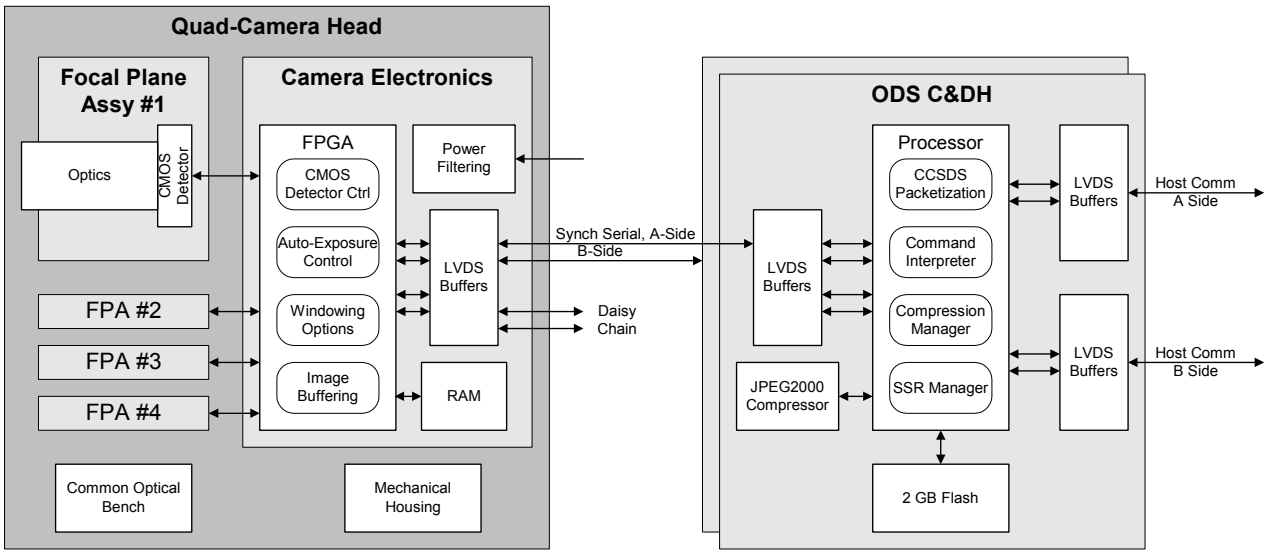


**Figure 8-4. Data Flow Block Diagram**

The primary requirements on the C&DH computer are for a large storage capacity, high throughput, and high-speed data compression. The general-purpose computation requirements (primarily C&DH housekeeping) are minor by comparison. The baseline configuration calls for a single board computer with four primary functional blocks: a moderate-performance general purpose CPU with high speed data throughput, a 1 gigabyte non-volatile (flash) memory, host communications (serial LVDS or RS-422), high-speed camera interface (serial LVDS), and a dedicated compression block running one or more JPEG2000 application-specific integrated circuits (ASICs). Collocated with the computer board is a power distribution board powering the C&DH and cameras, which includes motor controllers for the pan/tilt inspection assembly.

The system architecture allows for block redundancy in the C&DH system. Such redundancy is impractical in the camera assemblies within the allocated ODS mass and power budgets. But the imagers have high functional redundancy. Any single focal plane in the sail view assembly overlaps its neighbors, so that the loss of a single focal plane will result in only a small loss of coverage. And if a focal plane is lost, the inspection camera assembly provides a redundant capability to the sail view assembly.

## *8.4 Impacts of space environment on avionics requirements and design*

### 8.4.1 Radiation effects

Spacecraft electronics need to be designed to tolerate single event effects including upset, latchup, and functional interrupt. They can disable a spacecraft at or near the start of its mission. By contrast, we can select hardware known to tolerate specific levels of total ionizing dose, for a given orbit and mission duration. Orbits that spend significant time in or near the heart of the van Allen belts (~1.3-2Re) will see far higher radiation dosages than other missions, but these doses will be accumulated gradually. If the sailcraft starts in LEO and spirals upward, the ODS job of characterizing deployment and operational dynamics may be complete before the electronics fail. But if the spacecraft starts in a GTO-like orbit, passing through the heart of the belts even at the beginning of the mission, total dose accumulates much faster, and careful attention may be necessary to verify that the ODS electronics will last long enough.

### 8.4.2 Other space-environment effects on avionics

Radiation may be the most serious issue for most of the avionics, but other issues should not be neglected. They include thermal cycling and extreme temperatures (which may particularly affect solder joints on surface-mount parts), venting during boost (which can cause structural overloads), outgassing (which can contaminate optics and change equilibrium component temperatures), and electrical discharges during passes through auroral zones. There does not seem to be a particular need to focus on these issues at this phase of ODS development, because the key issues are fairly generic and familiar to spacecraft avionics developers.

## *8.5 Recommendations on avionics TRL gaps that need to be filled*

Most of the ODS avionics functions are routine spacecraft avionics functions, with technology readiness levels (TRLs) of 6-9. The exact TRL depends on whether ODS avionics uses hardware that has already flown. Routine functions include collecting non-imaging sensor data, switching devices on and off, formatting data for telemetry, validating commands and possibly code patches, and doing other supporting housekeeping and status checks.

Those aspects of the baseline avionics with low TRL are associated with high-throughput imaging: mostly controlling >20 SXGA imagers, capturing 80 frames/sec (total), and doing real-time JPEG2000 compression and centroiding. The two Mars Exploration Rovers have a similar numbers of cameras, mostly for self-inspection. But they do not have any high-rate capture or compression requirements, and they may not do centroiding at all.

The main key TRL gap is verifying that we can do JPEG2000 compression at a sustained rate of ~80 SXGA frames/second. JPEG2000 does not use frame-to-frame similarity, so a single frame test using a high-speed buffer may be adequate. We need to determine:

1. How fast we can download one stored SXGA image (using LVDS or another interface)
2. How long it takes to compress it (which may vary with the image and compression ratio)
3. How easily we can double-buffer, to download one image while compressing another.

Careful analysis of hardware specifications may eliminate most risk. But if JPEG2000 compression time varies with image content or compression ratio, we need tests on suitable images. And we do need good tests eventually (including radiation tests) to verify that there are no problems that may require our switching to raw-image capture plus later compression at lower rates, or switching to MPEG compressors if they allow higher throughput or compression.

Star trackers do bright-spot detection and centroiding. But the TRL is much lower for doing those tasks at ~80 SXGA frames/second on “noisy” solar sail images. We need to develop and test suitable algorithms, first on PCs and then on more flight-like hardware. It may be feasible to do the centroiding using mostly the same hardware used for conventional image compression.

# Section 9

# Photogrammetry Test of 10m Sail Quadrant

## *9.1 Scope and Challenges of the Test*

A proof-of-concept photogrammetry test was conducted using the ODS baseline camera configuration (Section 3) with commercial, off-the-shelf digital cameras and diffuse-white circular targets distributed on a 10m solar sail quadrant. This test demonstrated the feasibility of measuring solar sail shape with cameras located at two elevations on a relatively short longitudinal boom (perpendicular to sail plane) extended from the hub of the spacecraft.

Note that although good results were obtained after considerable effort in the image analysis phase, the ODS baseline camera geometry (four overlapping cameras per quadrant at lower station and one camera on pan-tilt at upper station of the camera mast) is unusually challenging compared with typical geometries used in high-precision, close-range photogrammetry tests where additional camera locations--typically around the periphery of the object--are permitted. Initial studies in Phase 1 concluded that to minimize changes in the existing solar sail designs (a customer Level 1 requirement) that mounting ODS cameras along a central boom was the only logical choice, and that the job of the ODS team was to do the best it could from this location. Section 3.1 discusses several other camera configurations that were considered.

The ODS baseline geometry is technically challenging for photogrammetry for several reasons, including: 1) the camera stations are closely spaced along the camera support mast (10% of sail edge dimension) and there is no camera separation perpendicular to the support mast, 2) the cameras view the sail at a relatively shallow angle so there is considerable target foreshortening in the images, and 3) camera self-calibration, which requires roving camera positions and roll diversity, cannot be performed. Recently the images acquired in this test were reanalyzed using more-advanced software (*Australis* [Ref. 9-1] vs. *PhotoModeler* [Ref. 9-2]) in an attempt to improve the robustness of the solution with better analysis approaches and

algorithms. However, to date these efforts have been unsuccessful. The ODS team will continue to evaluate and improve the robustness of the baseline camera configuration and data analysis procedures during Phase 2. In Phase 2 we will also conduct photogrammetric parametric studies and optimizations using *Australis* and other simulation tools.

## *9.2 Test Configuration*

The ODS proof-of-concept photogrammetry test used the 10m solar sail quadrant shown in Fig. 9-1. This seamed, 7-micron CP1 membrane was manufactured by SRS Technologies under a LaRC SBIR program and contains an early design of a shear compliant border to minimize membrane wrinkling. Dead weights on pulleys applied pre-tension loads of 5 lbs at each 45-deg corner. The test was conducted in air in the high-bay lab of Bldg. 1293 at NASA LaRC. Only static shape measurements were made; there was no attempt yet to measure structural dynamic characteristics (i.e., vibration properties). The room was darkened during the test except for a single illumination source, which was a 1000 W facility light (with built-in horizontal cylindrical reflector) located approximately 30 ft to the left and 30 ft above the center of the sail as viewed from the camera position of Fig. 9-1. The air handlers in the room were also turned off to avoid inadvertent movement of the membrane between photographs.

**Note:** The final ODS baseline camera configuration presented at the Phase 1 final review on January 14, 2004 specified camera platform heights of 15% (lower platform) and 25% (upper platform) of the edge sail dimension. The team selected these final values for the baseline shortly before the Phase 1 review, and there was not enough time to run another proof-of-concept test using these exact camera locations. The results presented in this section (and presented at the Phase 1 review) correspond to camera platform heights of 10% (lower platform) and 20% (upper platform) of the edge sail dimension. The platform separation distance is the correct baseline value of 10%, but both cameras are located 5% lower than in the baseline concept. Raising both camera platforms an additional 5% provides a slightly better viewing angle to the targets from the lower platform, which is particularly important with the L'Garde scalloped membrane design. Raising the upper platform still higher would improve both the stereo triangulation precision and our ability to inspect the sail particularly at distant locations. However, this option must be balanced with the associated increases in cost, integration complexity, and possible

dynamic interaction issues using a longer camera mast. We will re-examine these platform height selection decisions in Phase 2.

## *9.3 "Truth" Targets on Membrane Frame*

Forty-seven retroreflective targets on precision machined tool pieces as detailed in Fig. 9-1 were distributed on the rigid aluminum frame surrounding the membrane to provide a set of "truth" 3D coordinates in the test. (Hubbs Machine and Manufacturing, Inc. [Ref. 9-3] produced these targets.) The 3D location of each retroreflective target was measured to a 1-sigma accuracy of approximately 0.004 inches in a prior test using a state-of-the-art Geodetic Services *V-STARS* industrial photogrammetry system [Ref. 9-4]. These coordinates can be compared with corresponding 3D coordinates calculated with the ODS images to determine absolute ODS measurement accuracy, which is estimated to be at least 10x less than *V-STARS* accuracy. Relative ODS measurement accuracy can also be determined by comparing known separation distances of various target pairs with corresponding truth values as detailed in Fig. 9-1. The *V-STARS* system currently can only measure retroreflective targets, so we were unable at this time to also measure "truth" coordinates for the diffuse-white ODS targets on the membrane with this top-end system. We will investigate ways to circumvent this limitation in Phase 2. Nevertheless, by comparing *V-STARS* and ODS-calculated coordinates at numerous locations on the membrane boundary frame, the accuracy expected for the interior ODS target points--if they are centroided as accurately as the retroreflective targets--can be inferred. Of course, the diffuse white targets on the sail will probably not be centroided as accurately as the retroreflective targets because their contrast ratio with the surrounding background is lower.

This test used the INCA1 model camera having a measurement accuracy of approximately 1 part in 100,000 (1:100,000) of the object size. We recently upgraded this camera to the latest version, an INCA3 model, having a measurement accuracy of approximately 1 part in 160,000 (1:160,000) of the object size. The INCA3 camera used with the *V-STARS* software is the most accurate digital photogrammetry system available on the market today. It will be used in Phase 2 testing for the ODS program.

## *9.4 ODS Targets and Camera Description*

Figure 9-2 shows the grid of 52 targets placed on the membrane for these tests. The target spacing in the center region is approximately 1 m, and the spacing on the border is approximately 0.5 m. Targets were installed by hand and no attempt was made to precisely locate them. The target diameter was 1.25 inches. Figure 9-3 shows a close up of a typical target on the sail. The target material was standard bright-white Xerox paper, and the targets were attached using removable adhesive (3M remount spray adhesive) to allow easy removal if necessary.

Based on recent additional analyses, the recommended minimum number of targets per quadrant is now 100 (rather than 52). Therefore, the results provided in this section are conservative estimates of ODS measurement accuracy because adding additional targets to each quadrant should improve photogrammetric accuracy. The reason for this is that additional targets allow the software to make small adjustments more accurately in the calculated camera orientations (i.e., the 3D locations and pointing directions of the cameras). Errors in camera orientations, particularly the pointing directions, can significantly affect the photogrammetrically calculated 3D target coordinates.

A single off-the-shelf Olympus C-5050 digital camera, shown in Fig. 9-4, was used for all photography in this proof-of-concept test. It was pre-calibrated using the target grid and procedure supplied with the *PhotoModeler* software package, in which a grid of 100 targets is photographed from several viewing directions, the camera is rotated 90 degrees in some of the photographs, and then the images are analyzed simultaneously with a self-calibrating bundle adjustment algorithm. The consumer-grade Olympus C-5050 is a 5 megapixel (2560 x 1920) color CCD camera with an effective measurement resolution approximately equal to the ODS baseline scientific-grade 1.3 megapixel (1280 x 1024) monochrome CMOS camera. (Color cameras have significantly less resolution than monochrome units because of the color mask on the sensor and subsequent image interpolation, and consumer-grade cameras are manufactured to lower tolerances than scientific-grade cameras.) It has a built-in 3x motorized zoom lens that was used at two zoom settings (focal lengths of 7.1 and 11.3 mm) in the test.

For stability the camera was mounted on a tripod (adjustable to heights of 1m and 2m above the sail plane) and fired with a remote shutter release switch. The tripod was positioned 30 inches (0.8 m) behind the 90-deg corner of the aluminum boundary frame. All photography used an aperture setting of f/8 and an exposure time of 1.0 sec. The built-in flash was set to a low intensity that was sufficient to illuminate the retroreflective targets on the membrane boundary but did not wash out the diffuse white ODS targets on the membrane surface. The tripod was adjusted to two different heights, 1 m and then 2 m above the sail, and four images were shot at each height. The eight images were acquired in as short a period of time as possible (approx. 15 minutes) to maximize consistency of the data set. In Phase 2, we will use 8 synchronized scientific video cameras for additional ODS development tests of this type. With this new capability, all imagery will be acquired at exactly the same instant, just as it will be in space. These cameras will be capable of measuring both the static shape and the dynamics (i.e., vibration characteristics) of a sail quadrant system.

## *9.5 Imagery*

Figure 9-5 shows the approximate viewing areas of each photograph taken at the upper camera elevation (20% of the sail edge dimension above the sail plane). Viewing areas from the lower camera elevation (10% of the sail edge dimension above the sail plane) are similar but include additional sail area closer to the camera because of the perspective foreshortening effect. At both elevations, Camera Views 1-3 used a focal length of 11.3 mm and Camera View 4 used a focal length of 7.1 mm. At 11.3 mm the horizontal field of view is 35 degrees, and at 7.1 mm it is 53 degrees. Note that ellipses are plotted in this graphic for simplicity. The projected viewings areas are in fact trapezoidal, which are wider near the back of the sail than near the front.

Figures 9-6 and 9-7 show the four images from each camera elevation. The cameras were oriented to include both the membrane and the boundary support frame. In space, slightly more membrane area would be imaged since there would be no rear support frame (along the hypotenuse of the quadrant). Also, in space the inner and outer cameras (Cameras 1 and 3 in Fig. 9-5) will probably be rolled slightly to better fill the image areas, allowing more of an adjacent quadrant to be imaged rather then deep space at the top of the membrane.

The two white lines on the membrane were not used in this ODS proof-of-concept test. In another investigation they provided discrete boundaries for photogrammetric line tracking methods (tracking the shape of the horizontal seam lines). These methods were briefly examined but have not been successfully implemented to date. The ODS baseline configuration does not require these white lines for photogrammetry measurements.

Figure 9-8 shows close-up views from both camera elevations of several targets on the membrane. Notable aspects of this imagery are:

- Target contrast from Camera 3, which looks away from the single illumination source located above and to the left of the sail, is considerably higher than the contrast from Camera 1.
- Membrane creasing (caused by folding and handling) causes significant glints near several targets in the images from Camera 1, which will reduce target centroiding accuracy.
- Some target images are slightly non-elliptical due to membrane unflatness.
- Greater target foreshortening occurs at the lower camera station as expected due to the perspective.

## *9.6 Data Analysis Procedure and Results*

The eight images shown in Figs. 9-6 and 9-7 were analyzed as a single project using the commercial PhotoModeler photogrammetry software [Ref. 9-2]. Reference 9-5 details the data analysis procedure that was followed, and it will not be repeated here. In summary, the main steps are as follows:

- Mark the target locations in each image (known as “marking” or “centroiding”)
- Identify which points in the images refer to the same physical point (known as “referencing” or “correspondence”)
- Process, scale, and rotate the data
- Examine results and export for additional analyses

As mentioned earlier, the ODS geometry is technically challenging for photogrammetry for several reasons. A significant contributing factor is the relatively small angle between the two camera stations and the targets. For a vertical camera separation distance of 1 m (10% of sail edge dimension--the ODS baseline value), all targets further than 3.8 m from the cameras will have a relative viewing angle between the upper and lower camera stations of under 15 degs. Because the cameras are located 0.8 m behind the 90 deg corner, this region extends only 3.0 m into the sail quadrant. Fifteen degrees is the default minimum angle that PhotoModeler expects there to be between camera views to provide a robust, repeatable solution. Therefore, we needed to disable the default minimum value in the software and attempt a solution allowing smaller included angles for about half of the targets in the project. In order to have all angles above 15 degs requires a camera separation of at least 2.1 m (21% of sail edge dimension). Lengthening the camera mast for a flight experiment may unnecessarily complicate the design if acceptable solutions can be obtained at the shorter length. In Phase 2 we will measure the effects of greater camera separation distances using both experimental and simulated data sets.

The default PhotoModeler solution approach, which was followed here, uses a robust relative orientation calculation to estimate the camera 3D locations and orientation angles (known as the camera exterior parameters) prior to refining these values for each camera, in addition to computing the target 3D coordinates, in a free network (a.k.a. an inner constraints network) bundle adjustment. (Theoretically, a free network solution gives the minimum trace solution and is thus the most precise.) The relative orientation calculation makes no prior assumptions about the exterior parameters. In previous unrelated projects, it provided the correct solution the vast majority of the time. An alternative orientation approach is to resect each image individually using at least four control points per image. Resection is the technical term for calculating the 3D location and orientation angles (a.k.a. its pose) using control points. Control points are identifiable targets with known 3D coordinates. To obtain an accurate resection, the control points should be widely distributed in the image, preferably in three dimensions, and their coordinates must be known as accurately as possible. This is not always easy to achieve. In Phase 2 we will compare the effectiveness of using control points and camera resection against using a traditional relative orientation calculation.

PhotoModeler is best used in an iterative manner in most projects. That is, at the beginning of the data analysis only a few points and a few photographs are marked. Once perhaps 10 to 15 points are marked and referenced on three or four photographs, they are processed with the free-net bungle algorithm. Having confidence in that result, additional new markings and new photographs are added in stages, doing another bundle solution at each phase. This approach greatly minimizes the chances that errors will be made that are difficult to find or fix.

With the eight ODS images, this iterative analysis process often produced incorrect results in the early stages. Specifically, the computed camera locations and orientation angles were often poorly computed. If these values are not accurately calculated, subsequent bundle solutions will fail. Figure 9-9 shows an example of one of these intermediate and incorrect results. At this point, approximately 50 points have been marked and referenced and six of the eight images are included in the analysis. The computed camera locations are clearly incorrect, and the corresponding membrane shape is much more concave (curled up at the outer edges) than it should be.

However, after slowly adding additional points, and especially increasing the number of marked and referenced points that overlapping images had in common, PhotoModeler was eventually able to obtain an accurate solution, shown in Fig. 9-10. Visual examination showed all eight cameras to have the locations and orientations that were used in the test, and the sail membrane targets showed a uniformly concave shape with a maximum deflection at the center of the membrane as expected. On the periphery, the 3D coordinates of all 15 pairs of closely spaced retroreflective targets were also accurately computed.

Using these experiences and results as a starting point, in Phase 2 we will examine other data analysis approaches also, in particular those in *Australis*. We recently acquired and have begun successfully using the *Australis* photogrammetry package, written by Prof. Clive Fraser, who also wrote many principal parts of the *V-STARS* software when he was at Geodetic Services, Inc. several years ago. It has the same high computational accuracy and efficiency as *V-STARS,* but it also allows the import and analysis of TIFF images derived from arbitrary sources, something that *V-STARS* does not allow.

## *9.7 Measurement Accuracy*

ODS measurement accuracy, that is, the photogrammetric accuracy achieved using the eight images shown in Figs. 9-6 and 9-7, is now evaluated by comparison of the calculated 3D coordinates of the retroreflective targets on the boundary of the membrane with the "true" coordinates measured with the *V-STARS* system. As mentioned previously (repeated for emphasis), the *V-STARS* system currently can only measure retroreflective targets, so we were unable at this time to also measure "truth" coordinates for the diffuse-white ODS targets on the membrane with this top-end system. Nevertheless, by comparing *V-STARS* and ODS-calculated coordinates at numerous locations on the membrane boundary frame, the accuracy expected for any interior ODS target points--if they are centroided as accurately as the retroreflective targets--can be inferred.

Figure 9-11 shows the relative accuracy achieved for the results shown in Fig. 9-10. The term "relative" is used because only the separation distance of pairs of targets is evaluated, not the absolute, individual 3D target coordinates relative to a fixed reference frame. Relative measurement accuracy is determined using the 15 sets of Hubbs precision-machined "double-vector" targets, the 3 invar scale bars, and the *V-STARS* autobar located on the periphery of the membrane, all having precisely known dimensions (length in one direction for the Hubbs targets and scale bars, and length in all three directions for the autobar). See Fig. 9-1 for more information. Note that all of the Hubbs targets are oriented vertically (i.e., in the out-of-plane direction) while the other objects are oriented horizontally. In Fig. 9-11 the results for the 15 Hubbs targets are underlined. All of these pairs of targets are manufactured with a precise separation distance of 1.000 inches to an accuracy (which was verified in a previous *V-STARS* project) of +/-0.001 inches.

Among these results, the largest relative errors in the calculated separation distances using the ODS images occurred, not surprisingly, in the two rear corners of the testbed, with a global maximum relative error in the vertical direction of 0.060 inches, or 6%. It can be inferred that the targets on the membrane, which are located closer to the camera than the rear-corner boundary targets, will all have less than 6% relative error in the vertical direction if centroided with equal precision. For targets on the membrane, this relative error indicates the maximum

measurement error that would be expected using the ODS baseline configuration for a 1-inch change in membrane shape in the out-of-plane direction (due to vibration or thermal effects, for example). All Hubbs target pairs (i.e., the values underlined in Fig. 9-11) other than those at the two rear corners have relative measurement accuracies in the vertical direction under 3% (i.e., their measured values are between 0.970 and 1.030 inches).

The other values in Fig. 9-11 that are close to 1.000 are for additional double-vector targets located at the ends of three precision Brunson invar scale bars. These are all oriented in the X direction. All six values are comparable to those obtained for the 15 Hubbs targets oriented in the Z direction. There are also two tables in Fig. 9-11. This information compares the true dimensions of the scale bars and autobar with those calculated using the ODS images. Once again, the relative accuracies in the X and Z directions are about 2%. For the autobar, a relative accuracy measurement was also obtained in the Y direction. From the position of the autobar, the Y direction is oriented approximately along the line of sight of the cameras. Because imagers can only detect object coordinate variations normal to their line of sight, this result shows the lowest accuracy, 12%, as would be expected.

Table 9-1 and Figs. 9-12 and 9-13 show the absolute accuracy achieved for the results shown in Fig. 9-10. The term "absolute" is used because the target coordinates calculated photogrammetrically from the ODS images are compared with the absolute, individual 3D target coordinates (i.e., their true locations) relative to a fixed reference frame.

**Table 9-1. Accuracy of the ODS Photogrammetric Measurements**

| | Mean of 47 boundary targets, inches | Max. of 47 boundary targets, inches | Std. deviation (1 sigma) of 47 boundary targets, inches | Std. deviation / sail edge size |
|---|---|---|---|---|
| X direction: | -0.01 | 4.98 | 2.10 | ~ 1:200 |
| Y direction: | -3.62 | 6.64 | 2.83 | ~ 1:150 |
| Z direction: (out of plane) | 0.004 | 0.24 | 0.10 | ~ 1:4000 |
| Total vector: | 3.98 | 8.25 | 3.10 | ~ 1:125 |

Table 9-1 summarizes the results. Of particular interest for application of the ODS baseline measurement configuration to other solar sail sizes is the last column in the table, which lists the measurement accuracy achieved relative to sail edge dimension. Similar accuracies should be expected with other sail sizes using the same camera equipment if all physical dimensions in the design are scaled by an equal amount. The absolute measurement accuracy achieved in the Z direction (out of plane) is by far the largest of the three directions and is approximately 1 part in 4000 of the sail edge dimension. *And it is the Z direction that we certainly have the most interest in.* Note: Among the 47 targets used in this calculation, 20 are located on the back frame of the sail quadrant (along its hypotenuse) and thus are further from the cameras than the ODS targets on the membrane. Because accuracy decreases at larger distances, the numbers presented in Table 1-1 are in fact biased somewhat toward higher values than we would expect to be achieved for targets located on the membrane itself. In this sense they are conservative estimates of ODS measurement accuracy.

Figures 9-12 and 9-13 show the spatial distribution of the absolute measurement errors (total vectors and Z vectors only, respectively). In these plots, the dots indicate the true target locations with the vectors extending from the true target locations to the ODS-measured target locations, with a vector magnification factor applied for better visualization (magnification is x5 in Fig. 9-12 and x200 in Fig. 9-13). For the total error vectors (Fig. 9-12), the measurement errors are clearly predominately in the radial direction relative to the location of the cameras located at the hub of the sail. This is exactly what would be expected because imagers cannot measure along their line of sight. The total error vectors also grow uniformly larger with increasing distance from the cameras. This is also expected because photogrammetric accuracy decreases with distance due to the effects of perspective. Note that the total vectors are rotated to a top view in Fig. 9-12, but when viewed from any other direction the data looks essentially the same (i.e., the out-of-plane total error vector components are extremely small).

Figure 9-13 shows the distribution of the Z (out of plane) error components using an amplitude plotting scale of x200 (rather than x5 as in Fig. 9-12). These results show a random distribution pattern, indicated a negligible bias error in the results. The maximum Z direction

error among the 47 boundary targets is 0.24 inches, and the standard deviation of the results is 0.10 inches, or 1:4000 as shown in Table 9-1.

## *9.8 References*


9-1. Australis photogrammetry software, Photometrix Pty Ltd., website: http:// http://photometrix.com.au/.

9-2. PhotoModeler Pro photogrammetry software, Eos Systems, Inc., website: http:// http://www.photomodeler.com/.

9-3. Hubbs Machine and Machine and Manufacturing, Inc., optical targeting specialists, website: http://www.hubbsmachine.com/.

9-4. V-STARS industrial photogrammetry system, Geodetic Services, Inc., website: http:// http://www.geodetic.com/.

9-5. Pappa, R. S., Jones, T. W., Black, J. T., Walford, A., Robson, S., and Shortis, M. R., "Photogrammetry Methodology Development for Gossamer Spacecraft Structures," *Proceedings of the 3rd AIAA Gossamer Spacecraft Forum*, AIAA Paper 2002-1375, April 2002 (also published as NASA TM-2002-211739, June 2002).

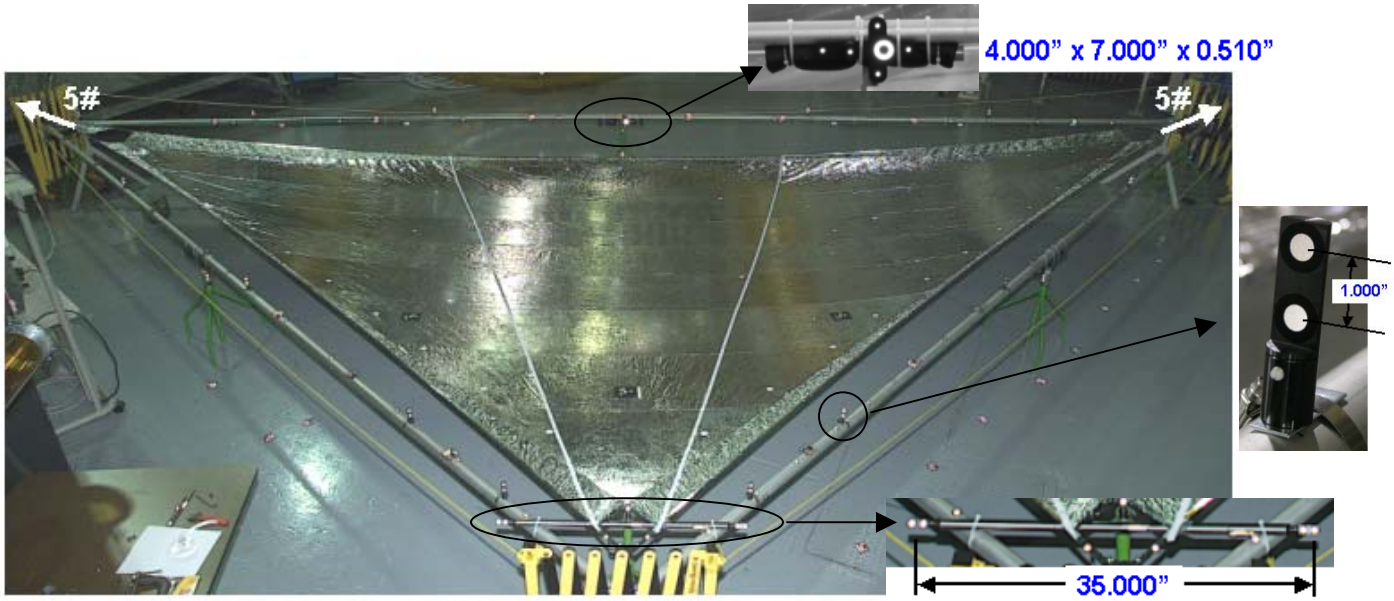


| Four Methods Used for Checking Measurement Accuracy: | Accuracy Checked | No. Targets |
|---|---|---|
| 15 Hubbs precision tooling pieces (1.000 +/- 0.001 inches) | Relative | 30 |
| 3 Scale bars (35.000 and 45.000 +/- 0.001 inches) | Relative | 12 |
| 1 V-STARS autobar (4.000 x 7.000 x 0.510 +/- 0.001 inches) | Relative | 5 |
| V-STARS photogrammetry survey (w/ GSI INCA camera) | Absolute | 47 TOTAL |

**Figure 9-1. SRS 10m sail quadrant used for ODS proof-of-concept photogrammetry test**

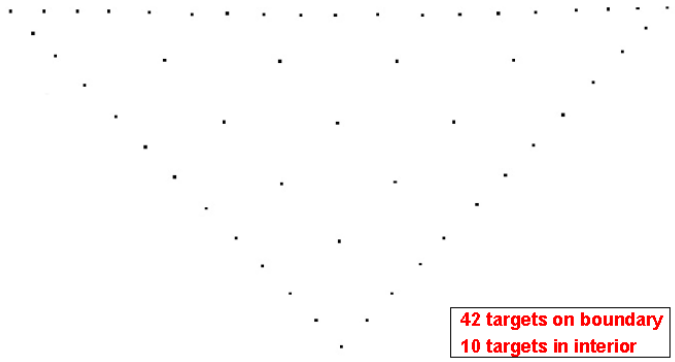


**Figure 9-2. Targets locations on membrane**

**Figure 9-3. Typical target**

**Figure 9-4. Olympus 5-megapixel digital camera used in test**

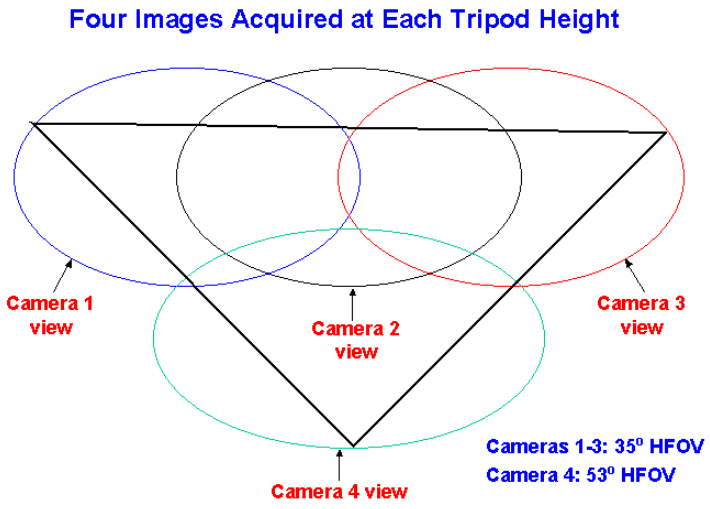


**Figure 9-5. Approximate viewing regions**

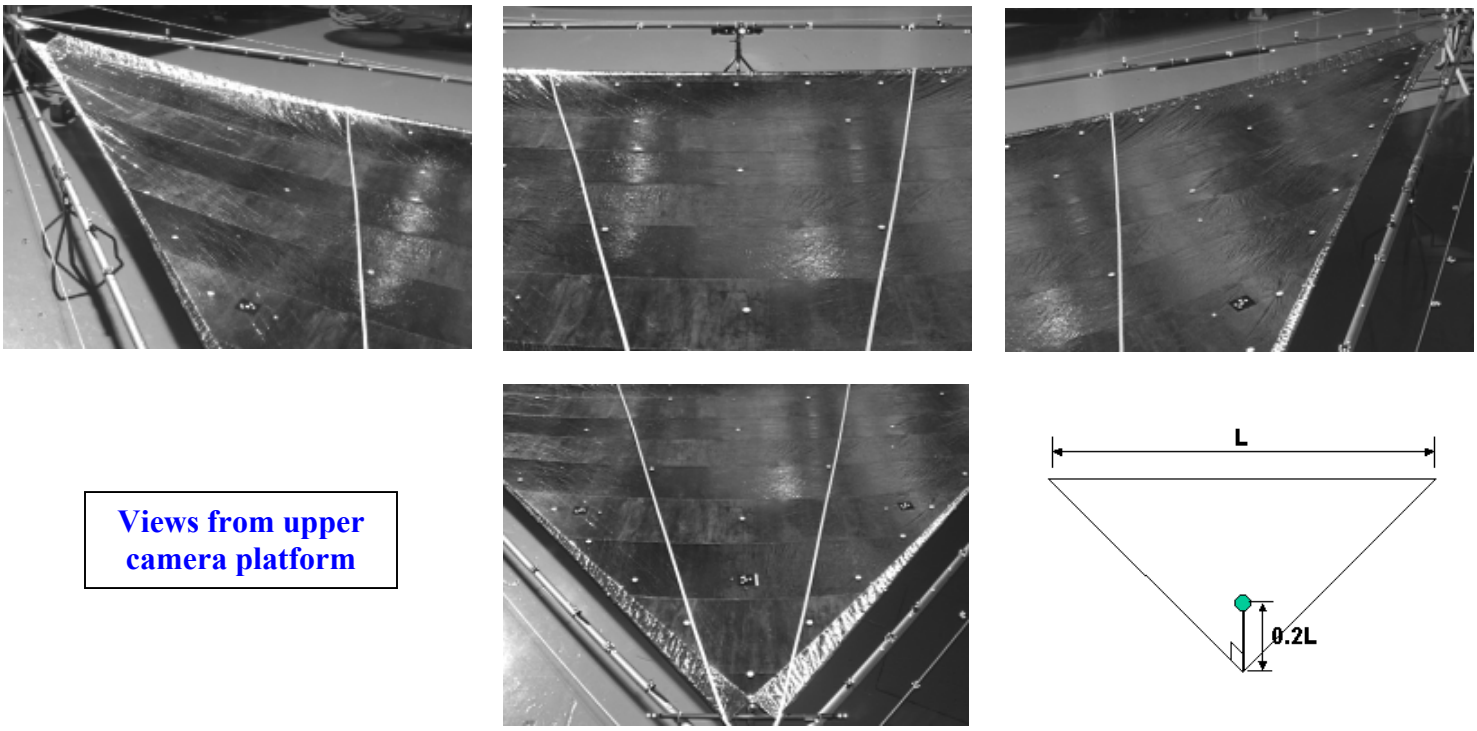


**Figure 9-6. ODS camera views from 2 m above sail (20% of sail edge dimension)**

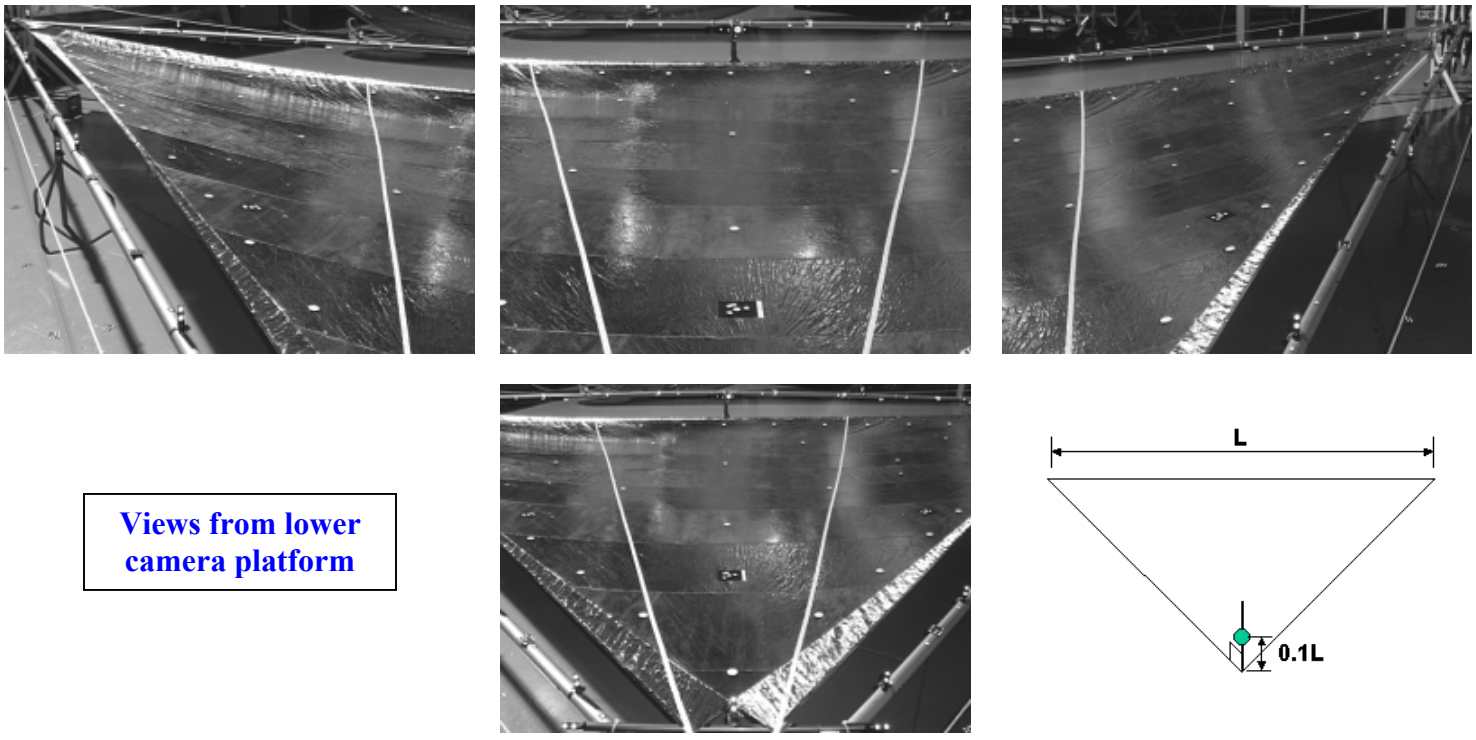


**Figure 9-7. ODS camera views 1 m above sail (10% of sail edge dimension)**

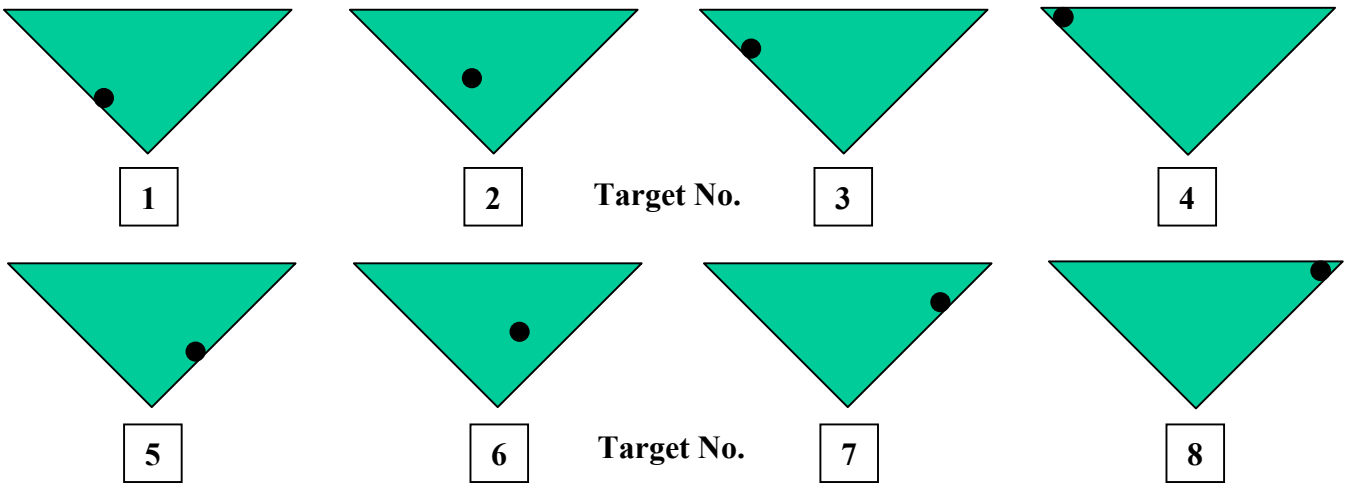


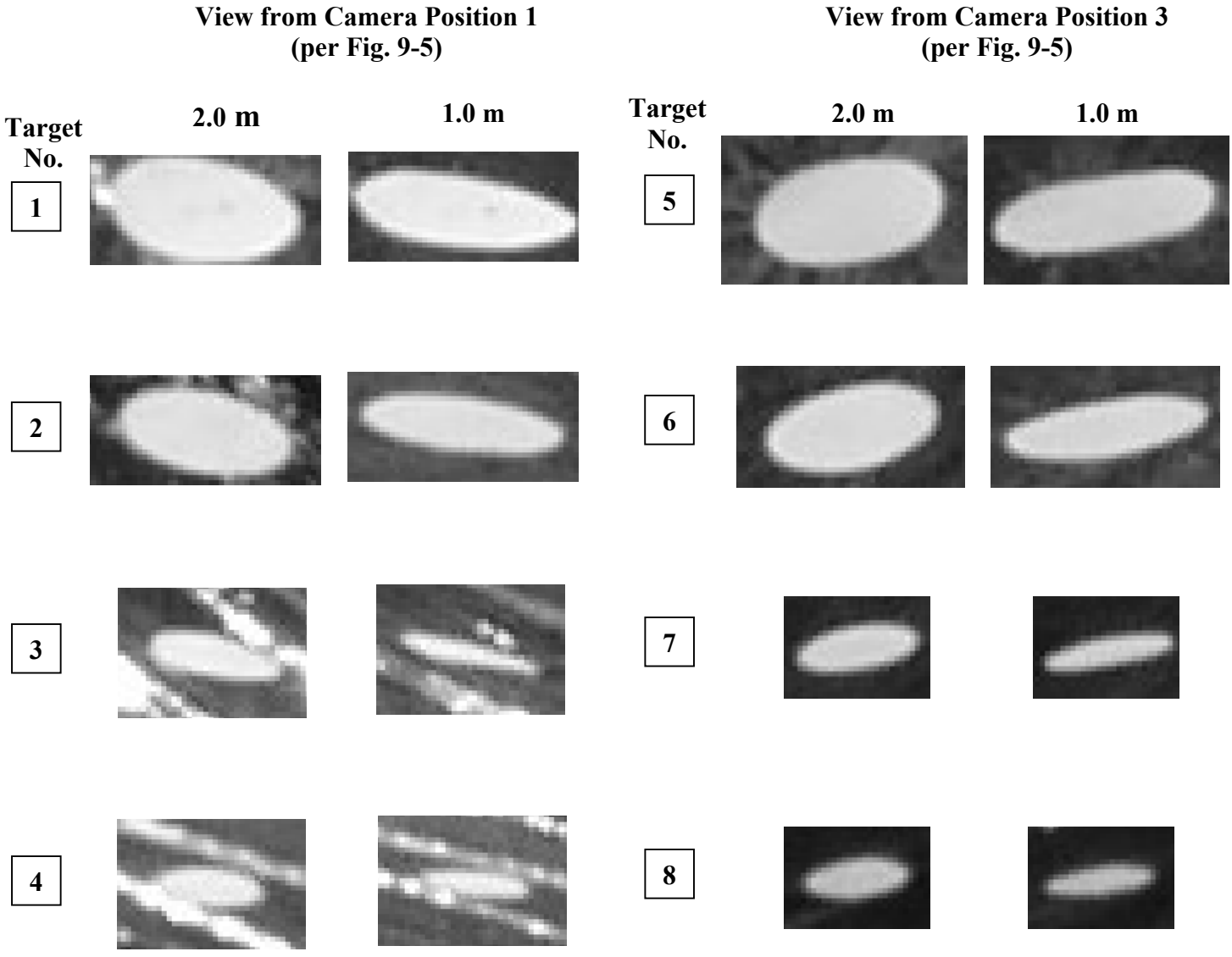


**Figure 9-8. Close up views of select targets from Camera Positions 1 and 3**

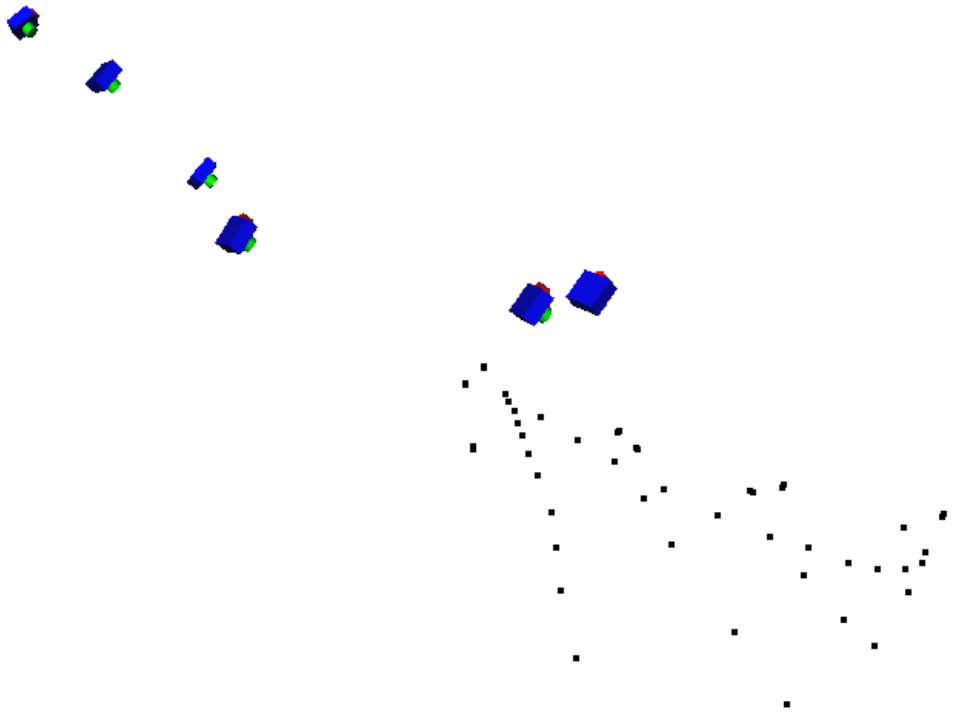

**Figure 9-9. One of many bad camera orientation results encountered during image analysis**

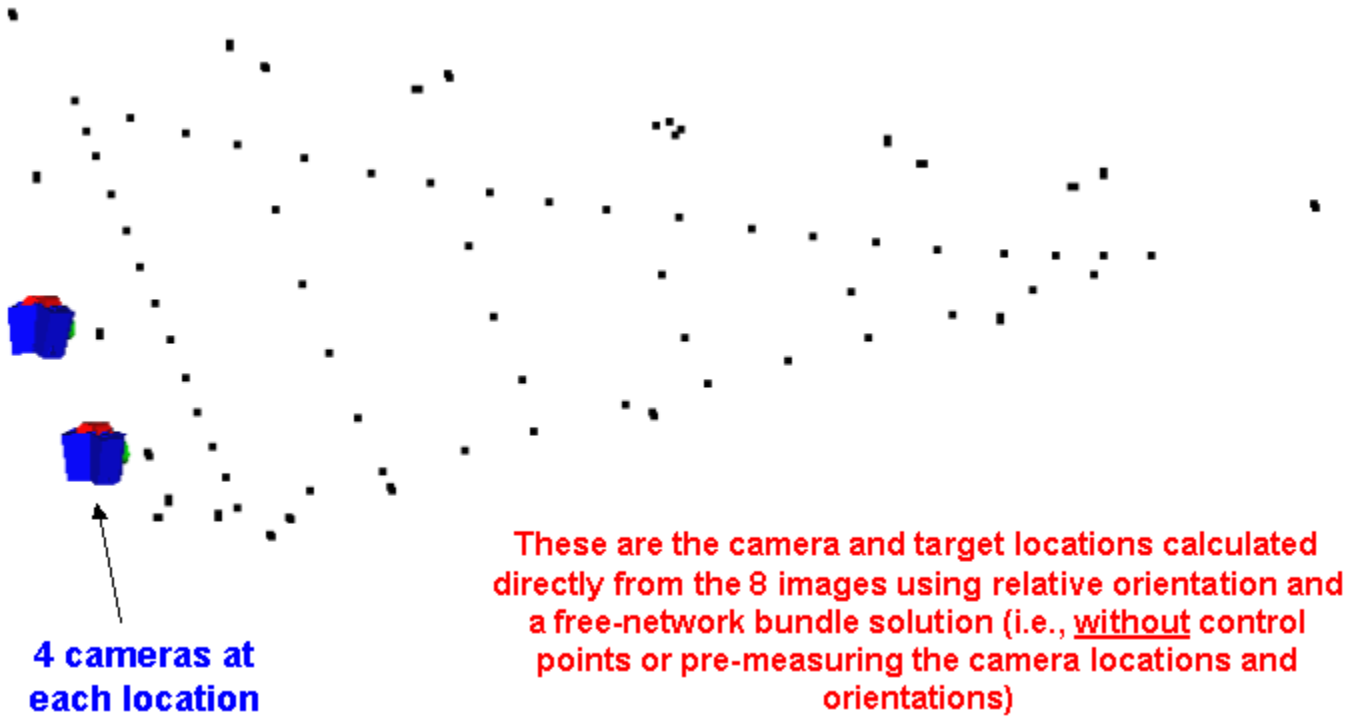


**Figure 9-10. Successful camera orientation and corresponding 3D point coordinates**

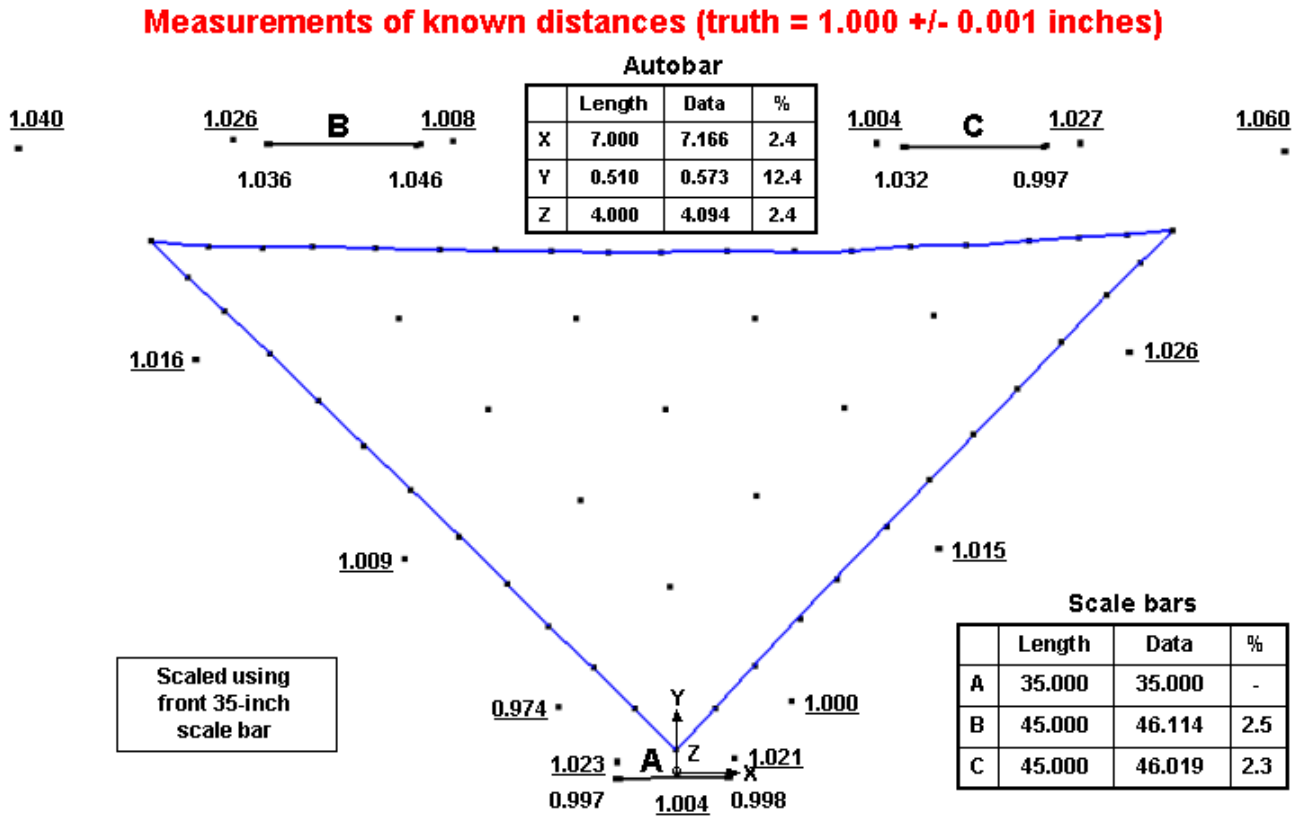


**Figure 9-11. ODS *relative* measurement accuracy with cameras 1 m and 2 m above sail**

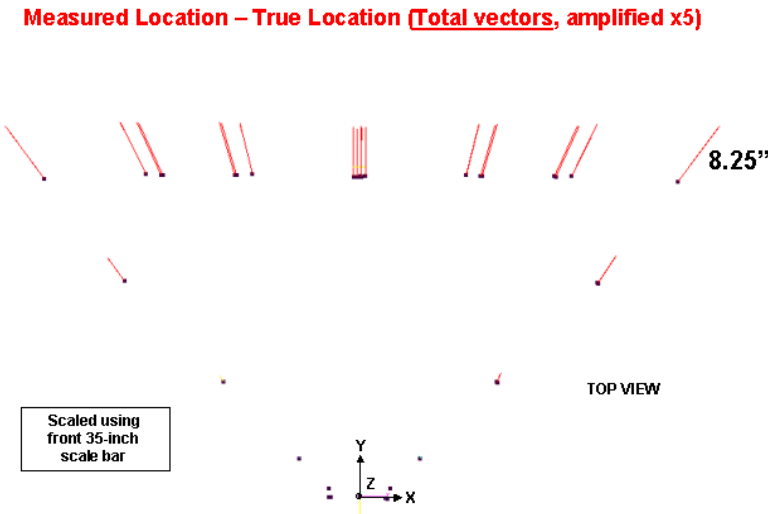


**Figure 9-12 ODS *absolute* measurement accuracy (i.e., measured location minus true location)**

**Total vectors shown. Dots indicate true 3D locations measured with V-STARS.**

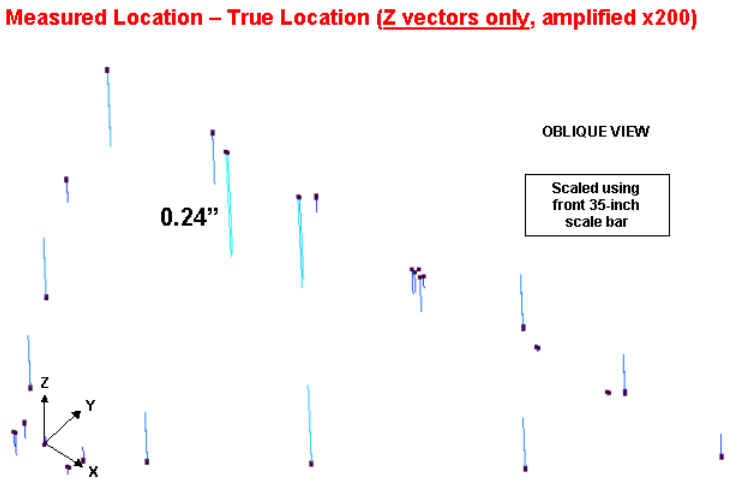


**Figure 9-13. ODS *absolute* measurement accuracy (i.e., measured location minus true location)**

**Z vectors shown. Dots indicate true 3D locations measured with V-STARS.**

# Section 10
# Known Interface Issues with Each Cycle 1 Sail Design

## *10.1 Common issues*

The issues listed below are common to both sail designs, but the answers may not be. Sections 10.2 and 10.3 show design-specific options for some of these common issues. The common issues identified to date include:

- Front vs back cameras and/or thermography: we need to study options overlooked in Phase 1
- Camera mast: design, ODS integration with mast, stability and knowledge of length
- Effects of ODS and camera mast on sail center of mass, static stability, and dynamics
- Stability and accuracy of knowledge of other sail dimensions ODS cannot estimate precisely
- Sail targets: number, pattern, design, attachment, location relative to folds, location accuracy
- Boom targets: same issues as sail targets, plus ensuring visibility over wide range of cases
- Visible and thermal appearance of membrane to ODS, and detectability of known anomalies
- Visible and thermal appearance of other interesting sail features, over a range of sun angles
- Sail slewing philosophy (affects glare: tilt same corner or quadrant towards sun, vs variable)
- Distributed wiring: protected or exposed, how attached, mass, possible need for redundancy
- Or tip/center wireless links: possible obstructions, need during deployment, redundancy
- Integration of distributed sensors with sail: accelerometers, load cells, strain, temperature, etc.
- Overall electrical integration of distributed ODS system with sail (power, data, grounding)
- Interfaces (if any) between ODS and sail during large-scale ground tests
- Possible schedule incompatibilities (we or they need decisions made before they are feasible)
- Implications of any required late design changes of sail or ODS on each other

## *10.2 Issues and options specific to ABLE sail design*

A concept for mounting the main ODS camera clusters on an ABLE-type deployable mast is shown below. A possible boom-camera view of retroreflective targets is shown at right.

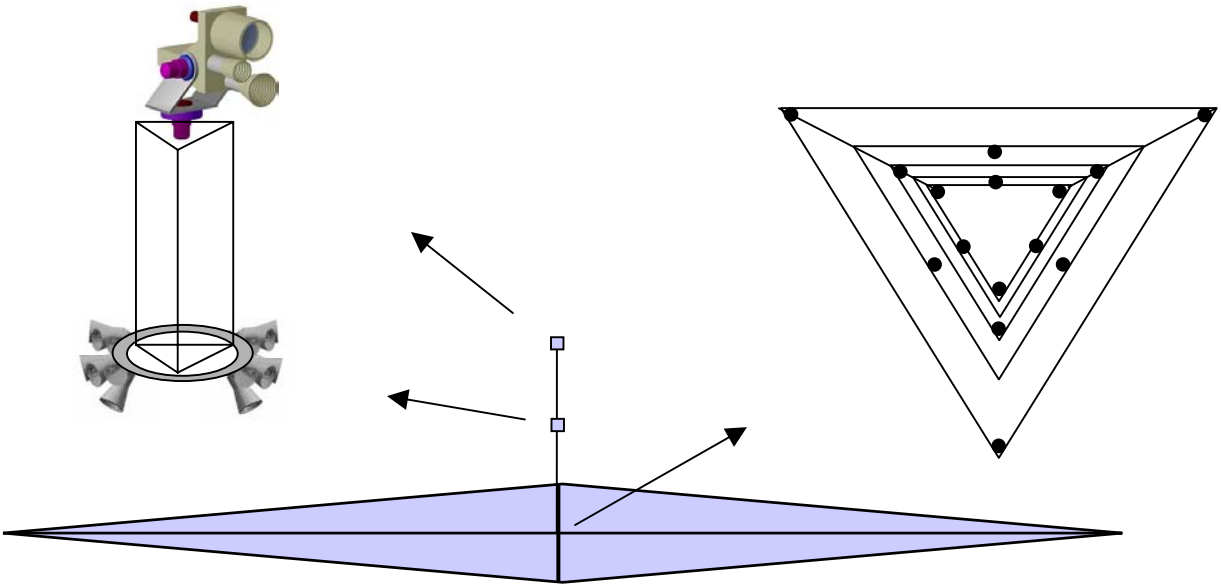

**Figure 10-1. ODS mounting on ABLE camera mast, and possible boom target pattern**

### 10.2.1 Relevant features of ABLE design

- The ABLE booms are deployed first, and then the sail.
- Deployment may be done while rotating edge-on to the sun, which might complicate imaging somewhat.
- The ABLE boom tips rotate as they deploy, and snap abruptly into place at full extension.
- Boom-view cameras must be offset from axis (a 1.3mm steel lanyard runs down the axis).
- A spreader bar on the mast tip rotates to effect roll. Moving ballast masses on the mast centerlines effect cant.

### 10.2.2 Boom-view cameras: position, coverage, and boom element visibility

Dave Murphy suggests we have targets at a maximum of 5 stations along the boom. On a 20m sail that puts the closest one at 2.84 m. To see a 0.4 m diameter boom at that distance requires a field of view of $8^{o}$. We need just 3/4 of the vertical height to see 3 targets at the corners of the bay, plus margin for misalignment and motion. How much margin is needed is TBD, but the other targets at each station will still stay in the view even after one leaves (or is occluded), and 2 of 3 should be enough for a good observation of boom bending and twist.

Putting the innermost targets at the middle of the battens allows a narrower camera field of view and hence more precision. There may be more in-plane bending than out-of-plane if peak bending is due to differences in support cable tension for adjacent quadrants. (This affects whether we use portrait or landscape image orientation.) We may want one extra target on the far end plate near the center (if we can do that without it being occluded by the central lanyard). This will help us know where the center of the boom tip is even if one or more of the other targets is occluded by boom cross-members inboard of that.

(Note: Additional studies may show that 3 accelerometers on each mast tip, plus targets on the sun-side face of the booms that are seen from the camera mast, is sufficient, and that we do not need cameras at the base of the booms and the targets described above. The cost/benefit ratio of doing so for a flight experiment may be too high.)

The lanyard is twisted by the action of the sail boom uncurling. From the camera viewpoint near the boom centerline, reflections off the lanyard are possible whether the camera is in front or behind the lanyard. The orientation that will cause glint is when a boom points towards the sun somewhat. When the sail deploys edge-on to the sun (while spinning), each camera may be pointed at the sun for a while. The potential for damage under these conditions must be checked.

The visibility of the boom elements themselves can be summarized as follows: the longeron is ~3mm in diameter, the batten ~2 mm. They are both graphite epoxy with a satin black appearance. The diagonals may present some glint. They are 0.3 mm stranded stainless steel cabling. The boom fittings have a diffuse tan coating.

## *10.3 Issues and options specific to L'Garde sail*

A concept for mounting the main ODS camera clusters on a L'Garde sail is shown below. The inflatable camera mast has a small offset at the base, so it can deploy around the carrier assembly, and is tilted for better clearance after deployment when the carrier is released and light pressure accelerates the sail backward away from the carrier. The cameras can mount offset to one side of the mast, so the mast can serve as a smooth bumper in case of carrier re-contact.

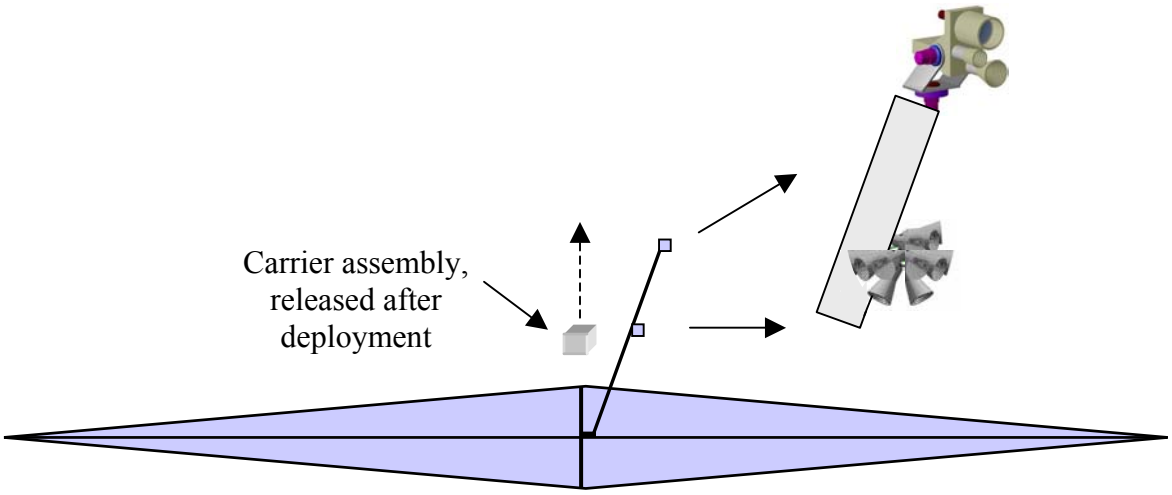


**Figure 10-2. ODS mounting on tilted camera mast, plus support package fly-away**

### 10.3.1 Relevant features of L'Garde design

- Membrane has a high-emittance thin iridescent black chrome coating on back.
- The booms have film over them so they can stay cooler, so their exact shape cannot be seen.
- Each boom has rings to support the sail, which can hold optical targets to image boom flex.
- The booms are aluminized internally and could act as a light pipe for data communication.
- Control assemblies at the tip may weigh ~200 grams and take <<10W power (maybe <1W).
- The sail's camber or depth/edge-length is likely to be in the 1%-5% range.
- L'Garde prefers that ODS not have wires running through the booms to the tip (heating, etc.).
- They want to minimize mass at boom tips (small compared to their ~200 gram tip vane assy).
- They do not want large moments from long camera masts at the boom tip.
- Their sail is light enough that ODS may affect axial CG location & hence sail stability.

### 10.3.2 Key mounting issues on L'Garde design

The carrier assembly needs to be on the sunward (front) side of the sail for the sail to fly away freely after it is deployed and released by the carrier. But the ODS camera platform needs to be there also. One option is to mount the camera boom slightly off center and tilted (10-15$^{o}$), to leave a "fly-away" margin between the carrier and the camera boom. Other options currently appear more difficult: discard the ODS camera boom with the carrier or perhaps deploy a second ODS.

An offset camera mast will move the sail center-of-mass toward one corner of the sail. Since they need a CM offset for slewing, it may be simplest if the sail corner closest to ODS is also the one that tilts toward the sun when the sail slews. This moves the maximum glare region further from the center of the sail. (Having a corner rather than mid-quadrant facing the sun should further reduce the area affected by glare, although it means poor viewing of part of one boom.) Having a fixed sun azimuth should also simplify keeping the camera mast cool, despite direct and reflected sunlight.

Note that the camera mast could use supporting guy lines between the sail plane and just under the main platform, if such lines don't make fouling more likely during flyaway. But the shorter length and lower loads (especially in bending) suggest to us that we don't need that.

The boom-view cameras on the L'Garde sail can mount forward of the sail plane, possibly within the triangle defined by the tensile truss structure. Targets can mount at the base of the V, at the supporting rings along the boom, and also at the top of some of the compressive members that define the V.

## *10.4 ODS Team Questions for Solar Sail Vendors*

### 10.4.1 ODS Primary-Equipment Accommodation

- What structure exists or can be provided to support ODS cameras (to achieve the desired views for photogrammetry)?
- What are limits to the size of extension booms, such that they will not adversely affect deployment, dynamics, or mass? (This answer will be very different for front-extension versus rear-extension masts.)
- Are there any special concerns regarding the accommodation of ODS support equipment (e.g., location, volume)?
- How are spacecraft support electronics to be accommodated? Is this yet definitive or is left as an exercise for a system contract (or proposal or study)?

### 10.4.2 Sail Targets

- What is the maximum target density (areal and mass) allowable? What other mechanical properties of targets must be specified (e.g., stiffness, thickness, etc.)?
- How will responsibility be allocated for the placement of ODS targets on the sail? Who is responsible for their specification? Who is responsible for their actual installation? Who is responsible financially for them and their installation?
- What can we say about accessibility to the sail, with or without targets, with respect to ODS activities, e.g., calibration?

### 10.4.3 Boom Targets

- What types of targets or retroreflectors can be attached to the masts?
- How will responsibility be allocated for the placement of ODS targets/reflectors on the masts? Who is responsible for their specification? Who is responsible for their actual installation? Who is responsible financially for them and their installation?
- What can we say about accessibility to the structure, with or without targets, with respect to ODS activities, e.g., calibration?

### 10.4.4 Mast-Tip Equipment

- Is any mast tip equipment besides accelerometers anticipated? What is the total allowable tip mass or total allowable additional tip mass beyond what is already contemplated?

- If “yes”, what is the power and data communications infrastructure anticipated? Can it be used as-is for accelerometer data? Can it be easily augmented?
- If “no”, will wired infrastructure be allowable (e.g., from a mast-deployment interference perspective)? What is an allowable linear mass density of such wiring? Stiffness? etc. What considerations are relevant with respect to mast deployment and interactions with wires (e.g., stowage, bending, etc.)? Is the mast structure useable as a power return?
- If wired infrastructure is not acceptable, what are the RF and optical properties of the booms and sails? What real estate can be made available at the mast tips for (solar) power generation?

### 10.4.5 Dynamics

- Is the sail structurally stable with respect to all sun angles? What is the maximum allowable off-normal sun angle?
- What reaction forces and torques are allowable for the PDS to impose on the ODS during deployment and operations?
- What are the intrinsic structural excitation sources and their magnitudes? Is there any need for artificial excitation to support dynamical (ODS) analysis? Can existing mechanisms provide such excitation?

### 10.4.6 Thermal

- What is the thermal conductivity of the sail material, both normal and transverse (in plane)?
- What are its expected $\alpha$ (front) and $\varepsilon$ (thermal, both front and back)?

# Section 11
# Technology Gaps and Risks for Bringing ODS to TRL 6

Sections 11.1 and 11.2 below list recognized technology gaps and perceived risks in getting the Optical Diagnostic System for Solar Sails to a NASA technology readiness level (TRL) of 6. Sections 11.3 through 11.10 recommend near-term development efforts in each area, mostly in the same order the topics were discussed in the main body of the report.

## *11.1 Key technology gaps that need to be filled to get ODS up to TRL 6*

Key technology gaps are listed below in estimated order of importance (critical items first):

1. Thermography: hardware selection, testing, and interpretation of imagery
2. Trade study: front side cameras (visible & IR) vs. back side cameras (visible & IR)
3. Cost/benefit study of cameras at hub for measuring bending/torsion of booms
4. Target requirements and test methods to validate them
5. Deriving sail shape and dynamics using cameras on lower platform only
6. Optimizing the height of both the upper and lower camera platforms
7. Photogrammetry and thermography instrument calibration techniques
8. Relevant ground tests of membrane optical properties
9. 80 Hz SXGA image compression at low power and mass w/space-qualifiable hardware
10. Design of both imagers and algorithms to handle high and variable noise in images
11. Efficient near-real-time SXGA image centroiding with minimum hardware and power

## *11.2 "Top Ten" known risks involved in getting ODS up to TRL 6*

The list below is taken from the Phase 1 final presentation. It is included here as an independent ODS status check, somewhat orthogonal to the list of technology gaps in Section 11.1.

1. Validity of targeting approaches
   – L'Garde targeting approach not yet demonstrated
   – AEC-ABLE / SRS targets not yet validated
   – Creases & wrinkles can significantly affect measurement accuracy

2. Uncertainty from ISP office about Level 1 requirements
   – Affects complexity of components purchased or built
   – Can affect schedule and cost

3. Camera design/placement affected by requirements of ground test program
   – Much less light
   – Vibration frequencies are much higher, so frame rates must go up ($f \sim 1/\text{Size}^2$)
   – The structure has much more sag in gravity than in space
   – We do not want the test program to drive the design

4. Procurement time
   – ISP getting required $$ to LaRC in sync with expenditures
   – Delays in subcontract award or component delivery

5. Compatibility of flight ODS with L'Garde carrier
   – Carrier flies away on sun side (interference with ODS mast?)

6. Compatibility of breadboard and prototype ODS with L'Garde boom cooling
   – L'Garde does not yet have a solution to this problem
   – Could affect how cameras are mounted at LaRC and Plum Brook

7. Buckling deflection of L'Garde booms is low (~ <2 cm for 10m sail)
   – Can sufficient vibration be excited to measure, without structural damage

8. Cycle 1 10m tests get delayed or have problems unrelated to ODS
   – Results in schedule slip to verification of Breadboard ODS

9. Method to place ODS system above sails in large-scale tests not yet well defined
   – Potential interference with other supports
   – Camera stability with pan-tilt movements

10. Transition to Phase 3 occurs just prior to start of new FY
   – Additional funds needed in ~ Sept. 2004 for Phase 3

## *11.3 Sail dynamic analyses*

### 11.3.1 How do thermal gradients, assembly errors, and creases affect membrane behavior?

During the study we realized that at least 3 different effects could swamp the intended uniform “few-ppm” tensile strain on solar sail membranes, and hence drastically change the planned uniform membrane tension. One effect is thermal gradients (see Section 6). Another is cumulative assembly errors. Large solar sails may necessarily involve step-and-repeat membrane assembly operations. This may lead to cumulative errors far larger than those found with sails small enough to assemble in deployed form on a flat surface. A third issue is the effect of creases, and intersecting creases that form puckers. The one saving grace about creases and puckers is that they straighten out at modest local membrane tension, and hence may provide passive slack management. This may help compensate for thermal gradients and assembly errors.

The task here is to understand the likely magnitude of these effects, and their combined effects on sail shape, dynamics, performance, and restrictions they may impose on sail operation. One potentially critical issue is to understand whether the effects of thermal gradients on sail shape could lead to positive feedback in the attitude control system, either due to the inherent geometry of the sail and its support structure, or due to plausible control-structure interactions: a possible control-induced flutter problem. Control interactions are a sail-developer responsibility, but developing sail dynamic models detailed and accurate enough to find inherent feedback mechanisms may be within the scope of ODS modeling, and could benefit later control stability studies by the sail developers.

### 11.3.2 What “natural” parameters summarize solar sail deviations from a plane?

The basic concepts in statistics (average, RMS error, and skewness) are amazing in their simplicity, completeness, and broad utility. Basic parameters of this sort might allow easy estimation of non-ideal sail performance due to billow, wrinkles, and creases. The question is what parameters might be most "natural." For example, we can probably develop a precise definition for the “mean sail plane” of a billowed sail that is unambiguous, measurable, and useful for various analytical purposes.

Root mean square (RMS) surface slope compared to that mean sail plane should summarize cosine losses due to scattering of reflections away from the mean direction of the reflection. This parameter properly combines all the effects of surface slopes, on all relevant scales, without worrying what causes them--at least when the combination of sun angle and billow depth are not sufficient to shade part of the membrane. The value can be inferred from the ratio of sail area projected onto the mean plane, compared to total sail area. Hence if we can estimate the in-plane displacement of the edges of the sail (caused by out-of-plane deformations), then we can infer RMS slope, without knowing the details of the out-of-plane (OOP) displacements. The thrust loss due to scattered reflections should be $4\boldsymbol{r}/(1+\boldsymbol{r})$ times the direct loss in area (which also affects thrust), where $\boldsymbol{r}$ is the sail reflectivity, assumed completely specular (which is a good approximation). A complementary parameter is the "average billow." This might be the difference between the mean OOP positions of the sail edge and the sail area. The CP shift due to billow may depend mainly on the product of this and the sail tilt angle to the sun, independent of details.

The effort here will be to look for a wider range of parameters like mean sail plane, RMS slope, and average billow, and use the models to estimate how well they can predict non-ideal sail behavior, and how readily their values can be derived from ODS and other flight data.

### 11.3.3 How can analytical models use ground and flight test data for verification?

ODS will generate large amounts of data: images, other sensor data, and (after processing on the ground) 3-D sail shape estimates. A key use of the data and shape estimates is structural model verification. Mission planners understandably like analytical models verified before using them to plan expensive missions. The question here is how to do that. Any model with a large enough number of input parameters can be made to fit any dataset, but that does not verify the model unless there is also reason for the specific inputs used. It is hard to describe this task in more detail than to say: it is everything that an intelligent modeler does between the time that he gets good-quality test or flight data, and the time he is ready to use his model to make predictions whose accuracy can be tested by later ground or flight experiments. Those predictions may span the range from thrust and thrust direction, to peak tensions at sail corner supports, to the

combined effects of sail control algorithms, sail structure, and thermal distortion. As ODS/sail tests are done, the data to drive this iterative loop become available, and progress can be made.

## *11.4 Image processing and display*

### 11.4.1 Real-time scanning for targets

It appears that the most time-consuming part of looking for targets in images may be the initial brute-force, pixel-by-pixel scan of the whole image. But low-level logic can scan for the target as it is transferred and provide indications of where to look in the image for good target candidates. The main near-term task is to understand what circuitry is required for this, and whether it might easily fit into an FPGA used for control of multiple imagers and image capture.

### 11.4.2 Automated target recognition, identification, centroiding, and characterization

Most photogrammetry still depends on manual target identification unless coded targets are used. Coded targets for ODS would have to be quite large, and manual target identification could be extremely time-consuming because of the large number of targets and images. Automating target identification should be easier than in many photogrammetric projects because the sail has high regularity in space and time, with its slowly moving, nearly planar square grid pattern of targets, plus linear boom, sail-edge, and seam features in approximately known locations. A useful effort might include working on automating the following tasks:

1. Find candidate targets and judge tentatively whether they are targets based on local tests.
2. Find their centroids (and eventually, their size, shape, orientation, and total brightness).
3. Judge which targets they are in a grid (and eventually provide a confidence estimation).
4. Interpolate positions for missing targets and look again for them with adjusted criteria.

### 11.4.3 Automating generation of accurate 3D sail shape estimates from ODS imagery

As noted in Section 3.2 and elsewhere in the report, the specialization of the two main ODS camera platforms means that ODS cannot do traditional 3D multi-viewpoint photogrammetry of the whole sail at one time. On the other hand, we will have high-quality images of the whole sail and targets, and a variety of real-world constraints on the interpretation of those images that allows us to infer considerable depth information in generating a 3D model of the sail. There seems to be no question that this can be done; the key issue is how to do that in the most accurate and efficient way. What makes this effort complicated is actually the wide variety of tools that may be able to assist the process, and the wide variety of derivative products that different approaches may provide, and the uses and relative value of those derivative products.

For example, any technique that can iteratively project ODS imagery onto a 3D sail model and adapt the model to better fit the imagery could be not only powerful but also intuitively useful because it ends with a potentially very accurate 3D model of the billowed sail that is also photo-realistic. If this sail model is compatible with one or more popular standard CAD display programs that allow users to easily change perspective, it may become an extremely powerful, intuitively useful tool for a wide range of analysts, including sail developers, program and mission planners, and others interested in solar sail technology. Even difficulties in local fitting of the model can be made visible, for example using an overlay that shows where the model thinks the targets should be, or residual errors. This allows users to evaluate solution accuracy, and perhaps (by seeing error patterns on the sail), to understand the reason for the errors.

The near-term effort here might start by collecting data on a wider range of computer programs that may be useful in image processing and display. Then we would find and talk with current users about the relative strengths and weaknesses of the programs, and put together a more detailed plan for the remaining development. In parallel with this, we would investigate the most useful forms for ODS image data products, with a strong emphasis on making them easily usable with a variety of existing widely used programs. For example, we have found that next-generation Digistar digital planetarium projectors from Evans and Sutherland will accept 3D model data in Windows ActiveX/DirectX format. Putting models into that format may

ensure the models can be used in a wide range of applications, from PC-based to planetarium-based.

### 11.4.4 Consider goals, lighting, and other issues for large-scale ODS ground tests

This is an effort that requires input from both the ODS team and the sail program. Section 4.2 of the report discussed lighting trades for large-scale combined ODS/sail tests. If we do indeed want realistic images we need "representative" lighting: selectable bright lights in several positions to simulate sunlight approaching the sail from different directions, with each light small enough to look like a sun-like source. We also need black backdrops wherever feasible so the sail itself looks appropriately dark. But we cannot hope to get realistic sail glint because large-scale ground tests necessarily apply higher membrane tensions and hence straighten out creases and puckers. So the more serious issue is to carefully think through the purposes of the large-scale tests, and to find out what is actually worth doing in those tests, and what other tests are needed if the original goals of such tests are best met in other ways. Large-scale tests are useful for ODS since they allow us to test our image-processing techniques, and they should be useful for modelers, sail developers, and mission planners by providing data on sail dynamics in test environments. But large-scale ODS/sail tests cannot provide all the kinds of developmental test data that ODS needs, so additional smaller-scale tests are needed as described in Section 11.5.

## *11.5 Mechanical and Optical Tests of Membrane Crease and Pucker*

### 11.5.1 The need for representative handling and lighting of representative membranes

The L'Garde flight sail will be metalized on both surfaces (aluminum on one side for reflectivity; a thinner chrome coating on the other side for emittance). The ABLE/SRS sail may be metalized on only one side. Despite the fact that the metal coatings are <5% as thick as the underlying plastic film, much of the memory of creases is due to the metals rather than the plastic because of their higher modulus and much lower yield strain compared to the plastic films, and the fact that the metals are on the surface, which maximizes strain in bending. Hence handling tests that seek to characterize crease or pucker formation and removal, and their effects

on sail glint and hence image quality, need to use films and coatings made of representative thicknesses of representative materials. And they must be handled in representative ways, at representative tensions. This cannot be done with large sail membranes in Earth gravity because gravity-induced tensions are far too high, whether the membrane is horizontal or vertical.

### 11.5.2 Handling tests to evaluate low-tension geometry of folded/unfolded membranes

The sail fold pattern will probably be z-folds in one direction followed by additional z-folds or rolling in the other direction. If the sail developers can provide data on how they expect the film to be secured against launch and depressurization (tightly clamped or not, etc.), it would be useful to have that data. When we deploy the film in ground tests, we need to take care to prevent tension spikes that would not occur in flight, and to provide "local unfolding" similar to that expected in flight with any pull-out tabs or other slack-management devices the sail is expected to use. On the other hand, if transient tension spikes are expected, for example at the end of deployment, it is important to try to mimic them in some way, or at least to do tests that bracket the range of expected peak tensions and their effects on creases, puckers, and other artifacts.

Once we have a way to mimic the expected handling of the sail membrane, at least insofar as it should affect crease and pucker formation and removal, then we can do realistic mechanical and optical tests on the membrane. Mechanical tests can look at the nonlinear stress-strain film response and see how that varies as a function of the peak tension in each direction since unfolding. A single exposure to "high enough" tension should take out most of the creases and puckers, much like shaking out a bed sheet after unfolding it. This should make the film behave much more like virgin film in both its mechanical and optical properties. We need to understand the extent of such changes. The sail developers may benefit because it may affect their thinking about imposing intentional transient peak tensions after deployment to straighten out creases and puckers before cumulative space exposure embrittles the membrane.

### 11.5.3 Optical testing of appropriately handled membranes

If mechanical tests show that traveling waves or other likely low-tension dynamics can "shake out" membrane creases and puckers without over-stressing the membrane or the boom structure, it is possible that glint will not be a problem. But if plausible handling can in some cases leave residual creases and possibly puckers, then careful glint testing seems necessary. The main purpose of these optical tests is to characterize glint intensity as a function of current tension, peak prior tension, and apparent local membrane tilt. The main emphasis should be on substantial local tilts because most of the sail is far from the "glare spot" and hence substantial local tilts are required to cause glint. Doing this test requires a small light source (not necessarily a point source) and good black baffling everywhere else. Then everything other than the light source that is viewed in specular reflections from the sail is far darker than the light source, and preferably fairly uniformly dark.

If the main ODS imaging cluster height is 15% of the sail edge dimension, then (neglecting billow) half of the sail area will be viewed at angles 69-78$^{o}$ from the normal, and ¾ of what is left will be viewed from 53-69$^{o}$. And the sun may generally be either near normal or near 35$^{o}$ from normal to the mean sail plane. So over ***most*** of the sail area, generating glint viewable by the cameras will require fairly significant local membrane tilts (due to creases, puckers, or wrinkles caused by uniaxial tension). One slope-error survey technique that has been used with solar concentrators is to image the reflection of a fluorescent tube off the non-ideal surface. Moving the tube allows a 1-dimensional scan of one component of the local membrane slope. Repeating this in two orthogonal scan directions allows evaluation of the glint statistics for slope components in each direction. Results for the two directions may differ because the order of folding and unfolding may result in different crease patterns.

### 11.5.4 Collecting and interpreting glint statistics

The key output from two 1D glint surveys may be a graph of the frequency of various angular deviations from flatness and the characteristic sizes of those features, which should vary with membrane thickness. This requires imaging on a scale far finer than that of a single pixel in a flight-size sail, or estimating the glinting feature size from its "excess brightness." This

assumes that the characteristic width of a reflecting region from a crease or pucker should be a function of the film thickness and tension far more than of the overall membrane size.

To limit the number of optical scans and post-processing runs required, it may be worth doing this test for two main cases, one with minimum peak tension after deployment, and one with much larger (but still plausible) peak tension, to see what difference that makes in glint statistics and potential noise in ODS imagery. Very informal manual tests may show several different types of behavior, each of which deserves characterization.

### 11.5.5 Diffuse membrane reflectivity

The same optical test setup used above can characterize "quasi-diffuse" membrane reflectivity after typical handling and with near-normal illumination and high-incidence viewing. In this case, it is very important that the main specular reflection from the membrane be trapped and absorbed fairly well so it doesn't illuminate the baffle regions the camera sees reflected in its view of the membrane. We can also mask the direct illumination of the sail and subtract the "surrounding background" intensity from the intensity of the masked region to reduce the effect of stray light. The purpose of the test is to see whether and how the effective diffuse sail reflectivity changes with handling, view angle, tension, or anything else. As mentioned in the "targetless imaging" section of the report (Section 4.3.1), such changes might provide useful diagnostic information. It may be worth testing some membranes before and after exposure to plausible events that might change diffuse reflectivity to see whether such changes do occur.

### 11.5.6 Target optical tests

One more set of very useful optical tests is imaging "handled" membrane samples with targets on them. The imaging can be done with far higher resolution than would be present in flight. The resulting image can be smeared in digital post-processing to simulate lower-resolution target images with various degrees of smearing, intra-pixel sensitivity variations, and so forth. These tests could characterize the brightness uniformity of the targets and the presence of any glinting features associated with the targets that might affect accuracy. For example, the painted targets shown at the Phase 1 final review caused slight local expansion of the film, which

caused local slackness around the edge of the target. At certain lighting angles, that causes glint from one side of the target but not the other. The result is centroiding errors. (If this can occur with flight-design targets, then we should use smaller targets than would otherwise be optimum for photogrammetric accuracy.) Target-induced glint might be present at very low tensions but not higher tensions. We can then do image recognition and centroiding off-line with images degraded by digital smearing and noise. This allows a better understanding of target visibility, recognition, and centroiding errors as a function of target size in pixels and glint and glare level.

## *11.6 ODS camera development*

Efforts are required here both on components (lenses, filters, lens shades and other stray-light-control features, imagers, and support circuitry) and system performance.

On the lenses, we should select and procure some "apparently suitable" stock lenses. We can take a few apart to see what may require changing for flight. Then we can contact the suppliers and determine their openness to making a small lot with any required changes, at a reasonable lot charge. Changes could include different spacers, better edge blackening, a smaller aperture, addition of a ceria-doped glass or colored glass front filter element, better venting, or tighter clearances to prevent relative shift in elements after shock or thermal cycling. If we can purchase modified lenses at a reasonable lot charge, then we can use stock lenses for most of the developmental testing. If nothing unpleasant is learned, then we would purchase custom lots. This should be done with enough lead-time that we can find a backup if necessary. If no suitable "modifiable" lens can be found, then an alternative path needs to be fleshed out--but the most nearly suitable stock lenses can still be used for most early development work.

For the imaging chips, we need to review the candidate datasheets more carefully and then choose at least two for testing. Many SXGA-class active pixel CMOS chips are available in "Evaluation/Development Kits (EDKs)," with PC-connected hardware and support software. This allows us to easily verify sensitivity and noise claims. We can also test an EDK for damage by focused sunlight. Nondestructive evaluation of the imaging chips is also useful. For example, for ~10 chips from the same batch, we can measure chip placement errors in the

ceramic package (offset, rotation, and tipping) and how much they vary. Another useful test for chips with glass covers is package bulge or breakage during fast depressurization in a vacuum chamber.

After these tests, we can substitute lenses selected above for the lens provided with the imager and do more useful ODS tests. Repeating the test described in Section 5.1.2 would be useful to quantify centroiding noise. We can also determine point spread function with a prototype lens, with and without color filters. Then, if the chips still look promising, it might be time for radiation testing of the imager and (in a proton environment) the lens to ensure it does not darken unacceptably, if we cannot find other radiation test data on those chips and optical glasses.

Then we can design and build prototype circuit boards and aluminum camera housings, assemble cameras, program any FPGAs as needed, and start testing for photogrammetric stability over temperature and shock. In parallel with this, we will be developing the rest of the avionics. When both are ready, we can test them together.

## *11.7 Thermography*

As noted in Section 6.7, it seems worthwhile to focus near-term thermography efforts on answering the following questions:

1. Are compact low-power imagers like the Omega likely to be flight-qualifiable?
2. Can front-side thermography with those imagers provide useful images of the sail?
3. What can such images tell us about sail properties, degradation, or other phenomena?

The ODS team has already purchased an Omega, so testing it will be convenient. The more difficult task is providing suitable thermal imaging test subjects. The long-wave emittance of the front of the sail (~0.03-0.05) may actually be less than that of a few meters of room air with typical humidity. So we may want to do many of the tests in vacuum with good cold plates, etc.

But many of the tests aimed at characterizing the imager are independent of the exact details of the object that is imaged, so we can use "any convenient subject" for many images.

Well over half the thermography effort might really be focused on characterizing what we can learn from front-side or back-side thermal images of sail materials, both virgin and also after plausible types of mistreatment, including sputtering, radiation, contamination, etc. Many of these material property tests might best be done at Surface Optics Corp. because those tests are done in carefully controlled environments that make it easy to distinguish surface property changes from temperature changes.

By testing materials over a range of conditions, angles, and wavelengths, we can determine "what is there to be seen" and whether it may need multi-spectral filters to adequately distinguish different conditions. That can tell us whether we may need an infrared filter wheel on the thermal imager, for example to split the 7.5-13.5 micron region into several bands so we can distinguish temperature changes, contamination, or other effects.

## *11.8 Distributed non-imaging sensors, datalinks, and support electronics*

The first effort here may be to find out from the sail developers what needs they have in their most recent sail designs for power and data transfer between the center and the boom tips, what sensors they are interested in, what concepts they are considering, and whether a 4-wire link weighing <1 g/m should be compatible with their boom design and not too hard to integrate. For the L'Garde design, we should find out whether a total ohmic heating of order 1W along a 50m wire is acceptable inside or in close proximity to their temperature-sensitive boom.

We should also look to see what commercial wiring might be available in this mass range. If none is available, it may be worth having a sample made for handling tests. (Using a robust polyimide coating should keep the costs well below those of the ProSEDS wire.) In parallel with this, we need to see what short-range wireless concepts may be most feasible and attractive, and

what the "overhead" is for providing power for wireless concepts. Then we should take a close look at the costs and risks of each option and recommend a wired or wireless solution.

In the area of sensors, we should take a fresh look at what will be most complementary to the imaging sensors and useful for understanding sail loads and dynamics and anomalies, to the extent we can predict the key issues and observables. Then we should purchase, evaluate, and test candidate sensors, first by themselves and then with candidate signal conditioning. Then we should make arrangements to have tests done with the sail booms to see whether there are any problems with deployment snagging (with wired concepts) or communication obstruction (in the case of wireless concepts). One sensor concept that we have not considered seriously but may be worth some attention is sensors and wiring concepts that are either inherent in or can be built into the membrane. For example, the resistance of the metal coating(s) between two regions may change with temperature, cumulative sputtering, or gross tearing. It may conceivably be worth measuring the resistance if a fairly low-risk way can be found to do that.

Another step is to integrate the sensors, communication links, and signal conditioning and do a variety of tests, hopefully including tests associated with the ABLE and L'Garde booms. We may want to consider circuit concepts that allow use of redundant separated cables in case one is damaged.

In parallel with this, we should look for radiation test data on candidate MEMS sensors. Such sensors are being considered for a wide variety of other programs, and radiation testing may be underway or planned. If we are very interested in a sensor that has not yet been tested, we should discuss it with radiation effects specialists to see whether there is any known reason for not using this sensor, and plan tests if it still seems prudent to use it. One final area is to periodically review progress in "Smart Dust" and other "local wireless network" concepts to see what new aspects may be relevant to distributed sensing on solar sails or other gossamer spacecraft.

## *11.9 Avionics*

In addition to the technology tasks just discussed relating to distributed systems, the technology gaps in the avionics area are mostly associated with high-throughput imaging. The key issues are controlling 6 clusters of 4 SXGA imagers, capturing 80 frames/sec, or perhaps more if reviews of sail dynamics and transient effects suggest a need for that, and figuring out how to do near-real-time JPEG2000 compression and centroiding using low-power, low-mass flight-qualifiable hardware.

The main key TRL gap is verifying that we can do JPEG2000 compression at a sustained rate of ~80 SXGA frames/second. JPEG2000 does not use frame-to-frame similarity, so repeatedly dumping a single frame from a single high-speed buffer may be adequate unless send/receive re-synchronization after switching channels is an issue. We need to determine:

1. Whether we can download stored SXGA images fast enough over ~7m (LVDS or ?)
2. How long compression takes (which may vary with the image and compression ratio)
3. How easily we can double-buffer, to download one image while compressing another.

Careful analysis of hardware specifications may eliminate most risk. But if JPEG2000 compression time varies with the image content or compression ratio, we need tests on suitable images. And we do need good tests eventually (including radiation tests) to verify that there are no problems that may require our switching to raw-image capture plus later compression at lower rates or possibly switching to MPEG compressors if they allow higher throughput or compression.

The centroiding task should be easier, but may not be able to take advantage of optimized single-purpose hardware the way JPEG2000 may be able to. Centroiding is mature technology, but doing it at 80 frames/second on “noisy” solar sail images is not. We need to develop and test suitable algorithms, first on PCs and then on more flight-like hardware. It may be feasible to do the centroiding using mostly the same hardware used for conventional image compression if a “mostly software” solution is used for the JPEG2000 compression.

Note: The fact that the avionics subsection is shorter than that for several other topics does not mean that avionics tasks are less important or require less effort. The high-TRL areas are just somewhat better defined so it doesn't take as long to describe what needs to be done about them.

## *11.10 Interface issues and integration planning*

The list below is copied from Section 10.1. These items are known interface issues that are common to both Cycle 1 sail designs (ABLE and L'Garde).

- Front vs back cameras and/or thermography: we need to study options overlooked in Phase 1
- Camera mast: design, ODS integration with mast, stability and knowledge of length
- Effects of ODS and camera mast on sail center of mass, static stability, and dynamics
- Stability and accuracy of knowledge of other sail dimensions ODS cannot estimate precisely
- Sail targets: number, pattern, design, attachment, location relative to folds, location accuracy
- Boom targets: same issues as sail targets, plus ensuring visibility over wide range of cases
- Visible and thermal appearance of membrane to ODS, and detectability of known anomalies
- Visible and thermal appearance of other interesting sail features, over a range of sun angles
- Sail slewing philosophy (affects glare: tilt same corner or quadrant towards sun, vs variable)
- Distributed wiring: protected or exposed, how attached, mass, possible need for redundancy
- Or tip/center wireless links: possible obstructions, need during deployment, redundancy
- Integration of distributed sensors with sail: accelerometers, load cells, strain, temperature, etc.
- Overall electrical integration of distributed ODS system with sail (power, data, grounding)
- Interfaces (if any) between ODS and sail during large-scale ground tests
- Possible schedule incompatibilities (we or they need decisions made before they are feasible)
- Implications of any required late design changes of sail or ODS on each other

# REPORT DOCUMENTATION PAGE

*Form Approved*
*OMB No. 0704-0188*



| 1. REPORT DATE *(DD-MM-YYYY)* | 2. REPORT TYPE | 3. DATES COVERED *(From - To)* |
|---|---|---|
| 01- 12 - 2004 | Technical Memoradum | |

**4. TITLE AND SUBTITLE**

Optical Diagnostic System for Solar Sails: Phase 1 Final Report

**5a. CONTRACT NUMBER**

**5b. GRANT NUMBER**

**5c. PROGRAM ELEMENT NUMBER**

**6. AUTHOR(S)**

Pappa, Richard S.; Blandino, Joseph R.; Caldwell, Douglas W.; Carroll, Joseph A.; Jenkins, Christopher H. M.; and Pollock, Thomas C.

**5d. PROJECT NUMBER**

**5e. TASK NUMBER**

**5f. WORK UNIT NUMBER**

23-800-92-62

**7. PERFORMING ORGANIZATION NAME(S) AND ADDRESS(ES)**

NASA Langley Research Center
Hampton, VA 23681-2199

**8. PERFORMING ORGANIZATION REPORT NUMBER**

L-19069

**9. SPONSORING/MONITORING AGENCY NAME(S) AND ADDRESS(ES)**

National Aeronautics and Space Administration
Washington, DC 20546-0001

**10. SPONSOR/MONITOR'S ACRONYM(S)**

NASA

**11. SPONSOR/MONITOR'S REPORT NUMBER(S)**

NASA/TM-2004-213511

**12. DISTRIBUTION/AVAILABILITY STATEMENT**

Unclassified - Unlimited
Subject Category: 39
Availability: NASA CASI (301) 621-0390

**13. SUPPLEMENTARY NOTES**

An electronic version can be found at http://techreports.larc.nasa.gov/ltrs/ or http://ntrs.nasa.gov

**14. ABSTRACT**

NASA's In-Space Propulsion program recently selected AEC-ABLE Engineering and L'Garde, Inc. to develop scale-model solar sail hardware and demonstrate its functionality on the ground. Both are square sail designs with lightweight diagonal booms (<100 g/m) and ultra-thin membranes (<10 g/m2). To support this technology, the authors are developing an integrated diagnostics instrumentation package for monitoring solar sail structures such as these in a near-term flight experiment. We refer to this activity as the "Optical Diagnostic System (ODS) for Solar Sails" project. The approach uses lightweight optics and photogrammetric techniques to measure solar sail membrane and boom shape and dynamics, thermography to map temperature, and non-optical sensors including MEMS accelerometers and load cells. The diagnostics package must measure key structural characteristics including deployment dynamics, sail support tension, boom and sail deflection, boom and sail natural frequencies, sail temperature, and sail integrity. This report summarizes work in the initial 6-month Phase 1 period (conceptual design phase) and complements the final presentation given in Huntsville, AL on January 14, 2004.

**15. SUBJECT TERMS**

Solar Sails, Optical Diagnostics, In-Space Propulsion Program, Photogrammetry, Thermography, Space Flight Experiments, Instrumentation

| 16. SECURITY CLASSIFICATION OF: | | | 17. LIMITATION OF ABSTRACT | 18. NUMBER OF PAGES | 19a. NAME OF RESPONSIBLE PERSON |
|---|---|---|---|---|---|
| a. REPORT | b. ABSTRACT | c. THIS PAGE | | | STI Help Desk (email: help@sti.nasa.gov) |
| | | | | | 19b. TELEPHONE NUMBER *(Include area code)* |
| U | U | U | UU | 146 | (301) 621-0390 |